THE SPATIAL LOCALIZATION OF TARGETED ALPHA MODULATIONS IN CONCURRENT EEG-FMRI DURING VISUAL ENTRAINMENT

Cilia Pauline Jaeger

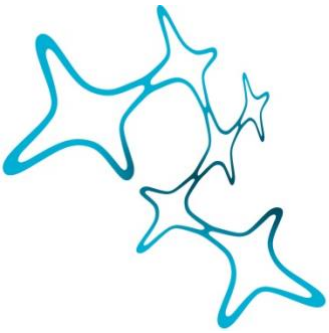

Graduate School of
Systemic Neurosciences
LMU Munich

Dissertation der
Graduate School of Systemic Neurosciences
Der Ludwig-Maximilians-Universität München

March, 2022

Supervisor
Dr. Afra M. Wohlschläger
Klinikum rechts der Isar
Technical University of Munich

First Reviewer: Dr. Afra M. Wohlschläger
Second Reviewer: Dr. Christian Sorg
Third Reviewer: Prof. Dr. Erich Schröger

Date of Submission: 16 March 2022
Date of Defense: 10 0ctober 2022

Dedicated to my family,

especially to

my grandfather Prof Eckhard Hoffmann

ABSTRACT

Coordination of neural communication is ubiquitous in cognition. The alpha oscillation (8- 13 Hz) is the predominant neural oscillation in the posterior cortex and has been associated with a broad range of cognitive processes. The alpha oscillation is thought to facilitate information processing and binding of context-relevant incoming sensory input by gating cortical excitability through phasic bouts of inhibition. Yet it is not well understood how information transfer emanates from modulations in the alpha rhythm. Spatially localizing the brain regions involved in alpha-mediated information processing will give further insight into the origin and role of the alpha oscillation. Evidence suggests that visual rhythmic stimuli can entrain the alpha oscillation. The entrainability of the alpha rhythm can be utilized to systematically study controlled alpha modulations. However, the peak alpha frequency varies across individuals, which has been ignored in most previous entrainment studies.

In my research I investigated the spatial localization of targeted alpha modulations using concurrent EEG-fMRI. In my first study, I implement an entrainment paradigm targeting individual differences in the peak alpha frequency. I evaluate the efficacy of entrainment by comparing degree of synchronicity during entrainment at the individual alpha frequency to control frequencies. I also show that degree of synchronicity as measured by imaginary coherency in EEG and BOLD connectivity in fMRI serves as an appropriate proxy for entrainment. Increased synchronicity across the occipitoparietal cortex was observed at rhythmic stimulation at the IAF as compared to rhythmic stimulation of control frequency in both EEG and fMRI.

In my second study, I implement the entrainment paradigm in a concurrent EEG-fMRI study and show that EEG and fMRI whole brain connectivity complement each other with each contributing to differently to the assessment of overall connectivity. I also show that co-fluctuations in connectivity reveal novel insights on long-range thalamocortical connections involved in visual processing. My results contribute functional evidence for previously observed thalamo-cortical structural connectivity and show a novel application of studying dynamic connectivity changes during sensory stimulation. In the future, this application can be translated to other modalities and other neural oscillations and provide clearer insight into the specific roles of individual neural oscillations in cognition.

TABLE OF CONTENTS

ABSTRACT....IV

TABLE OF CONTENTS....V

LIST OF FIGURES....VII

LIST OF ABBREVIATIONS....VIII

INTRODUCTION....1

1.1 Neural oscillations....1

1.1.1 Neural oscillations in cognition....1

1.1.2 EEG: Neural underpinning of oscillations....1

1.1.3 Features of neural oscillations as mechanisms for neural communication....2

1.2 Role of the alpha oscillation....3

1.2.1 Alpha oscillation in visual cognition....3

1.2.2 Cellular circuitry of alpha's role in gaiting by inhibition....5

1.2.3 fMRI: alpha-correlated BOLD signal....6

1.3 Studying neural oscillations with concurrent EEG-FMRI....7

1.3.1 Neural underpinnings of the BOLD signal....7

1.3.2 Electrophysiological brain connectomes....7

1.3.3 Correlating EEG and fMRI in concurrent measurements....8

1.3.4 Methodological challenges in concurrent EEG-fMRI....10

1.4 Entrainment: Modulating the alpha oscillation....11

1.5 Variability in alpha peak frequency....14

1.6 Aims of the thesis....14

PROJECT I:....17

TARGETED RHYTHMIC VISUAL STIMULATION AT INDIVIDUAL SUBJECTS' INTRINSIC ALPHA FREQUENCY CAUSES SELECTIVE INCREASE OF OCCIPITOPARIETAL BOLD-FMRI AND EEG FUNCTIONAL CONNECTIVITY....17

Abstract:....18

2.1 Introduction:....19

2.2 Methods:....21

2.3 Results:....27

2.4 Discussion: 29
2.5 References: 34
Appendices: 41
PROJECT II: 46
ALPHA-MEDIATED LONG-RANGE CONNECTIVITY DURING RHYTHMIC VISUAL STIMULATION IN CONCURRENT EEG-FMRI STUDY 46
Abstract: 47
3.1 Introduction: 48
3.2 Methods: 50
3.3 Results: 56
3.4 Discussion: 59
3.5 References: 63
Appendices: 68
GENERAL DISCUSSION: 80
4.1 Summary 80
4.2 Limitations and future applications of alpha entrainment 80
4.3 Cross-frequency coupling 81
4.4 Hierarchical architecture of neural oscillations 84
4.5 Adaptability of oscillations 85
4.6 Clinical relevance: neural oscillations in the context of illness 87
4.7 Advancements in multi-modal imaging techniques 89
4.8 Conclusion and future outlook 92
REFERENCES: 94
CURRICULUM VITAE 122
ACKNOWLEDGEMENTS 122
LIST OF PUBLICATIONS 124
AFFIDAVIT 125
DECLARATION OF AUTHORSHIP: 126

LIST OF FIGURES

Figure 1.1: Gaiting by inhibition hypothesis……4
Figure 1.2: Entrainment theory of neural oscillations…….12
Figure 2. 1: Visual Paradigm…….. 23
Figure 2. 2: Significant EEG functional connectivity…….28
Figure 2. 3: Significant BOLD functional Connectivity…….29
Figure 3.1: Stimulation Paradigm……52
Figure 3.2: Significant Connectivity in EEG and fMRI……..57
Figure 3.3: Trial-by-trial covariance between EEG- and fMRI-derived connectivity……59

LIST OF ABBREVIATIONS

AAS	Average artifact subtraction
ACPC	Anterior commissure posterior commissure
ADHD	Attention-deficit-hyperactivity disorder
ANOVA	Analysis of variance
BOLD	Blood oxygen level-dependent
DAN	Dorsal attention Network
DC	Degree centrality
DMN	Default mode network
ECG	Electrocardiogram
ECoG	Electrocorticography
EEG	Electroencephalogram
EPI	Echo planar imaging
FDG	Fluorodeoxyglucose
FFT	Fast Fourier transform
fMRI	Functional magnetic resonance imaging
FPN	Frontoparietal network
GABA	Gamma-aminobutyric acid
GLM	General linear model
HRF	Hemodynamic response function
Hz	Hertz
IAF	Intrinsic alpha frequency
ICA	Independent component analysis
iCOH	Imaginary coherency
IFG	Inferior frontal gyurs
LFP	Local field potentials
MFG	Medial frontal gyrus
MNI	Montreal Neurological Institute
MPRAGE	Magnetization prepared rapid acquisition gradient echo
MR	Magnetic resonance
NBS	Network-based statistics
PCC	Partial canonical correlation

PET	Positron emission tomography
PSC	Percent signal change
RF	Radio frequency
ROI	Region of interest
SFG	Superior frontal gyrus
SMN	Sensorimotor network
SPL	Superior parietal lobe
SSVEP	Steady-state visually evoked potentials
TR	Acquisition time
tACS	Transcranial alternating current stimulation
VAN	Ventral attention network
V1	Visual area 1

INTRODUCTION

1.1 Neural oscillations

1.1.1 Neural oscillations in cognition

The brain is regarded as a self-organizing, highly complex structure that coordinates the interplay between interconnected and functionally segregated processes to adapt to ever-changing cognitive dynamics. Neural communication between distributed populations of neurons allows for the integration of functionally segregated information that gives rise to cognition and consciousness (Donner & Siegel, 2011; Lopes da Silva, 2013; Siegel et al., 2012). However, understanding how the brain regulates coordination of activity between large neural assemblies has been a central question in cognitive neuroscience. Scientists have proposed that neural oscillations, defined as rhythmic fluctuation of neural activity in distinct frequency bands, may be governing neural communication by modulating synchronicity of brain activity across distributed regions (Fries, 2005a, 2015). Neural oscillations are the most prominent feature in the electroencephalogram (Berger, 1929; Hari & Salmelin, 1997) and can be divided into specific frequency bands thought to have distinct roles in cognition.

1.1.2 EEG: Neural underpinning of oscillations

In 1924, Hans Berger's invention of the electroencephalogram (EEG), marked a pivotal moment in cognitive neuroscience, as for the first-time neural activity could be measured non-invasively in humans. The EEG signal is composed of the summation of local field potentials (LFPs) induced by synchronous post-synaptic activity of large populations of pyramidal cells organized radially along the cortical columns in layer V (Buzsáki et al., 2012; Da Silva, 2009). The excitation of post-synaptic cells creates charge differences (through the opening and closing of ion channels) along the dendritic membrane forming dipoles in the extracellular matrix, which propagate radially throughout the cortex to the scalp electrodes (Buzsáki et al., 2012). Over time, the counteraction between excitatory and inhibitory neural activity leads to fluctuations in the local field potentials that form rhythmic oscillations in the EEG signal (Buzsáki & Draguhn, 2004; Lopes da Silva, 2013). These neural oscillations can be decomposed into distinct frequency bands: delta (2-4 Hz), theta (4-8 Hz), alpha (8-12Hz), beta (13-30Hz), and gamma (30-140 Hz) band (Keitel & Gross, 2016; Lopes da Silva, 2013) The physiological constraints of the underlying neural circuitry, such as time constants of

synaptic activity, give rise to specific frequencies of neural oscillations (Buzsáki et al., 2012; Buzsáki & Draguhn, 2004). Neural oscillations of specific frequency bands seem to play an important role in several cognitive processes and can act across sensory modalities (Siegel et al., 2012b). For example, the alpha oscillation has been associated with anticipatory attention, temporal attention, memory retention, and visual perception (Foxe & Snyder, 2011; Wolfgang Klimesch, 2012). Oscillations of different frequency bands have also been linked to the same cognitive process, such as the alpha and theta band in working memory (Klimesch, 1999; Li et al., 2017; Sauseng et al., 2002) and attention (Fiebelkorn & Kastner, 2019; Keller et al., 2017). The non-specific and cross-modal properties of neural oscillations brings into question on how exactly alterations in oscillatory patterns impact cognition and psychiatric disorders (Başar, 2013; Uhlhaas & Singer, 2006). Developing techniques to localize and experimentally modulate neural oscillations is crucial to advance the understanding of the role of neural oscillations in neural communication.

1.1.3 Features of neural oscillations as mechanisms for neural communication

Two key features of oscillations: frequency and phase, are at the center of regulating neural communication. A somewhat periodic, recurring pattern, such as periods of neural firing and rest, leads to a cyclical pattern that repeats over time. The rate of repetition is termed the frequency of an oscillation. The position within a given cycle of an oscillation is defined as the phase. Two oscillators of the same frequency can synchronize when their phases align. This phase-coupling between neural assemblies allows for information flow between two functionally segregated brain regions during the excitatory phase of their oscillatory activity (Fries, 2015; Varela et al., 2001). Similarly intrinsic brain rhythms can synchronize with external rhythms, thus rhythmically sampling the environment (Busch & Vanrullen, 2010; Lakatos et al., 2019a; Landau & Fries, 2012). As more oscillators synchronize in phase, the amplitude of the synchronized oscillation increases, which is defined as the power of an oscillation (Thut, Veniero, et al., 2011). Cross-frequency coupling occurs when either the phase of a higher frequency and lower frequency intermittently align (phase-phase coupling) or when the phase of a low frequency modulates the amplitude of a higher frequency (phase-amplitude coupling) (Canolty & Knight, 2010; Helfrich et al., 2016). In this sense the phase of long-range low frequency oscillations can regulate the number of cell populations recruited for local sensory processing at higher frequencies (Siegel et al., 2012a), thus, parcellating brain activity and processing of sensory input across time. This is often referred to as the

"communication by coherence" hypothesis (Fries, 2015). Ongoing changes in frequency, phase and power of neural oscillations have been associated with working memory (Roux & Uhlhaas, 2014; Sauseng et al., 2002), attention (Fiebelkorn & Kastner, 2019; Landau & Fries, 2012), and sensory processing of the external environment (Haegens & Zion Golumbic, 2018; Rufin VanRullen, 2016).

1.2 Role of the alpha oscillation

1.2.1 Alpha oscillation in visual cognition

The most prominent oscillation in EEG during wakeful rest is the posterior alpha oscillation (7-12 Hz) (Niedermeyer & Lopes da Silva, 1999). Initially alpha was thought to reflect cortical idling, as high alpha power observed during eyes-closed, resting wakefulness, diminish with cognitive demand (Pfurtscheller et al., 1996)). But evidence from visual working memory and spatial attention studies suggest the alpha oscillation has a more active role in regulating cortical excitability. Increased posterior alpha power in task-irrelevant regions correlated with increased memory load during working memory retention (Haegens et al., 2010; Sauseng et al., 2009). Increased alpha power in the unattended hemisphere correlated with decreased detection of distractor items in spatial attention tasks (B. F. Händel et al., 2011; Thut et al., 2006; Worden et al., 2000). In visual perception, high pre-stimulus alpha power was associated with decreased visual discrimination/detection (Ergenoglu et al., 2004b; Lange et al., 2013; Van Dijk et al., 2008). This suggests the alpha rhythm has an inhibitory role that inhibits task-irrelevant brain regions (Wolfgang Klimesch et al., 2007b).

However, studies investigating the phase of pre-stimulus alpha lead to further insight into the role of alpha. Studies looking pre-stimulus alpha phase during visual detection tasks showed difference in alpha phase of detected and non-detected stimuli (Busch et al., 2009; Mathewson et al., 2009). In a concurrent EEG-fMRI study by Scheeringa and colleagues (2011), a decrease in BOLD activity in V1 was correlated with stimuli presented at the peak of alpha phase as compared to stimuli arriving at the trough of the alpha phase. Combined these results show the influence of high alpha power occurs at a certain phase of the alpha cycle rather than over the entire cycle (Mathewson et al., 2011). The alpha rhythm therefore rather reflects variability in cortical excitability. Subsequently the alpha rhythm gates information flow across the visual processing stream by regulating the neural excitability

with alpha phase and neural gain, or the recruitment of synchronized neural populations, through alpha power.

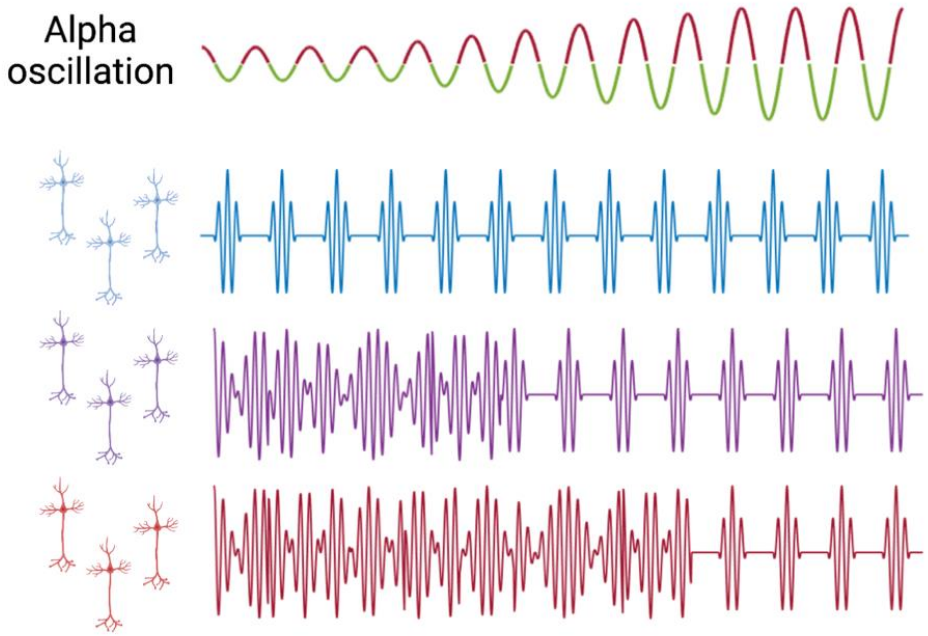

Figure 1.1: Gaiting by inhibition hypothesis. Graphical illustration of the gaiting by inhibition hypothesis coined by (Jensen et al 2011). It is proposed that the alpha oscillation regulates neural activity of local sensory neural populations through both power and phase. The parts of the alpha cycle in red indicate inhibitory phase and the green indicates the excitatory phase of the alpha oscillation. As the alpha power increases, the activity of the different underlying neural populations (as indicated by different colors) oscillating in the gamma frequency becomes more synchronized. Oscillations in the figure were generated with a customized Matlab script and the figure was composed with BioRender.com

Early studies implementing attentional cues to elicit changes in posterior alpha power already suggest that modulation of the alpha rhythm lies under top-down control (Hanslmayr et al., 2007; Snyder & Foxe, 2010). More recent studies showed that expectancy of stimulus presentation induced through temporal cueing induced alpha phase modulations (Samaha et al., 2015). Furthermore, studies implementing a two-choice visual detection task and analyzing false alarm trials (trails in which no visual stimuli was presented but subjects subjectively perceived seeing a stimulus) showed alpha power correlated with subjective confidence or judgement rather than with visual discrimination ability (Iemi et al., 2017; Samaha et al., 2017). Similar findings were found in a two-choice auditory discrimination task (Wöstmann et al., 2019). These studies provide evidence for modulation of alpha phase and power in sensory areas lying under top-down control.

1.2.2 Cellular circuitry of alpha's role in gaiting by inhibition

In visual processing, the selective binding and integration of sensory input requires the coordination of both feedforward and feedback inputs (Felleman & Van Essen, 1991; Lamme et al., 1998; Spillmann & Werner, 1996), which are also known respectively as bottom-up and top-down processes. The dynamic relaying between higher- and lower-order areas has been extensively studied and is thought to occur either through direct cortico-cortical or indirect cortico-thalamo-cortical interactions (Sherman & Guillery, 2013; Womelsdorf et al., 2014). In the context of neural oscillations, phase coupling of neural activity between frequencies is thought to reflect dynamic relaying of feedforward and feedback information across cortico-cortical and cortico-thalamic connections. Yet due to the spatial limitations of EEG, it is still not known through which pathways neural oscillations coordinate neural activity. The origins of alpha generators have been extensively studied in invasive electrophysiology studies in animals, which have found alpha oscillations to originate from deep, infragranular layers in sensory cortices (Buffalo et al., 2011; Spaak et al., 2012). Rhythmic activity from inhibitory interneurons suppresses neural excitability vertically across cortical columns (Spaak et al., 2012; Van Kerkoerle et al., 2014) and gait inhibition of cortical excitability in local sensory regions. This rhythmic inhibition correlates with local amplitude changes of the alpha rhythm (Haegens et al., 2015). Studies comparing thalamic spike rate between attended and unattended trials showed that increased thalamic spiking and increased cortical alpha-thalamic coherence during attended trials in primates (Bollimunta et al., 2011; Saalmann et al., 2012). Furthermore, bursts of thalamic firing is thought to correlate with the rhythmic inhibition dictated by alpha phase (Vijayan & Kopell, 2012; Womelsdorf et al., 2014). Thalamic projections primarily target outputs in supragranular layer (Sherman & Guillery, 2005), which is in line with studies find alpha activity across cortical layers (Bollimunta et al., 2011; Haegens et al., 2015; Scheeringa et al., 2016). Yet measurements of alpha activity in cortical and subcortical layers on a microscopic level gives little information on the macroscopic, long-range relaying of information. Concurrent EEG-fMRI can be implemented to overcome the poor spatial resolution of EEG and study long-range connections by means of alpha phase coherency non-invasively in humans.

1.2.3 fMRI: alpha-correlated BOLD signal

Mixed results have been reported correlating BOLD and the alpha oscillation. The variability in results partially arises from different modalities of the alpha oscillation being correlated with the BOLD signal during task or rest. Studies correlating high alpha power with fMRI seed-based connectivity during rest have shown decreased connectivity between V1 and other visual areas yet increased BOLD connectivity between V1 and the thalamus and prefrontal areas (Scheeringa et al., 2012), suggesting local inhibition in sensory areas may occur through long-range connectivity along thalamocortical pathways. Ongoing fluctuations in alpha phase correlated with connectivity in frontoparietal networks, which has been associated with top-down modulation of initiation and change in attentional control (Sadaghiani et al. 2012). During a visual attention task, trial-by-trial alpha power negatively correlated with the BOLD response (Scheeringa et al., 2009), whereas pre-stimulus alpha power did not correlate with the evoked BOLD response in occipital regions (Scheeringa et al., 2011a). However, stimulus arriving at the peak of the alpha phase correlated with a reduced BOLD signal in visual areas (Scheeringa et al., 2011b). These findings support the role of alpha as gaiting by inhibition. These studies used alpha measures derived from globally averaged or electrode signals at the scalp, which does not accurately portray spatial information of the alpha oscillation (Lai et al., 2018; Wirsich et al., 2020). A study examining source-localized alpha power during a selective attention task showed that occipital alpha power contralateral to the attended stimuli correlated with the BOLD response in down-stream ventral visual areas, which the authors interpreted as gaiting of information flow between early and downstream visual areas for attended stimuli (Zumer et al., 2014). Furthermore, Zumer et al found an inverse correlation between the BOLD signal in the dorsal attention network and alpha power (Zumer et al., 2014). In resting state studies, spatial networks of phase-phase coupled source-localized alpha sources correlated with the fMRI default mode network (Brookes et al., 2011), somatosensory and visual network (Hipp et al., 2012). A study analyzing the spatial distribution of transient changes in alpha power and phase coupling of the precuneus with other brain regions was highly correlated with occipital parietal regions that were associated with a dorsal higher order functional connectivity network in both modalities (Vidaurre et al., 2018c). However, other band-limited neural oscillations, such as the beta band, also correlate with fMRI functional networks including the default mode network (Wirsich et al., 2020), somatosensory network and visual network (Hipp et al., 2012). More research is needed to understand how ongoing alpha-correlated functional connectivity networks vary during visual perceptual tasks.

1.3 Studying neural oscillations with concurrent EEG-FMRI

1.3.1 Neural underpinnings of the BOLD signal

To understand how the BOLD signal correlates with neural oscillations in EEG signal, it is first important to understand how the BOLD signal reflects neural activity. The BOLD signal indirectly measures neural activity by measuring the ratio of deoxygenated to oxygenated blood within a brain region (Ogawa et al., 1992). During synaptic activity, the opening of ion channels and transmission of neurotransmitters uses ATP, which requires oxygen to regenerate (Attwell & Iadecola, 2002). At the site of neural activity, initially there is more deoxygenated hemoglobin, followed by an increase in local cerebral blood flow and oxygenated hemoglobin (Attwell & Iadecola, 2002; Logothetis, 2008). The delayed response of the cerebral blood flow following oxygen consumption is about six seconds and is often modeled with a canonical hemodynamic response function (HRF) (Friston, 2002; Lindquist et al., 2009). Under rest, slow fluctuations in the fMRI signal across discrete cortical regions oscillating with a frequency of less than 0.1 Hz are observed (Fox, Corbetta, et al., 2006; Lowe et al., 1998). The spatial reconfiguration of functional connectivity networks at this ultraslow frequency has been associated with distinct cognitive processes such as attention (Fox, Snyder, et al., 2006), cognitive control (Dosenbach et al., 2007; Vincent et al., 2008), and sensory processing (Beckmann et al., 2005; De Luca et al., 2005). It has become of increasing interest to understand how these connectivity dynamics relate to distinct cognitive processes.

1.3.2 Electrophysiological brain connectomes

Mapping the spatial configuration of neural oscillations in distinct frequency bands has been at the center of understanding the roles of neural oscillations. Band-specific EEG signal indexes synchronous fluctuations in neural activity between excitatory and inhibitory states at a given frequency (Musall et al., 2014). Measures of synchronicity, such as phase coherency, serve as good measures for mapping the interaction between tightly coupled brain regions (Bowyer, 2016). Like with fMRI time series, covariation in coherency across time between brain regions, can be considered a proxy for functional connectivity. However due to radial volume conductance of local field potentials in the brain, EEG electrodes pick up mixed signal from different neural sources (Buzsáki et al., 2012) preventing accurate separation of

neural sources. Scientists have circumvented the issue of poor spatial resolution in EEG, by reconstructing spatial source estimates from scalp EEG data (Schoffelen & Gross, 2009a). Local, inter-connected, and functionally homogenous populations of cells (over 1 cm^2) show high degree of synchronization and subsequent local increase in signal to noise ratio (Murakami & Okada, 2006; P. Nunez & Srinivasan, 2006). Taken together with the geometry of the head and estimates of tissue conductance, the spatial location of underlying neural sources can be estimated (Schoffelen & Gross, 2009a). However, the effects of field spread and volume conductance cannot entirely be eliminated in source space. The so-called signal leakage in source space can lead to artificially high phase- or amplitude-coupling between two sources (Lai et al., 2018; Schoffelen & Gross, 2009a). For phase coupling connectivity analyses, signal leakage can be corrected for by removing zero-phase lag interactions. Using only the imaginary part of phase coherence between two sources inherently removes zero-phase lag interactions (Nolte et al., 2004; Sadaghiani et al., 2022). An equivalent technique can be applied for amplitude-coupling across sources by orthogonalizing all possible region pairs (Colclough et al., 2015; Hipp et al., 2012). In concurrent EEG-fMRI studies, the high spatial resolution of fMRI can complement electrophysiological connectomes and studies have shown networks derived from both modalities spatially overlap (Brookes et al., 2011; Hipp et al., 2012; Wirsich et al., 2020).

1.3.3 Correlating EEG and fMRI in concurrent measurements

The observation that full-band EEG (i.e. the raw EEG signal composed of all neural oscillations) fluctuates at infra-slow frequencies (Monto et al., 2008) and correlates with fluctuations in resting state networks (Hiltunen et al., 2014) lead to the hypothesis that long range connectivity in both faster neural oscillation and in slow fluctuating fMRI signal may represent similar functional dynamics (Engel et al., 2013; Mostame & Sadaghiani, 2021). Fluctuations within specific resting state networks have also been associated with fluctuations in power of band-limited neural oscillations (Jann, Kottlow, et al., 2010; Mantini et al., 2007). The earliest studies used specific EEG features and related these with changes in resting state networks in fMRI (Laufs et al. 2003, Scheeringa et al 2011, de Pasquale et al 2010). However these studies relied heavily on a priori hypotheses of the spatial relationship of the two modalities within a given network of interest (Huster et al 2012). Data-driven approaches have shown that low frequency-specific EEG networks overlap with canonical resting state functional connectivity networks (Brookes et al., 2011; Deligianni et al., 2014;

Wirsich et al., 2017). Yet static functional connectivity networks hold little information on how electrophysiological and fMRI networks change over time.

An increasing trend in neuroscience is studying dynamic changes in brain connectomes, or distributed connections in the brain exhibiting coupling of neural or vascular signals, using multi-imaging modalities. The coupling and uncoupling of functionally related brain regions organized in networks may reflect macroscopic neural activity patterns that underly cognition (Hutchison et al., 2013). As mentioned in section 1.5, functional coupling in fMRI occurs at an ultraslow frequency and remains relatively stable over time in distinct functional networks under rest (Bright et al., 2020). However, the vascular response in fMRI and neural response measured through EEG are vastly different in nature and while they share signal arising from the same neural origins, they also may represent different neural properties (Hermes et al., 2017; Sepideh Sadaghiani & Wirsich, 2020). Data-driven electrophysiological connectivity studies have shown networks to be modulated on a fast time scale (100ms - 300ms) (Baker et al., 2014; Vidaurre et al., 2018c). Fast network is undetectable in fMRI. The use of source-localized electrophysiological connectivity in combined EEG-fMRI studies, has become increasingly popular as EEG may add complementary information about spatial reorganization of network dynamics on a faster time scale (Sadaghiani et al., 2022). A few, but nominal studies have shown that the spatio-temporal organization of ongoing functional connectivity networks derived from electrophysiology correlate with fMRI-derived functional connectivity networks (Sadaghiani & Wirsich, 2020; Vidaurre et al., 2018; Wirsich et al., 2020). Temporal dynamics of functional connectivity networks have shown to be frequency-specific (Mostame & Sadaghiani, 2021), which provides evidence for frequency-specific information exchange. Although there is considerable overlap between frequency-specific connectivity networks in rest (Wirsich et al 2020) and in task (Nentwich et al., 2020). When putting these electrophysiological connectomes into the context of hierarchical organization of communication in the brain during segregation and integration, it has been proposed that dynamic relaying of information between higher and lower order brain areas can occur simultaneously through communication in and between neural oscillations (Florin & Baillet, 2015; Fries, 2015; Sadaghiani et al., 2022). However, to what extent these neural oscillations play a role in either top-down or bottom-up relaying of information is not known. Furthermore, the type of long-range pathways, either through cortical or subcortical connections, remains to be elucidated. An external stimulus can be implemented to activate long-range connections involved in visual processing. I propose studying concurrent

electrophysiological and fMRI connectivity under visual stimulation to activate connections involved in visual processing.

1.3.4 Methodological challenges in concurrent EEG-fMRI

The strong magnetic field in an MR scanner poses safety and data quality issues and in combined EEG-fMRI due to the electromagnetic induction. The biggest safety concern is radiofrequency-related heating of electrodes that may cause burning. Increased field of view, shorter TR times or scanner magnetic field strength can increase radiofrequency magnetic field magnitude and must be adjusted accordingly (Lemieux et al., 1997). This often poses a tradeoff between smaller field of view or longer acquisition times (TR) in the fMRI. Furthermore, the switching of the magnetic field gradients causes induces large currents in the EEG electrodes, which are 400 times larger than neurophysiological signal (Allen et al., 2000). Also, any movement inside of the magnetic field including pulsatory movement of arterial blood vessels induce electric currents that are measured by the scalp electrodes (Yan et al., 2009, 2010). The gradient and the ballistocardiogram artifact can be removed using a sliding window approach to subtract an adaptive artifact template (Allen et al., 2000). However, this reduces the signal to noise ratio by smoothing out the signal. Therefore, only large effects in the EEG signal can be tested in concurrent EEG-fMRI. Furthermore, the slightest muscular movements are amplified in the EEG signal, requiring stringent movement-related artifact removal and many trial repetitions. In the fMRI, the scalp electrodes can cause field inhomogeneities and signal loss (Bonmassar et al., 2001). It is therefore advised to test experimental paradigms in EEG and fMRI separately before attempting concurrent EEG-fMRI studies to account for reduced signal to noise ratio.

The synergistic benefit of concurrent EEG-fMRI to increase temporal and spatial resolution also poses the largest challenge in data analysis methods. Fluctuations in EEG and fMRI signal occur on vastly different time scales. Correlating these time scales often is requires averaging EEG features across fMRI acquisition times to create a comparable time course or deconvolving fMRI time course to the sampling rate of the EEG signal (Abreu et al., 2018). Averaging across fMRI acquisition times results in EEG features that correlate with fMRI better in low frequencies (Deligianni et al., 2014). Correspondingly, dynamic functional connectivity analyses using sliding window approaches have to find a window length that is large enough to be informative about fMRI (Leonardi & Van De Ville, 2015; Shine et al.,

2016), yet small enough to see considerate changes in EEG (Chang et al., 2013; Wirsich et al., 2020). One way to overcome this is to compare variance of time varying EEG and fMRI connectivity under different experimental conditions. Spatially, the resolution of source-estimated EEG features corresponds ~1-2cm^3. Whereas the spatial resolution in fMRI is ~2-3mm^3. However, in connectivity studies time series are averaged across parcellated brain regions making spatial scales comparable between EEG and fMRI.

1.4 Entrainment: Modulating the alpha oscillation

Accumulating evidence supports that rhythmic activity and synchronization across distributed brain areas governs communication. Synchronization may occur either bi-directionally between two independent oscillators (Lakatos et al., 2019a; A. Pikovsky et al., 2001; Varela et al., 2001) or one oscillator may unidirectionally drive synchronization of other oscillators through phase resetting (Lakatos et al., 2019a; A. Pikovsky et al., 2001; Schroeder & Lakatos, 2009). The latter is termed entrainment. Visual sensory sampling of external stimuli occur rhythmically within the theta and alpha band range (Rohenkohl & Nobre, 2011; Rufin VanRullen, 2016) and it has been proposed that entrainment of neural oscillators to external stimuli predictively prepares the brain for effective information flow and sensory binding by segregating regions oscillating within phase from those out of phase (Fries, 2015; Lakatos et al., 2019a; Ronconi et al., 2018). Entrainment has also been shown to be supramodal with entrainment occurring across sensory modalities (see Bauer et al., 2020 for a review). In a natural setting, entrainment is thought to lie under top-down control, as increased coherency in frequency-specific oscillation bands have been associated with anticipatory attention and temporal sampling of the environment (Fiebelkorn et al., 2013; Rohenkohl & Nobre, 2011; VanRullen et al., 2011). By its supramodal nature of driving synchronization across brain regions and across modalities, entrainment has been proposed to selectively alter functional connectivity patterns (Helfrich et al., 2019; Lakatos et al., 2019a). Yet this remains to be tested.

The concept of entrainment has also been employed by scientists to experimentally drive modulatory changes in brain activity with external rhythmic stimuli (de Graaf et al., 2013; Mathewson et al., 2012; Spaak et al., 2014; Thut et al., 2011) and test for the communication by coherency hypothesis (Lakatos et al., 2019; Van Diepen et al., 2019). Repetitive transcranial stimulation or rhythmic light stimulation are non-invasive tools commonly used

to induce neural entrainment. A 10 Hz electrical pulse administered with transcranial alternating current stimulation (tACS) showed entrainment of the alpha rhythm evaluated by increase in alpha power and phase locking between neural alpha and the external rhythm (Helfrich et al., 2014). Studies employing rhythmic flickering light at 10 Hz have shown increased alpha phase locking (de Graaf et al., 2013; Mathewson et al., 2012) and alpha power (Spaak et al., 2014). These studies also showed behavioral fluctuations in response to entrained alpha during a visual perception.

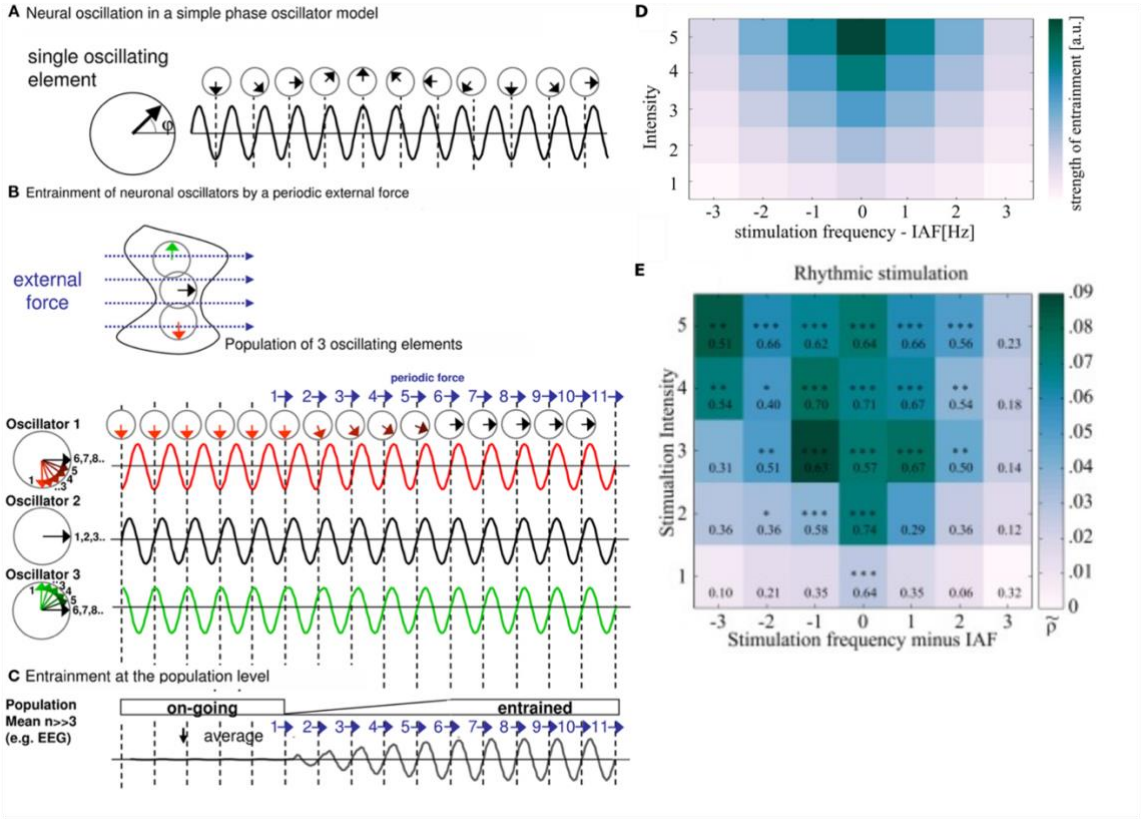

Figure 1.2: Entrainment theory of neural oscillations. A) Schematic of phase angles of a neural oscillation. B) Theoretic entrainment of uncoupled neural oscillators to an external driving force. C) Effects of entrainment over time portrayed by increased synchronization and increase in neural power. Figures A, B, and C were adapted with permission from Thut, et al., 2011. D) Arnolds Tongue principle of entrainment. Strength of entrainment is thought to increase with intensity of light stimulus and/or decreased distance of driving frequency from IAF. E) Experimental phase locking index plotted for different stimulation strengths and driving frequencies. Figure D and E were adapted with permission from Notbohm, et. al., 2016.

However, it is still debated whether rhythmic light stimulation truly drives synchronization of intrinsic oscillations to the external rhythm or whether rhythmic stimulation evokes the superposition of steady-state visually evoked potentials (SSVEPs) on intrinsic neural oscillations (Capilla et al., 2011; Haegens & Zion Golumbic, 2018; Keitel et al., 2014, 2019). The sudden increase in luminance elicits a strong visual evoked response (Regan, 1982).

Rhythmic presentation of flickering light thus elicits a steady-state visual evoked response that induces strong phase coherency within visual areas and subsequently increases oscillatory power (Capilla et al., 2011). In part, previous analysis methods investigating alpha power are insufficient in discerning between increase in amplitude of intrinsic neural oscillations or SSVEPs (Keitel et al., 2019; Van Diepen et al., 2019). Any rhythmic activity with a sinusoidal wave shape will induce an increase in spectral power (Keitel et al., 2019; Zoefel et al., 2018) making measures of oscillatory power insufficient for measuring degree of entrainment. The strong steady-state evoked response will also artificially increase phase locking between the external light stimulus and neural oscillations (Van Diepen & Mazaheri, 2018; Rufin VanRullen, 2016). Measures of phase coupling between neural sources serve as a better proxy for measuring degree of entrainment. Further concerns have raised that entrainment of neural oscillations to rhythmic stimuli in sensory areas can only occur if synchronization of ongoing neural oscillations is observed in the absence of external stimuli (Haegens & Zion Golumbic, 2018).

A nominal EEG study comparing degree of entrainment, as measured by phase coherency, at rhythmic and arrhythmic flickering at the intrinsic alpha frequency (IAF) and neighboring control frequencies showed the highest degree of entrainment occurred for rhythmic stimulation at the IAF (Notbohm et al., 2016; Notbohm & Herrmann, 2016). Due to the phenomena of resonance, less energy is required to drive synchronization of two oscillatory sources, when the frequency of the driving force approaches the frequency of the intrinsic oscillation (Notbohm & Herrmann, 2016; A. Pikovsky et al., 2001). The Arnold's Tongue principle can be applied in entrainment paradigms to control for transient evoked responses due to light stimulation that are superpositioned on ongoing neural activity by flickering at control frequencies near the frequency of the intrinsic neural oscillations and comparing degree of phase coherency to rhythmic stimulation at the intrinsic frequency. It remains to be clarified whether the spatial distribution of entrained alpha mimics intrinsic alpha maps. Comparing source-localized alpha connectivity maps under rest and under entrainment would clarify the effect of rhythmic light flicker on ongoing neural activity and help classify spatial distribution of modulated alpha.

1.5 Variability in alpha peak frequency

Inter- and intra-subject variability in the peak alpha frequency have been reported (Barzegaran et al., 2017; Haegens et al., 2014; Klimesch et al., 1996; Notbohm & Herrmann, 2016). Alterations in the peak alpha frequency and amplitude of the alpha band have been reported during aging and in neurodegenerative diseases (Klimesch, 1999; Uhlhaas & Singer, 2006). Variability is also observed in age-matched, healthy individuals. A study localizing alpha sources showed some individuals present with more than one peak alpha frequency with lower alpha frequencies being localized in occipitoparietal regions and higher alpha frequencies being localized in occipitoparietal regions (Barzegaran et al., 2017). The alpha peak frequency also shifts with cognitive demand (Haegens et al., 2014a; Maurer et al., 2015; Mierau et al., 2017). Recent research suggests that brain oscillations are coupled with rhythms of the body, such as breathing rate and heart rate, and that the frequency of band-limited neural oscillations may adapt to optimize cross-frequency coupling across the brain and body (Klimesch, 2018). It has also been proposed that shifts in the alpha peak may optimize temporal sampling and integration of sensory input during cognition (Mierau et al., 2017; Samaha et al., 2015), in which areas with different alpha peak frequencies may be processing functionally distinct information (Barzegaran et al., 2017; Christoph S. Herrmann et al., 2016; Mierau et al., 2017). The alpha peak frequency has also been shown to correlate with amplitude of the vascular response to light stimulation in visual areas with higher alpha frequencies exhibiting a reduced hemodynamic response (Koch et al., 2008). However, it is still unclear whether there are several alpha generators or shifts in the alpha peak frequency measured at the scalp represent localized shifts in one alpha oscillator over time. Studying modulations in individual-specific alpha oscillations on a group level will take into account interindividual variability in the alpha oscillation and alpha-related BOLD response and will help clarify differential findings.

1.6 Aims of the thesis

Although many advances have been made in classifying the functional role of the alpha oscillation in visual perception as gaiting information flow by inhibition, it is still debated how modulatory changes in the alpha rhythm govern visual perception and awareness. In part many of these studies looked at correlational changes in the alpha rhythm and behavior. Since other canonical neural frequency bands, such as theta and delta (Helfrich et al., 2017, 2019;

Sauseng et al., 2015), have also been correlated with attention and top-down modulation of neural processes and may use phase to govern information flow (Landau & Fries, 2012; VanRullen, 2016), it proves difficult to disentangle the role of the alpha rhythm. Combined EEG-fMRI studies prove useful in creating spatiotemporal maps of neural oscillations. Combined EEG-fMRI resting state studies have mapped transient changes in the alpha rhythm to higher order posterior areas, frontoparietal areas and the default mode network (Brookes et al., 2011; Chang et al., 2013; Vidaurre et al., 2018c). However other canonical frequency bands also correlate with these functional connectivity networks under rest (Hiltunen et al., 2014; Hipp et al., 2012; Wirsich et al., 2020). It has been suggested that transient changes in alpha-functional connectivity maps may reflect changes in information processing during cognitive processes such as visual perception. This remains to be tested experimentally.

In my PhD project I attempt to address several limitations of previous studies investigating the role of the alpha rhythm. Most previous observations on the alpha oscillation were derived from correlational findings from spontaneous changes in the alpha rhythm. I intend to study controlled modulations to the alpha rhythm by using rhythmic flickering light to entrain the ongoing neural oscillations. However, individuals present with variable peak alpha frequencies, which have been overlooked in most previous entrainment studies. I take advantage of the Arnold's tongue principle, that states entrainment should be strongest when the driving frequency matches the frequency of the receiving source, by targeting individual's intrinsic alpha frequency. I propose rhythmic flickering light entrains ongoing neural oscillations by driving increased synchronization in posterior occipital and parietal alpha networks. In the first part of my study, I set up and test an entrainment paradigm to test neural synchronization in both EEG and fMRI during light entrainment of the IAF. Taking the methodical limitations of separating visual-evoked response from ongoing neural activity in the alpha rhythm into consideration, I use neighboring frequencies and arrhythmic stimulation to control for synchronous activity induced by SSVEPs. Source localized alpha phase coherency in the EEG and fMRI-derived functional connectivity are used as a proxy for neural synchronization in the alpha rhythm. I hypothesize the degree of entrainment, as measured by increased synchronicity, should be strongest for the stimulation at the intrinsic alpha frequency as compared to arrhythmic stimulation and rhythmic stimulation at neighboring frequencies in both EEG and fMRI imaging modalities.

I also develop a novel application of concurrent EEG-fMRI by studying functional connectivity changes during visual entrainment. Recent advances in time-varying connectivity methods in concurrent EEG and fMRI have shown dynamic modulation of functional connectivity correlates across different time scales during rest. I build on these findings by investigating fMRI- and neurophysiology-derived functional connectivity during visual stimulation. I argue by externally modulating the alpha rhythm with an external light stimulus, alpha modulations are imposed along the visual pathway allowing us to study upstream connectivity changes involved in visual perception. The entrainment paradigm from my first study was implemented in a concurrent EEG-fMRI study to investigate whole brain connectivity changes involved in visual processing. I predicted stimulation at the IAF should increase long-range connectivity between visual and higher order areas. The novel technique of looking at concurrent task-based connectivity shows the potential of concurrent EEG-fMRI connectivity in spatial localization of hierarchical brain connections during task.

PROJECT I:

TARGETED RHYTHMIC VISUAL STIMULATION AT INDIVIDUAL SUBJECTS' INTRINSIC ALPHA FREQUENCY CAUSES SELECTIVE INCREASE OF OCCIPITOPARIETAL BOLD-FMRI AND EEG FUNCTIONAL CONNECTIVITY

Cilia Jaeger[1,2,3], Rachel Nuttall[1,2,5], Juliana Zimmermann[1,2], James Dowsett[4], Christine Preibisch[1,2,6], Christian Sorg[1,2,7], Afra Wohlschlaeger[1,2]

[1]Department of Diagnostic and Interventional Neuroradiology, Klinikum rechts der Isar, Technical University of Munich, Munich, Germany

[2]TUM Neuroimaging Center (TUM-NIC), Klinikum rechts der Isar, Technical University of Munich, Munich, Germany

[3]Graduate School of Systemic Neuroscience, Ludwig Maximilian University, Planneg-Martinsried, Germany

[4]Department of Psychology, Ludwig Maximilian University, Munich, Germany

[5] Department of Anesthesiology, Klinikum rechts der Isar, Technical University of Munich, Munich, Germany

[6]Clinic for Neurology, Klinikum rechts der Isar, Technical University of Munich, Munich, Germany

[7]Department of Psychiatry, Technical University of Munich, Munich, Germany

Abstract:

Neural oscillations in distinct frequency bands are ubiquitous in the brain and play a role in many cognitive processes. The "communication by coherence" hypothesis, poses that the synchronization of low frequency oscillations regulates information flow across long-range connections. Specifically, the posterior alpha frequency band (7-12 Hz) is thought to gate bottom-up visual information flow by inhibition during visual processing. Evidence shows that increased alpha phase coherency positively correlates with functional connectivity in resting state connectivity networks, supporting alpha mediates neural communication through coherency. However, these findings have mainly been derived from spontaneous changes in the ongoing alpha rhythm. In this study, we experimentally modulate the alpha rhythm by targeting individuals' intrinsic alpha frequency with sustained rhythmic light to investigate alpha-mediated synchronous cortical activity in both EEG and fMRI. We hypothesize increased alpha coherency and fMRI connectivity should arise from modulation of the IAF as opposed to control frequencies in the alpha range. Sustained rhythmic and arrhythmic stimulation at the IAF and at neighboring frequencies within the alpha band range (7-12 Hz) was implemented and assessed in a separate EEG and fMRI study. We observed increased cortical alpha coherency in the visual cortex during rhythmic stimulation at the IAF as in comparison to rhythmic stimulation of control frequencies. In the fMRI, we found increased functional connectivity for stimulation at the IAF in visual and parietal areas as compared to other rhythmic control frequencies by correlating time courses from a set of regions of interest for the different stimulation conditions and applying network-based statistics. This suggests that rhythmic stimulation at the IAF frequency induces a higher degree of synchronicity of neural activity across the occipital and parietal cortex, which supports the role of the alpha oscillation in gating information flow during visual processing.

Key words: entrainment, alpha oscillation, individual alpha frequency, visual flicker, imaginary coherency, fMRI connectivity, EEG-fMRI, occipitoparietal cortex

2.1 Introduction:

Neural oscillations play an important role in cognition by regulating neural communication between brain regions. Specifically, low frequency oscillations, arising from the synchronization of neural activity across distributed neural assemblies, are thought to serve as a mechanism for information flow across long-range connections.[1,2] The alpha oscillations (7-12 Hz) are the most prominent neural oscillations in EEG during wakeful rest.[3,4] They are low-frequency oscillations thought to gate communication between local sensory processes in visual perception through inhibition.[5,6]

Power of alpha oscillations has been associated to inhibition. In resting state fMRI studies, an inverse correlation between BOLD activity and alpha power in occipital regions has been reported.[7–9] These findings suggest the alpha rhythm acts as an inhibitory oscillation dampening cortical excitability in sensory areas when alpha power is high.[10–13] Evidence from visual detection studies support the 'gating by inhibition' hypothesis. Visual task performance correlated with pre-stimulus alpha phase[14,15] suggesting neural activity gets enhanced then suppressed within a cycle or phase of the alpha oscillation. An increase in alpha power arises from the synchronization of neural activity in more neural populations, which subsequently gates information flow.[2,5,16,17]

The prime source of information on neural oscillations are electrophysiological measurements, in particular scalp EEG. Although scalp EEG is well suited for studying neural oscillations with high temporal resolution, exact source reconstruction of the neural origin of oscillators is limited in EEG[18] due to the underlying static electromagnetic inverse problem.[19] Therefore, localization of alpha oscillation generators presents a problem, which limits the characterization of the distinct neural processes giving rise to the alpha oscillation.

Functional MRI represents the method of choice for spatial localization at rather high resolution and can be used to assist source localization of electrical neural oscillations. However, fMRI studies on long-range connectivity associated with the alpha rhythm report mixed results. A study correlating alpha power and BOLD functional connectivity found the primary visual cortex positively correlated with areas associated with the default mode network, yet negatively correlated with other visual areas.[9] The strength in functional connectivity between the default mode network and dorsal attention network also inversely

correlate with spontaneous alpha power.[20] Whereas, a positive correlation between spontaneous increase in alpha phase coherency and BOLD connectivity within the frontoparietal attention network [21] and a dorsal default mode network.[22] Divergent findings may be explained by the fact that two different EEG measures, amplitude and phase coherency, are being compared to BOLD functional connectivity. However, neural communication is thought to arise from temporal coupling of neural activity across neural populations[2,23]It is therefore conducive to use statistical measures assessing temporal coupling of spatially distinct neural activity in both modalities, such as phase coherency in EEG[24,25] and BOLD function connectivity.[26] Furthermore, these studies investigated spontaneous changes in alpha rhythm in concurrent measurements. Studying experimentally modulated changes in the alpha rhythm in a controlled manner would be more informative in classifying top-down, long-range connections associated with the alpha rhythm.

Several studies have shown evidence that rhythmic light stimulation can entrain ongoing neural oscillations in the visual pathway.[27–29] Entrainment, defined as the synchronization of neural oscillation to an external rhythmic stimulus,[27,30] allows for selective alterations in the alpha frequency band. One study, taking individual variability in individual peak intrinsic alpha frequency (IAF) into account, showed increased alpha phase synchronicity occurring with decreased distance of the stimulation frequency from the IAF.[31,32] The study showed that entrainment of neural oscillators follows the Arnolds tongue principle,[31,33] which states phase synchronicity and entrainment increases when the driving flicker frequency approaches the peak frequency of the neural oscillators. ,[31,33] Thus showing entrainment of the intrinsic alpha rhythm with rhythmic light. A study by Parkes et al. (2004) reported a decreased BOLD response in V1 for rhythmic stimulation in the alpha range as compared to arrhythmic stimulation. They concluded the decreased BOLD response reflected increased inhibition due to entrainment of the alpha oscillation, that differed from the event-related BOLD response to random flicker-induced luminance changes during arrhythmic stimulation. However, the question still remains whether entrainment of the IAF induces similar increase in alpha-mediated cortical synchronicity in EEG and fMRI.

In line with the communication by coherency theory, we propose that entrainment of the alpha oscillation should increase synchronous neural activity as measured by increased alpha phase coherency and BOLD functional connectivity. In this study, a novel light stimulation tool was used that can be adjusted to sub-millisecond precision allowing for frequency steps

of 0.01 Hz or finer. Participants intrinsic alpha frequency was determined from eyes-closed, resting-state EEG measurement. Flicker-stimulation at the IAF and neighboring frequencies of the alpha range were assessed during independent EEG- and fMRI experiments. Degree of synchronicity was assessed across stimulation conditions using source-localized imaginary coherency in the EEG study and correlation matrices in the fMRI study.

2.2 Methods:

2.2.1 Participants:

All participants gave written consent before participation and had normal or corrected-to-normal vision. Although the studies were conducted during different time periods, some of the participants chose to participate in both studies. The study was approved by an in-house ethics committee at TUM School of Medicine at the Technical University Munich.

2.2.1.1 EEG study participants: 16 young, healthy individuals (10 females, mean age = 26.2 years, SD = ± 3.0 years) participated in an EEG study. One subject was excluded from the analysis due to excessive noise during the testing session, resulting in 15 participants (9 females, mean age = 26.3, SD = ± 3.0 years).

2.2.1.2 fMRI study participants: 25 young, healthy participants (15 females, mean age = 28.7 years, SD = ± 2.7 years) were recruited for a separate fMRI study. Two subjects did not have a visible alpha peak frequency and the study was discontinued after the resting state EEG measurement. One subject exhibited rapid fatigue during the study and was subsequently excluded. Four more subjects were excluded for excessive head movements. The data of the remaining 18 subjects (12 females, mean age = 26.0 years, SD = ± 2.4 years) were subjected to the data analysis.

2.2.2 Visual Entrainment Design:

For clarification, the visual entrainment experiment was conducted separately for EEG and fMRI acquisitions. To allow for comparisons across studies, the same entrainment paradigm was used and subjects were lying in supine position in both experiments. The visual entrainment paradigm consisted of a radial flickering checkerboard, which was presented for

20 seconds followed by the presentation of a black blank screen with a red fixation cross for 10 seconds in the EEG paradigm or 50 seconds in the fMRI paradigm (Figure 1A). A longer interstimulus interval was introduced in the fMRI experiment to account for the slower BOLD response and post-stimulus undershoot. The experiment was presented through Presentation software (Neurobehavioral Systems, http://www.neurobs.com) and projected by a projector onto a screen 1.5 meters behind the participants head and viewed by a mirror (visual angle 70°). The flickering rate of the checkerboard was controlled via a custom-built LCD glass placed in front of the beamer. The LCD glass darkens to a nearly opaque screen when voltage is applied to it, which was controlled through a microcontroller (Arduino Uno, Scarmagno, Italy) allowing flickering at any required frequency. Each flicker frequency was created with a 50% duty cycle, i.e., the LCD screen was dark for half of the cycle and transparent screen for the other half. A total of fourteen flicker conditions were presented, including the following frequencies: the individual subject's IAF, 7, 8, 9, 10, 11, and 12 Hz, which were presented both rhythmically and arrhythmically. The arrhythmic frequency stimulation was achieved by jittering the period of the stimulation frequency up to 25% (i.e. ± 12.5% from the flicker frequency) while maintaining the 50% duty cycle to keep the average luminance the same across all flicker conditions. (Figure 1B). The presentation of all conditions was individually randomized for each subject.

In both EEG and fMRI, the fourteen flicker conditions were presented once per session. For the EEG experiment, three sessions lasting approximately 8 minutes were obtained, resulting in 3 repetitions of each flicker condition per subject. For the fMRI experiment, two sessions of the entrainment paradigm lasting approximately 16 minutes were obtained for each subject, resulting in two repetitions of the fourteen flicker conditions per subject.

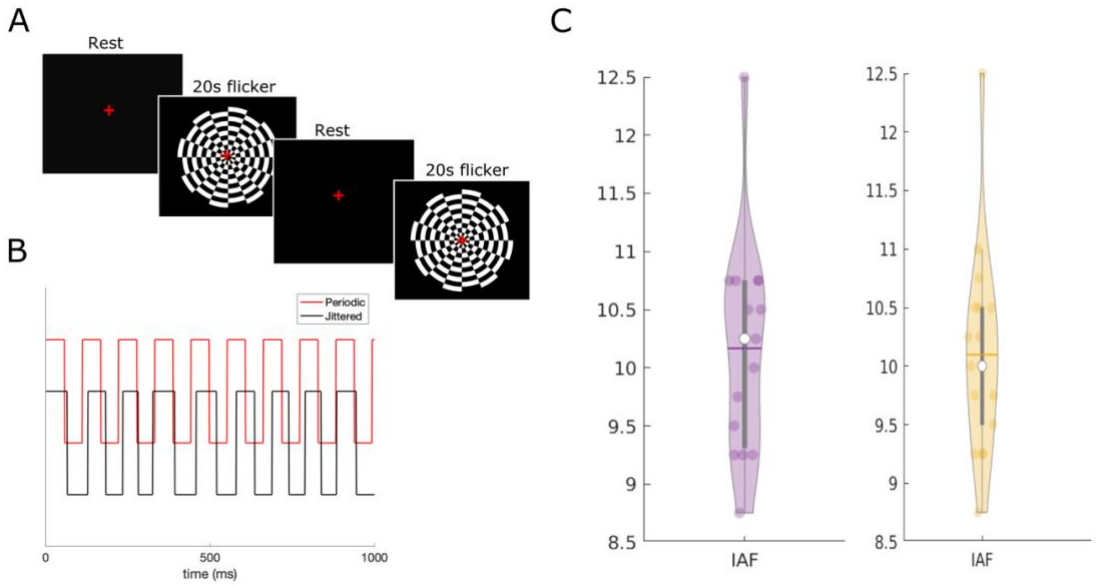

Figure 2. 1: Visual Paradigm. A) Subjects were presented with a blank screen for 50 seconds in the fMRI study (10 seconds for the EEG only study) followed by 20 seconds flickering circular checkerboard. Subjects were asked to continuously fixate on the red fixation cross. The checkerboard flickered via a shutter glass inserted in front of the projector for 14 stimulation conditions (the subject's IAF, 7 Hz, 8 Hz, 9 Hz, 10 Hz, 11 Hz, 12 Hz, rhythmic and arrhythmic stimulation for each frequency). B) The arrhythmic condition (black) was randomized with up to 25% jitter of the stimulation frequency. The rhythmic condition is presented in red. C, D) Boxplots indicating the distribution of the peak alpha frequency (determined from 1 minute resting state, eyes closed EEG recordings) across 15 participants that were recruited for the EEG (C) and fMRI (D) studies, respectively. Peak alpha frequencies ranged from 8.75 to 12.5 Hz (interquartile range: 9.31 - 10.75 Hz; red) for EEG subjects (C) with a median and mean IAF of 10.25 Hz and 10.17 ± 0.93 Hz, respectively. The peak alpha frequency ranged from 8.75 Hz to 12.5 Hz (interquartile range 9.5Hz – 10.5Hz; red) for fMRI subjects (D) with a median / mean IAF across subjects of 10 Hz and 10.1 ± 0.85 Hz, respectively.

2.2.3 EEG Data:

2.2.3.1 Data acquisition:

EEG data were recorded for i) the entrainment paradigm using EEG in the first experimental group, and ii) determining the IAF frequency shortly before performing the fMRI entrainment experiment in the second experimental group. All EEG data was acquired from 64 MR-compatible scalp electrodes (EASYCAP GmbH, Germany), which was placed according to the 10/10 system. The online reference and ground electrode were located at FCz and AFz respectively. Impedance was kept below 10 kΩ. Data was acquired with a sampling rate of 1000 Hz and a software-based high-pass filter of 10 seconds was used to prevent DC saturation. All recordings were performed using BrainVision Recording Software (Brain Products, Germany).

2.2.3.2 Determination of IAF by resting state EEG:

The IAF was determined from one-minute eyes-closed resting state EEG performed shortly before the entrainment paradigm. Subjects were in supine position in a dark room to keep the body position of the subjects consistent with the fMRI scanning session. The one-minute resting state EEG was segmented into 4 second segments. For each of the following electrodes, O1, O2, Oz, P1, P2, and Pz, the EEG signal was extracted and processed as follows. To account for slow signal drift, each segment was baseline corrected to the average power of the segment, which was calculated from a fast Fourier transform with 50% overlap and a Hanning window taper. The maximum alpha peak frequency was determined for electrodes O1, O2, Oz, P1, P2, Pz with a resolution of 0.25 Hz. If a subject did not have a single peak frequency across all aforementioned electrodes, then the frequency of the most common peak was determined across the six electrodes.

2.2.3.3 EEG preprocessing

The flicker paradigm EEG data was segmented into 20 second epochs corresponding to the stimulation blocks and concatenated across all three sessions for all rhythmic and arrhythmic frequencies. Data was then down sampled to 500 Hz and band pass filtered to range from 1 to 30 Hz. Channels that either flat lined for 5 seconds, exceeded a high-frequency noise standard deviation of 4, or exceeded a correlation of 0.8 with nearby channels were excluded (Clean RawData Plugin, EEGLAB).[35] Data was re-referenced to the average and further denoised using an independent component analysis. All components that were not labeled as brain by the ICLabel toolbox (Swartz Center for Computational Neuroscience, https://sccn.ucsd.edu/wiki/ICLabel) were removed. Bad electrodes were re-interpolated using the re-referenced and ICA-denoised data. Using the Artifact Subspace Reconstruction algorithm in EEGLAB any data segment surpassing 20 standard deviations of calibrated clean data or segments in which 25% of channels exceeded 7 standard deviation of average channel power were removed. The 20 seconds of data for each flicker frequency condition were then divided into 4 second epochs with no overlap. The spectral content ranging from ±1 Hz around the stimulation frequency was calculated for each 4 second segment using a Fourier transform with a DPSS taper.

2.2.3.4 Source localization of imaginary coherency value

To reconstruct alpha sources from the scalp EEG, volume conductance across the head was calculated from a template boundary element model as implemented in Fieldtrip, (www.fieldtriptoolbox.org)[36]. The 64-electrode position files were manually aligned to the T1 template in MNI space. The Fourier coefficients for each 4-second epoch were projected into source space using the partial canonical correlation (PCC) algorithm[37,38] with a regularization parameter set at 10%. Imaginary coherence was calculated for each dipole pair for each flicker condition from the complex part of the Fourier-transformed data. The imaginary part of the coherence spectrum has been shown to be unaffected by volume conductance and thus eliminates spurious coherency caused by volume conductance.[39] The source-localized coherency values were parcellated into 90 regions using the AAL atlas.[40] Cerebellar regions were excluded as source projection into deep subcortical structure becomes less reliable.

2.2.3.5 Statistical test of group coherency effects

The parcellated coherency matrices for all flicker conditions were entered into an ANOVA for all subjects with flickering frequency as a factor with fourteen levels. Significance testing correcting for multiple comparison was performed using the Network-Based Statistical Toolbox (NBS)[41], which implements a non-parametric clustering approach. The NBS toolbox uses mass univariate testing of a hypothesis of interest on each connection between all node pairs. The NBS toolbox then corrects for multiple comparison using a cluster-based, non-parametric random permutation approach. Since we hypothesized that rhythmic stimulation at the IAF elicits higher degree of synchronization than stimulation at other rhythmic frequencies due to increased entrainment with the driving flicker frequency at the IAF,[30–32] comparison rhythmic stimulation at the IAF more significant than all other rhythmic flicker frequencies was tested using network-based statistics To ensure increases in cortical coherency was an effect of entrainment rather than measures of the underlying ongoing alpha oscillation, the comparison rhythmic versus arrhythmic flicker conditions and vice versa were also tested.

2.2.4 Experimental FMRI Data:

2.2.4.1 Image data acquisition and processing:

Imaging data was acquired on a 3T Phillips Ingenia scanner with a 32-channel head coil. A structural scan (MPRAGE, TE 3.3 ms, TR = 7.264 ms, flip angle = 8°, TI = 1060 ms, FoV = 240 mm x 240 mm x 170 mm, voxel size = 0.75mm³, matrix size = 320 x 320; 227 sagittal slices) and two functional scanning sessions were acquired. Nine hundred and eighty whole-brain echoplanar imaging (EPI) scans (TE = 30 ms, TR = 1000 ms, flip angle =70°, FoV = 192mm x 192mm x 115mm, matrix 64x62, voxel size = 3mm^3, 36 slices, slice thickness = 33 mm with a 0.2mm interslice gap) were acquired with a multiband factor of 2 and a SENSE factor of 2.

2.2.4.2 Image preprocessing for fMRI connectivity analysis

The fMRI data was preprocessed using the CONN toolbox.[42] Anatomical and functional images were re-oriented to the ACPC axis. Functional images were head motion-corrected and co-registered to the T1-anatomical image. Four subjects showed head movement exceeding a threshold of 2mm/2° movement/rotation in any direction and were excluded from further analyses as mentioned in section 1 (participants). The anatomical data was segmented into six tissue probability maps and subsequentially normalized to Montreal Neurological Institute (MNI) standard brain space. The functional images were then also MNI normalized using identical transformations. The preprocessed EPI time series were despiked using a wavelet-based approach (BrainWavelet Toolbox),[43] and further denoised with the CONN Toolbox by regressing out head motion effects using the Friston24[44] movement parameters. To reduce cardiac and respiratory effects, signal from white matter and cerebrospinal fluid (obtained from individual masks in MNI space) were removed through a linear regression. The residuals were high pass filtered with a temporal bandpass filter of 0.08 Hz to account for slow scanner drift.

2.2.4.3 Network-based connectivity analysis across rhythmic flicker conditions

The whole brain time series were parcellated into 360 regions using the Glasser Atlas.[45] Time series were averaged within each parcel. 56 regions (Supplementary Table 2) corresponding to occipital parietal cortex spatially overlapping with significantly connected areas in the EEG study were selected for the subsequent connectivity analysis. The parcellated time series were extracted for each stimulation condition resulting in twenty time points per flicker condition per session. Cross-correlation matrices were created from the 56 regions of interest for each flicker condition and averaged across the two scanning sessions per subject. Cross-correlation matrices for all flicker frequencies and subjects were entered into an ANOVA.

Significance testing correcting for multiple comparison was performed using the NBS toolbox (see Methods section 3.5 for a more detailed explanation). For each frequency condition (7, 8, 9, 10, 11, 12 Hz and the IAF) as well as for the comparison between rhythmic and arrhythmic stimulation, significance was tested for the t-contrast rhythmic stimulation at a given flicker frequency against all other rhythmic flicker frequencies.

2.3 Results:

EEG connectivity during stimulation at and near the IAF:

Individual participant's peak alpha frequency, measured during resting-state one-minute eyes closed EEG, ranged between 8.75 and 12.5 Hz with a mean peak frequency of 10.17 ± 0.93 Hz (Figure 1). To quantify the degree of entrainment at the IAF as compared to neighboring frequencies, connectivity in source projected EEG was measured by evaluating alpha-band limited phase synchrony using imaginary coherence. Rhythmic stimulation at the IAF resulted in increased alpha phase coherency across occipitoparietal regions and across the left and right hemisphere (Figure 2A, mass univariate testing at $p < 0.05$; 1000 random permutations, $p < 0.05$). Increased coherency in occipitoparietal regions was also observed at rhythmic stimulation at 10 Hz (Figure 2B). However, across subjects the mean peak alpha frequency centered around 10 Hz and thus stimulation at 10 Hz may have also elicited a high degree of entrainment. The contrast rhythmic IAF compared to all other rhythmic frequencies excluding 10 Hz elicited higher interhemispheric connectivity in the visual cortex. This effect confirms that rhythmic stimulation at the IAF elicits higher degree of synchronicity than neighboring frequencies. Rhythmic stimulation elicited significantly higher alpha phase coherency across region pairs than arrhythmic stimulation across frequencies (Supplementary Figure 1). No significant phase coherence were found across region pairs for arrhythmic stimulation compared to rhythmic stimulation.

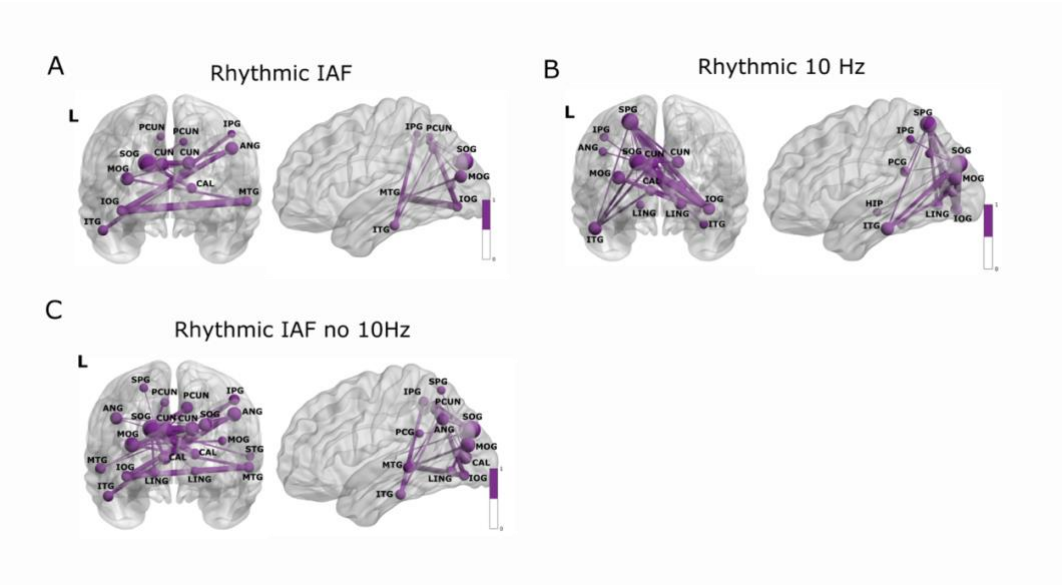

Figure 2. 2: Significant EEG functional connectivity. Significant EEG functional connectivity was measured using imaginary coherency between region pairs for a given flicker frequency contrasted against other flicker frequencies (each connection tested at p-value of 0.05). A non-parametric permutation test was performed on supra-threshold connections to account for multiple comparisons (NBS, 1000 iterations, significance at $p < 0.05$). Significant connections at contrasts: A) rhythmic IAF versus all other rhythmic flicker frequencies, B) rhythmic 10 Hz versus all other rhythmic flicker frequencies, and C) rhythmic IAF as compared to all other flickering frequencies excluding 10 Hz. All other rhythmic flicker frequencies (7, 9, 11, 12 Hz) did not result in any significant connections. The average IAF value was 10.1 Hz, which may explain the strong connections seen at rhythmic 10 Hz. Brain networks were visualized with BrainNet Viewer.(Xia et al., 2013)

<u>BOLD connectivity analysis during visual stimulation:</u>

The degree of functional connectivity between nodes, as measured by cross-correlation of parcellated fMRI time series, was assessed using network-based statistics as a proxy for degree of entrainment across flicker conditions. Most notably, rhythmic stimulation at the IAF induced significantly more connected networks that ranged across occipital and parietal regions and across hemispheres as compared to rhythmic stimulation at all other frequencies (mass univariate testing at $p < 0.001$; 5000 random permutations, $p < 0.001$; Figure 4A). In the fMRI data, for rhythmic stimulation at 9Hz (Figure 4B), 11 Hz (Figure 4C), and 12 Hz Figure 4D) significant connections were detected between parietal and occipital regions. The comparison of rhythmic versus arrhythmic stimulation at the IAF resulted in increased occipital connectivity of BOLD signals, while the reversed comparison was not significant (Supplementary Figure 1C). Visual stimulation at the IAF did not show any significant decrease in BOLD signal amplitude as compared to arrhythmic stimulation or other control frequencies (see Supplementary information and Supplementary Figure 2).

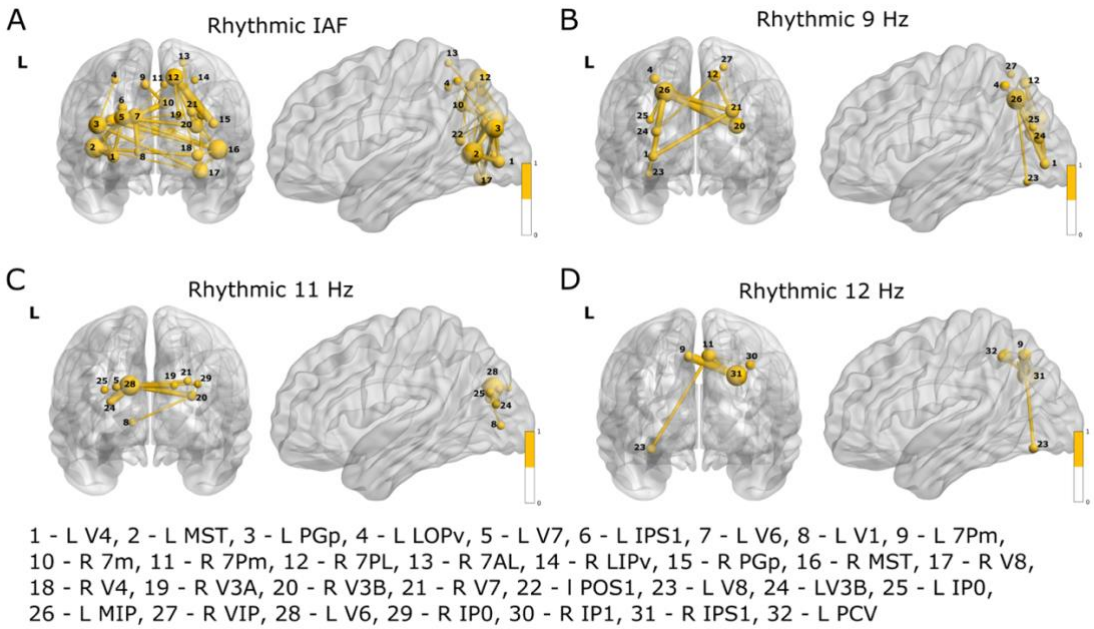

Figure 2. 3: Significant BOLD functional Connectivity. Significant BOLD function connectivity for the t-contrasts A) rhythmic IAF greater than rhythmic all other flicker frequencies, B) rhythmic 9 Hz greater than rhythmic all other flicker frequencies, C) rhythmic 11 Hz greater than all other rhythmic flicker frequencies, and D) rhythmic 12 Hz greater than all other flicker frequencies. No significant clusters were observed for rhythmic 8 Hz greater than all other flicker frequencies, rhythmic 10 Hz greater than all other flicker frequencies, and rhythmic 12 Hz greater than all other flicker frequencies. A threshold of $p < 0.001$ was used to obtain supra-threshold connectivity components. Each component was subject to family-wise error rate correction through permutation testing ($P < 0.001$, 5000 permutations).

2.4 Discussion:

This study, to our knowledge, is the first, to evaluate alpha-modulated cortical synchronicity changes in both an EEG and an fMRI study. A novel light stimulation tool was used to target individuals' intrinsic alpha frequency. Rhythmic and arrhythmic control frequencies were used to ensure entrainment at the IAF independent of synchronicity changes induced by steady-state visually evoked potentials. Results show both an increase in synchronicity across occipitoparietal regions in both the EEG and fMRI study for rhythmic stimulation at the IAF as compared to all other rhythmic flicker frequencies from within the alpha range. These findings suggest that targeted entrainment at the IAF leads to enhanced synchronization of neural activity across neural ensembles as measured by coherency in the EEG. Increase in synchronous neural activity thus drives a synchronized increase in neural gain in visual and parietal areas, as reflected by the increase in fMRI connectivity. The higher degree of

synchronicity between fluctuating neural activity in the visual cortex suggests gated processing of incoming visual sensory input.

There is still a debate in the literature whether rhythmic light stimulation truly drives synchronization of intrinsic oscillations to the external rhythm or whether rhythmic stimulation evokes the superposition of steady-state visually evoked potentials (SSVEPs) on intrinsic neural oscillations.[30,46,47] In part, analysis methods investigating alpha power are insufficient in discerning between different sources oscillating within the same frequency, i.e., intrinsic neural oscillations or SSVEPs.[17,47,48] Phase coupling between two oscillatory sources provides a more accurate measure of synchronicity between neural oscillations and external rhythms.[30,49] Although it has been noted that measure of alpha phase locking to external stimuli are sensitive to amplitude and phase changes elicited by evoked potentials,[50,51] we argue that comparing degree of phase coupling to control conditions with equal amounts of energy, or luminance, serves as an accurate measure of entrainment. In this study, the arrhythmic conditions were used as a control for phase changes to the ongoing alpha rhythm induced by evoked potentials. The arrhythmic condition mimicked the rhythmic condition with equal luminance and only slight phase shifts per cycle. The arrhythmic condition should therefore elicit a similar visually evoked response as the rhythmic condition.[32,34,46] In our results there was no significant phase coherence neither for the arrhythmic condition in the EEG (Supplementary Figure 2) nor for the fMRI stimulation at the IAF (Supplementary Figure 3), supporting the conclusion that the observed significant connectivity reflects entrainment of ongoing neural oscillations.

Entrainment of the alpha rhythm in part proves difficult because of inter- and intra-subject variability. The alpha peak frequency has been observed to shift with age, neurological disorders,[52] and also varies across age-matched individuals.[53,54] Recent studies assessing peak alpha frequency across experimental condition also noted a shift in the peak alpha frequency up to 0.2Hz per hour.[55] Alpha peak frequency shifts have been associated with cognitive demand[54,56] and spontaneous fluctuations in the resting state alpha peak frequency has been observed to be inversely associated with BOLD signal change in the visual cortex.[57] In this study, the peak alpha frequency across subjects varied between 8.75 and 12.5 Hz in both the EEG and fMRI cohort and were centered between 10 and 10.5 Hz. A high degree of synchronicity was therefore observed for the 10 Hz condition in the EEG study (Figure 2) and the 9 Hz condition in the fMRI study (Figure 3). Notbohm et al. (2016), showed that at a

given light intensity, stimulation at a frequency near the IAF will also elicit entrainment. This suggests that the alpha rhythm is adaptable and may be able to shift its peak frequency to match either external or intrinsic temporal rhythms,[58,59] allowing for better temporal integration and processing of sensory information.[60,61]

Even though rhythmic visual stimulation has been extensively used in fMRI studies of the visual cortex,[62,63] only a few studies have investigated changes in the BOLD signal amplitude response in the visual cortex under rhythmic[64,65] and arrhythmic visual stimulation[34] across different flicker frequencies including the alpha range. In general, a decreased BOLD response was found for rhythmic flicker in the alpha range as compared to lower or higher flicker frequencies[64,65] and in comparison to arrhythmic stimulation in the alpha range.[34] These previous studies had small sample sizes of six to seven subjects, sampled only few flicker frequencies in the alpha range and did not consider variability in the alpha peak frequency across individuals. Our results show no significant difference in the BOLD response amplitude between rhythmic and arrhythmic stimulation (Supplementary Figure 2). Although the BOLD signal amplitude was lower for rhythmic stimulation at the IAF, 10 Hz and 12 Hz. We are quite confident that an increase in trial number and thus power may have resulted in significant findings. Nevertheless, the degree of jitter in the arrhythmic condition may also have not been large enough to interrupt the ongoing alpha rhythm. Yet, a significantly higher degree of synchronicity for rhythmic stimulation at the IAF compared to arrhythmic stimulation (Supplementary Figure 3) suggests that a 25% jitter was sufficient to interrupt the intrinsic alpha oscillation. In comparison to previous studies, our study also specifically targeted the individually measured IAF and used a finer frequency resolution of 1Hz intervals within the alpha range.

Moreover, our findings also particularly depend on the question what signal transformation must be considered when interpreting EEG and fMRI results that arise from different neurophysiological signals. The event-related BOLD response can be considered as a superposition of spontaneous and task-related activity.[66,67] The vascular and metabolic contributions to the BOLD amplitude response reflect the average level of synaptic activity in a local area, while EEG signal measures the summation of LFPs induced by the synchronous activity of neural populations.[68] Taking this into consideration in the current study, the BOLD amplitude response in V1 may reflect the superposition of both the visual-evoked responses induced by the increase in luminance upon presentation of the checkerboard, which is

observed across all conditions as mean luminance was kept constant, and changes in BOLD connectivity as induced by entrainment of alpha rhythm. Since an evoked response, and subsequent neural activity, will be present in V1 for all flicker conditions, the BOLD amplitude may not be sensitive enough in V1 to show entrained BOLD effects.

When investigating the alpha-BOLD relationships, it is important to understand the neural basis of alpha power and alpha phase as well as the BOLD amplitude response and functional connectivity as these may represent different neural modalities. In the literature, mixed results have been reported when comparing the alpha rhythm to the BOLD signal. Studies that analyzed BOLD amplitude response and alpha power have shown an inverse relationship in visual cortex.[8,69] However, another study by Scheeringa et al. (2012) investigating BOLD connectivity and alpha power in resting state has shown decreased connectivity across visual areas, yet increased connectivity between the visual cortex and default mode network. Variability in alpha phase has been correlated with variable BOLD amplitude response in V1.[70] High alpha phase synchronicity correlated positively with functional connectivity in frontoparietal areas during rest.[71] More recently, a study investigating transient changes in alpha power and phase coherency between the PCC and the cortex in resting state, showed increased alpha power as well as phase synchronicity in occipital parietal regions associated within a higher order cognitive network.[72] In our study, visual entrainment at the IAF elicited increased phase synchronicity and BOLD connectivity in similar regions, suggesting that entrainment may induce a higher degree of coherency in top-down parietal regions and sensory visual areas. Yet visual stimulation may cause synchronicity changes that differ from spontaneous fluctuations in the alpha rhythm and BOLD connectivity under rest.

We note that direct comparisons between alpha coherency and fMRI connectivity could not be inferred in this study as participants varied across the two studies and EEG and fMRI data were not acquired simultaneously and subjects varied across the study. We observed variability in the intrinsic alpha peak frequency across individuals and across the EEG and fMRI study. Interindividual differences in peak alpha frequency has also been correlated with regional differences in cerebral blood flow,[73]which suggest a variable BOLD response across individuals. Despite variability across the two studies, rhythmic stimulation at the IAF increased connectivity across similar regions in the occipital parietal cortex.

In conclusion, we showed that rhythmic stimulation at the IAF results in increased alpha coherency and fMRI connectivity across the occipitoparietal cortex as compared to other rhythmic flicker frequencies due to increased entrainment with the driving external light force at the IAF and stronger modulation of synchronous neural activity. A replication of entrainment in a future concurrent EEG-fMRI studies investigating the synchronicity in the alpha rhythm and BOLD signal during entrainment, as well as during rest, would help clarify whether entrainment at the IAF activates the same neural processes as spontaneous fluctuations in intrinsic alpha frequency. Finally, future studies investigating behavioral outcomes during experimental modulations of the alpha rhythm during entrainment in concurrent EEG-fMRI would provide definitive evidence for the communication by coherence hypothesis.

2.5 References:

1. Fries P. A mechanism for cognitive dynamics: neuronal communication through neuronal coherence. *Trends Cogn Sci*. 2005;9(10):474-480. doi:10.1016/J.TICS.2005.08.011
2. Fries P. Rhythms For Cognition: Communication Through Coherence. *Neuron*. 2015;88(1):220. doi:10.1016/J.NEURON.2015.09.034
3. Berger H. Über das Elektrenkephalogramm des Menschen. *Arch für Psychiatr und Nervenkrankheiten 1929 871*. 1929;87(1):527-570. doi:10.1007/BF01797193
4. Hari R, Salmelin R. Human cortical oscillations: a neuromagnetic view through the skull. *Trends Neurosci*. 1997;44–49.
5. Jensen O, Mazaheri A. Shaping functional architecture by oscillatory alpha activity: Gating by inhibition. *Front Hum Neurosci*. 2010;4:186. doi:10.3389/FNHUM.2010.00186/BIBTEX
6. Mathewson KE, Lleras A, Beck DM, Fabiani M, Ro T, Gratton G. Pulsed out of awareness: EEG alpha oscillations represent a pulsed-inhibition of ongoing cortical processing. *Front Psychol*. 2011. doi:10.3389/fpsyg.2011.00099
7. Goldman RI, Stern JM, Engel J, Jr, Cohen MS. Simultaneous EEG and fMRI of the alpha rhythm. *Neuroreport*. 2002;13(18):2487. doi:10.1097/01.WNR.0000047685.08940.D0
8. Scheeringa R, Petersson KM, Oostenveld R, Norris DG, Hagoort P, Bastiaansen MCM. Trial-by-trial coupling between EEG and BOLD identifies networks related to alpha and theta EEG power increases during working memory maintenance. *Neuroimage*. 2009;44(3):1224-1238. doi:10.1016/j.neuroimage.2008.08.041
9. Scheeringa R, Petersson KM, Kleinschmidt A, Jensen O, Bastiaansen MCM. EEG Alpha Power Modulation of fMRI Resting-State Connectivity. *Brain Connect*. 2012;2(5):254. doi:10.1089/BRAIN.2012.0088
10. Ergenoglu T, Demiralp T, Bayraktaroglu Z, Ergen M, Beydagi H, Uresin Y. Alpha rhythm of the EEG modulates visual detection performance in humans. *Cogn Brain Res*. 2004;20(3):376-383. doi:https://doi.org/10.1016/j.cogbrainres.2004.03.009
11. Romei V, Brodbeck V, Michel C, Amedi A, Pascual-Leone A, Thut G. Spontaneous Fluctuations in Posterior α-Band EEG Activity Reflect Variability in Excitability of Human Visual Areas. *Cereb Cortex (New York, NY)*. 2008;18(9):2010-2018.

doi:10.1093/cercor/bhm229

12. Klimesch W, Sauseng P, Hanslmayr S. EEG alpha oscillations: The inhibition-timing hypothesis. *Brain Res Rev*. 2007. doi:10.1016/j.brainresrev.2006.06.003
13. Iemi L, Chaumon M, Crouzet SM, Busch NA. Spontaneous Neural Oscillations Bias Perception by Modulating Baseline Excitability. *J Neurosci*. 2017. doi:10.1523/JNEUROSCI.1432-16.2017
14. Busch NA, Dubois J, VanRullen R. The Phase of Ongoing EEG Oscillations Predicts Visual Perception. *J Neurosci*. 2009;29(24):7869-7876. doi:10.1523/JNEUROSCI.0113-09.2009
15. Mathewson KE, Gratton G, Fabiani M, Beck DM, Ro T. To See or Not to See: Prestimulus α Phase Predicts Visual Awareness. *J Neurosci*. 2009;29(9):2725-2732. doi:10.1523/JNEUROSCI.3963-08.2009
16. Palva S, Palva JM. Functional roles of alpha-band phase synchronization in local and large-scale cortical networks. *Front Psychol*. 2011. doi:10.3389/fpsyg.2011.00204
17. Van Diepen RM, Foxe JJ, Mazaheri A. The functional role of alpha-band activity in attentional processing: the current zeitgeist and future outlook. *undefined*. 2019;29:229-238. doi:10.1016/J.COPSYC.2019.03.015
18. Nunez PL, Silberstein RB, Cadusch PJ, Wijesinghe RS, Westdorp AF, Srinivasan R. A theoretical and experimental study of high resolution EEG based on surface Laplacians and cortical imaging. *Electroencephalogr Clin Neurophysiol*. 1994;90(1):40-57. doi:10.1016/0013-4694(94)90112-0
19. Michel CM, Murray MM, Lantz G, Gonzalez S, Spinelli L, Grave De Peralta R. EEG source imaging. *Clin Neurophysiol*. 2004;115(10):2195-2222. doi:10.1016/J.CLINPH.2004.06.001
20. Chang C, Liu Z, Chen MC, Liu X, Duyn JH. EEG correlates of time-varying BOLD functional connectivity. *Neuroimage*. 2013;72:227-236. doi:10.1016/J.NEUROIMAGE.2013.01.049
21. Sadaghiani S, Scheeringa R, Lehongre K, et al. Alpha-Band Phase Synchrony Is Related to Activity in the Fronto-Parietal Adaptive Control Network. *J Neurosci*. 2012. doi:10.1523/JNEUROSCI.1358-12.2012
22. Vidaurre D, Hunt LT, Quinn AJ, et al. Spontaneous cortical activity transiently organises into frequency specific phase-coupling networks. *Nat Commun 2018 91*. 2018;9(1):1-13. doi:10.1038/s41467-018-05316-z
23. Siegel M, Donner TH, Engel AK. Spectral fingerprints of large-scale neuronal

interactions. *Nat Rev Neurosci 2012 132*. 2012;13(2):121-134. doi:10.1038/nrn3137

24. Lopes da Silva F. EEG and MEG: relevance to neuroscience. *Neuron*. 2013;80(5):1112-1128. doi:10.1016/J.NEURON.2013.10.017
25. Marzetti L, Della Penna S, Snyder AZ, et al. Frequency specific interactions of MEG resting state activity within and across brain networks as revealed by the multivariate interaction measure. *Neuroimage*. 2013;79:172-183. doi:10.1016/J.NEUROIMAGE.2013.04.062
26. Stephan KE, Friston KJ. Functional Connectivity. *Encycl Neurosci*. 2009:391-397. doi:10.1016/B978-008045046-9.00308-9
27. Herrmann CS. Human EEG responses to 1-100 Hz flicker: Resonance phenomena in visual cortex and their potential correlation to cognitive phenomena. *Exp Brain Res*. 2001. doi:10.1007/s002210100682
28. Mathewson KE, Prudhomme C, Fabiani M, Beck DM, Lleras A, Gratton G. *Making Waves in the Stream of Consciousness: Entraining Oscillations in EEG Alpha and Fluctuations in Visual Awareness with Rhythmic Visual Stimulation*.; 2012.
29. Spaak E, de Lange FP, Jensen O. Local Entrainment of Alpha Oscillations by Visual Stimuli Causes Cyclic Modulation of Perception. *J Neurosci*. 2014. doi:10.1523/JNEUROSCI.4385-13.2014
30. Lakatos P, Gross J, Thut G. A New Unifying Account of the Roles of Neuronal Entrainment. *Curr Biol*. 2019;29(18):R890-R905. doi:10.1016/J.CUB.2019.07.075
31. Notbohm A, Herrmann CS. Flicker Regularity Is Crucial for Entrainment of Alpha Oscillations. *Front Hum Neurosci*. 2016. doi:10.3389/fnhum.2016.00503
32. Notbohm A, Kurths J, Herrmann CS. Modification of Brain Oscillations via Rhythmic Light Stimulation Provides Evidence for Entrainment but Not for Superposition of Event-Related Responses. *Front Hum Neurosci*. 2016. doi:10.3389/fnhum.2016.00010
33. Pikovsky A, Rosenblum M, Kurths J, Hilborn RC. Synchronization: A Universal Concept in Nonlinear Science. *Am J Phys*. 2002;70(6):655. doi:10.1119/1.1475332
34. Parkes LM, Fries P, Kerskens CM, Norris DG. Reduced BOLD response to periodic visual stimulation. *Neuroimage*. 2004;21(1):236-243. doi:10.1016/j.neuroimage.2003.08.025
35. Delorme A, Makeig S. EEGLAB: an open source toolbox for analysis of single-trial EEG dynamics including independent component analysis. *J Neurosci Methods*. 2004;134:9-21. http://www.sccn.ucsd.edu/eeglab/. Accessed February 13, 2022.
36. Oostenveld R, Fries P, Maris E, Schoffelen JM. FieldTrip: Open source software for

advanced analysis of MEG, EEG, and invasive electrophysiological data. *Comput Intell Neurosci*. 2011;2011. doi:10.1155/2011/156869

37. Schoffelen JM, Gross J. Source connectivity analysis with MEG and EEG. *Hum Brain Mapp*. 2009;30(6):1857-1865. doi:10.1002/HBM.20745
38. Zhuang X, Yang Z, Cordes D. A technical review of canonical correlation analysis for neuroscience applications. *Hum Brain Mapp*. 2020;41(13):3807-3833. doi:10.1002/HBM.25090
39. Nolte G, Bai O, Wheaton L, Mari Z, Vorbach S, Hallett M. Identifying true brain interaction from EEG data using the imaginary part of coherency. *Clin Neurophysiol*. 2004;115(10):2292-2307. doi:10.1016/J.CLINPH.2004.04.029
40. Rolls ET, Huang CC, Lin CP, Feng J, Joliot M. Automated anatomical labelling atlas 3. *Neuroimage*. 2020;206(August 2019):116189. doi:10.1016/j.neuroimage.2019.116189
41. Zalesky A, Fornito A, Bullmore ET. Network-based statistic: identifying differences in brain networks. *Neuroimage*. 2010;53(4):1197-1207. doi:10.1016/J.NEUROIMAGE.2010.06.041
42. Whitfield-Gabrieli S, Nieto-Castanon A. Conn: a functional connectivity toolbox for correlated and anticorrelated brain networks. *Brain Connect*. 2012;2(3):125-141. doi:10.1089/BRAIN.2012.0073
43. Patel AX, Kundu P, Rubinov M, et al. A wavelet method for modeling and despiking motion artifacts from resting-state fMRI time series. *Neuroimage*. 2014;95(100):287-304. doi:10.1016/J.NEUROIMAGE.2014.03.012
44. Friston KJ, Williams S, Howard R, Frackowiak RSJ, Turner R. Movement-related effects in fMRI time-series. *Magn Reson Med*. 1996;35(3):346-355. doi:10.1002/MRM.1910350312
45. Glasser MF, Coalson TS, Robinson EC, et al. A multi-modal parcellation of human cerebral cortex. *Nature*. 2016;536(7615):171. doi:10.1038/NATURE18933
46. Capilla A, Pazo-Alvarez P, Darriba A, Campo P, Gross J. Steady-State Visual Evoked Potentials Can Be Explained by Temporal Superposition of Transient Event-Related Responses. *PLoS One*. 2011;6(1):e14543. doi:10.1371/JOURNAL.PONE.0014543
47. Keitel C, Keitel XA, Benwell CSY, Daube C, Thut XG, Gross XJ. Stimulus-Driven Brain Rhythms within the Alpha Band: The Attentional-Modulation Conundrum. 2019. doi:10.1523/JNEUROSCI.1633-18.2019
48. Cohen MX, Gulbinaite R. Rhythmic entrainment source separation: Optimizing

analyses of neural responses to rhythmic sensory stimulation. doi:10.1101/070862

49. Lowet E, Roberts MJ, Bonizzi P, Karel J, De Weerd P. Quantifying Neural Oscillatory Synchronization: A Comparison between Spectral Coherence and Phase-Locking Value Approaches. *PLoS One*. 2016;11(1):e0146443. doi:10.1371/JOURNAL.PONE.0146443
50. Van Diepen RM, Mazaheri A. The Caveats of observing Inter-Trial Phase-Coherence in Cognitive Neuroscience. *Sci Reports 2018 81*. 2018;8(1):1-9. doi:10.1038/s41598-018-20423-z
51. Muthukumaraswamy SD, Singh KD. A cautionary note on the interpretation of phase-locking estimates with concurrent changes in power. *Clin Neurophysiol*. 2011;122(11):2324-2325. doi:10.1016/J.CLINPH.2011.04.003
52. Uhlhaas PJ, Singer W. Neural synchrony in brain disorders: relevance for cognitive dysfunctions and pathophysiology. *Neuron*. 2006;52(1):155-168. doi:10.1016/J.NEURON.2006.09.020
53. Klimesch W. EEG-alpha rhythms and memory processes. *Int J Psychophysiol*. 1997;26(1-3):319-340. doi:10.1016/S0167-8760(97)00773-3
54. Haegens S, Cousijn H, Wallis G, Harrison PJ, Nobre AC. Inter- and intra-individual variability in alpha peak frequency. *Neuroimage*. 2014;92(100):46-55. doi:10.1016/J.NEUROIMAGE.2014.01.049
55. Benwell CSY, London RE, Tagliabue CF, et al. Frequency and power of human alpha oscillations drift systematically with time-on-task. *Neuroimage*. 2019;192:101-114. doi:10.1016/J.NEUROIMAGE.2019.02.067
56. Maurer U, Brem S, Liechti M, Maurizio S, Michels L, Brandeis D. Frontal Midline Theta Reflects Individual Task Performance in a Working Memory Task. *Brain Topogr*. 2015;28(1):127-134. doi:10.1007/S10548-014-0361-Y/FIGURES/3
57. Babu Henry Samuel I, Wang C, Hu Z, Ding M. The frequency of alpha oscillations: Task-dependent modulation and its functional significance. *Neuroimage*. 2018;183:897. doi:10.1016/J.NEUROIMAGE.2018.08.063
58. Helfrich RF, Schneider TR, Rach S, Trautmann-Lengsfeld SA, Engel AK, Herrmann CS. Entrainment of brain oscillations by transcranial alternating current stimulation. *Curr Biol*. 2014;24(3):333-339. doi:10.1016/J.CUB.2013.12.041
59. Cecere R, Rees G, Romei V. Individual differences in alpha frequency drive crossmodal illusory perception. *Curr Biol*. 2015;25(2):231-235. doi:10.1016/J.CUB.2014.11.034

60. Samaha J, Postle BR. The Speed of Alpha-Band Oscillations Predicts the Temporal Resolution of Visual Perception. *Curr Biol*. 2015. doi:10.1016/j.cub.2015.10.007
61. Mierau A, Klimesch W, Lefebvre J. State-dependent alpha peak frequency shifts: Experimental evidence, potential mechanisms and functional implications. *Neuroscience*. 2017;360:146-154. doi:10.1016/J.NEUROSCIENCE.2017.07.037
62. Ogawa S, Tank DW, Menon R, et al. Intrinsic signal changes accompanying sensory stimulation: functional brain mapping with magnetic resonance imaging. *Proc Natl Acad Sci U S A*. 1992;89(13):5951-5955. doi:10.1073/PNAS.89.13.5951
63. Kwong KK, Belliveau JW, Chesler DA, et al. Dynamic magnetic resonance imaging of human brain activity during primary sensory stimulation. *Proc Natl Acad Sci*. 1992;89(12):5675-5679. doi:10.1073/PNAS.89.12.5675
64. Singh M, Kim S, Kim T-S. Correlation between BOLD-fMRI and EEG signal changes in response to visual stimulus frequency in humans. *Magn Reson Med*. 2003;49(1):108-114. doi:10.1002/mrm.10335
65. Ozus B, Liu HL, Chen L, Iyer MB, Fox PT, Gao JH. Rate dependence of human visual cortical response due to brief stimulation: an event-related fMRI study. *Magn Reson Imaging*. 2001;19(1):21-25. doi:10.1016/S0730-725X(01)00219-3
66. Fox MD, Snyder AZ, Zacks JM, Raichle ME. Coherent spontaneous activity accounts for trial-to-trial variability in human evoked brain responses. *Nat Neurosci*. 2006;9(1):23-25. doi:10.1038/NN1616
67. Becker R, Reinacher M, Freyer F, Villringer A, Ritter P. How Ongoing Neuronal Oscillations Account for Evoked fMRI Variability. *J Neurosci*. 2011;31(30):11016-11027. doi:10.1523/JNEUROSCI.0210-11.2011
68. Hermes D, Nguyen M, Winawer J. Neuronal synchrony and the relation between the blood-oxygen-level dependent response and the local field potential. *PLOS Biol*. 2017;15(7):e2001461. doi:10.1371/JOURNAL.PBIO.2001461
69. Mayhew SD, Bagshaw AP. Dynamic spatiotemporal variability of alpha-BOLD relationships during the resting-state and task-evoked responses. *Neuroimage*. 2017;155:120-137. doi:10.1016/J.NEUROIMAGE.2017.04.051
70. Scheeringa R, Mazaheri A, Bojak I, Norris DG, Kleinschmidt A. Modulation of Visually Evoked Cortical fMRI Responses by Phase of Ongoing Occipital Alpha Oscillations. *J Neurosci*. 2011. doi:10.1523/JNEUROSCI.4697-10.2011
71. Sadaghiani S, Scheeringa R, Lehongre K, et al. Alpha-band phase synchrony is related to activity in the fronto-parietal adaptive control network. *J Neurosci*.

2012;32(41):14305-14310. doi:10.1523/JNEUROSCI.1358-12.2012

72. Vidaurre D, Hunt LT, Quinn AJ, et al. Spontaneous cortical activity transiently organises into frequency specific phase-coupling networks. *Nat Commun*. 2018;9(1). doi:10.1038/S41467-018-05316-Z
73. Jann K, Koenig T, Dierks T, Boesch C, Federspiel A. Association of individual resting state EEG alpha frequency and cerebral blood ow. 2010. doi:10.1016/j.neuroimage.2010.02.024
74. Xia M, Wang J, He Y. BrainNet Viewer: A Network Visualization Tool for Human Brain Connectomics. *PLoS One*. 2013;8(7). doi:10.1371/journal.pone.0068910
75. Eickhoff SB, Stephan KE, Mohlberg H, et al. A new SPM toolbox for combining probabilistic cytoarchitectonic maps and functional imaging data. *Neuroimage*. 2005;25(4):1325-1335. doi:10.1016/j.neuroimage.2004.12.034

Appendices:

Appendix A: Supplementary methods

To replicate previous findings from Parkes et al. (2004), the BOLD time series were extracted from V1 for each hemisphere separately, using probability maps obtained from Anatomy Toolbox(Eickhoff et al., 2005) as masks. The mean BOLD time series were extracted from the normalized functional images for each ROI and high-pass filtered (0.0078 Hz, 128 sec) for each scanning session, to account for slow scanner drift across the scanning sessions. The BOLD time series were segmented into the 20 second stimulation blocks for each stimulation condition. For each scanning session, the baseline BOLD time series was determined by averaging the last 20 seconds of all 50 second baseline periods that occurred in between stimulation blocks. Only the last 20 seconds were used to ensure that the BOLD signal had returned to baseline. The BOLD percent signal change (PSC) for each stimulation block was then calculated for each session as:

$$BOLD\ PSC = \frac{BOLD\ stimulation - \ mean\ BOLD\ baseline_{30-50\ seconds}}{mean\ BOLD\ baseline_{30-50\ seconds}} * 100$$

The BOLD PSC was then averaged across scanning session and across subjects respectively for a given ROI. The averaged evoked BOLD response is visualized in SI Figure 2. Then the last 10 seconds of the BOLD percent signal change of each stimulation condition were averaged together to make our data comparable with Parkes et al (2004). No Significant difference was found across the last 10 seconds of stimulation data between rhythmic and arrhythmic stimulation for a given frequency.

Appendix B: Supplementary figures

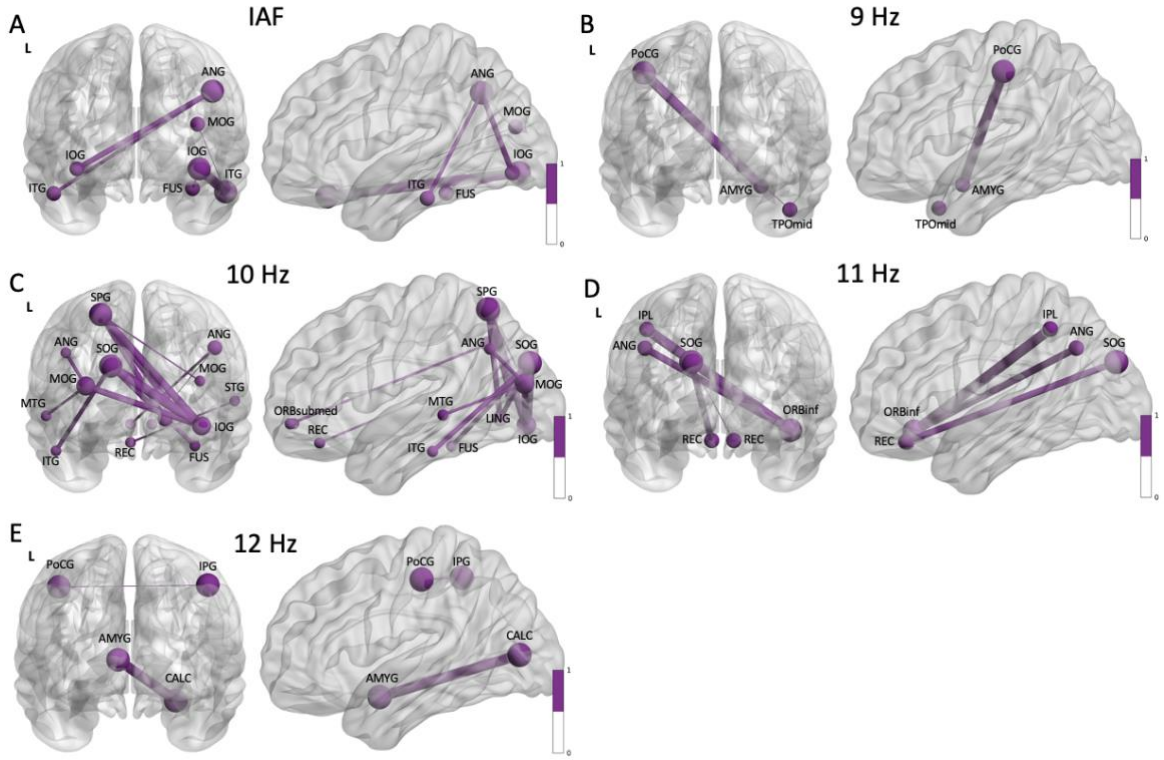

Supplementary Figure B.1: Significant clusters for rhythmic greater than arrhythmic stimulation in EEG. Significant clusters were corrected for multiple comparisons using False Discovery Rate. Significant clusters ($p_{FDR} < 0.05$, 1000 Permutations) were found for: A) IAF, B) 9 Hz, C) 10 Hz, D) 11 Hz, and E) 12 Hz. No significant clusters for rhythmic greater than arrhythmic stimulation at 7 Hz and 8 Hz.

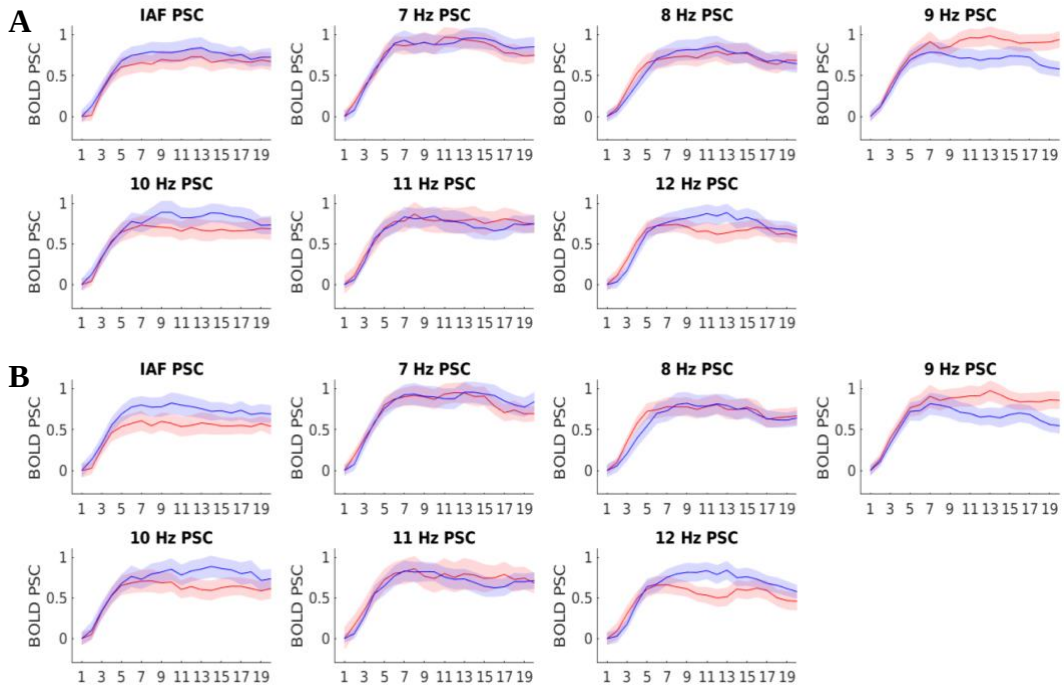

Supplementary Figure B.2: BOLD percent signal change in V1 for each flicker condition at rhythmic stimulation (red) and arrhythmic stimulation (blue) for each flicker condition averaged across A) left V1 and B) right V1. The shaded area indicated the standard error of the mean. No significant difference was found between rhythmic and arrhythmic stimulation for a given flicker frequency when averaging the last 10 seconds of each stimulation block.

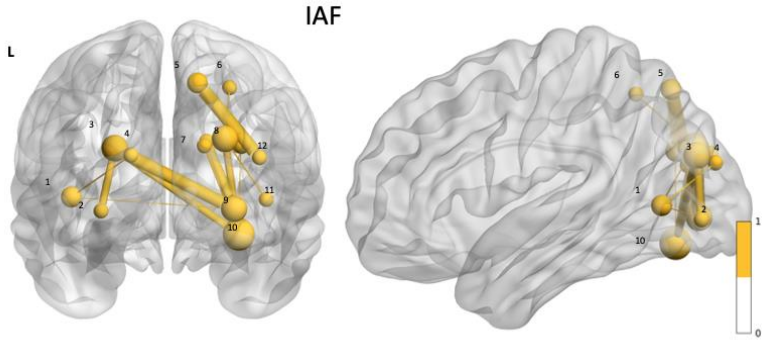

1 – L MST, 2 – L V4, 3 – L V7, 4 – L V3A, 5 – R 7PL, 6 – R LIPv, 7 – R V3A, 8 – R V7, 9 – R V4, 10 – R V3, 11 – R MST, 12 - R PGp

Supplementary Figure B.3: Significant clusters for rhythmic greater than arrhythmic stimulation in fMRI. Significant clusters ($p_{NBS} < 0.001$, 5000 Permutations, mass univariate testing at $P < 0.001$) were found for rhythmic versus arrhythmic stimulation at the IAF. No significant clusters were found for the contrast arrhythmic versus rhythmic stimulation at the IAF.

Appendix C: Supplementary Tables

Supplementary Table C.1: AAL atlas regions abbreviations

Abbreviation	AAL Region
PCUN	Precuneus
SOG	Superior Occipital Gyrus
MOG	Medial Occipital Gyrus
IOG	Inferior Occipital Gyrus
ITG	Inferior Temporal Gyrus
CUN	Cuneus
CAL	Calcarine Gyrus
IPG	Inferior Parietal Gyrus
ANG	Angular Gyrus
MTG	Medial Temporal Gyrus
LING	Lingual Gyrus
FFG	Fusiform Gyrus
SPG	Superior Parietal Gyrus
PCG	Posterior Cingulate Gyrus
IPL	Inferior Parietal Lobe
PoCG	Postcentral Gyrus
AMYG	Amygdala
TPOmid	Middle Temporal Pole
REC	Gyrus rectus
ORBinf	Inferior orbital frontal gyrus

Supplementary Table C.2: Glasser atlas regions of interest

Abbreviation	Glasser Region
R, L V1	Primary Visual Cortex
R, L MST	Medial Superior Temporal Area
R, L V6	Sixth Visual Area
R, L V2	Second Visual Area
R, L V3	Third Visual Area
R, L V4	Fourth Visual Area
R, L V8	Eighth Visual Area
R, L V3A	Area V3A
R, L V7	Seventh Visual Area
R, L IPS1	Intraparietal Sulcus Area 1
R, L V3B	Area V3B
R, L PCV	Precuneus Visual Area
R, L 7Pm	Medial Area 7p
R, L 7m	Area 7m
R, L POS1	Parieto-Occipital Sulcus Area 1
R, L 7AL	Lateral Area 7A
R, L 7Am	Medial Area 7A
R, L 7PL	Lateral Area 7P
R, L 7PC	Area 7PC
R, L LIPv	Area Lateral Intra Parietal Ventral
R, L VIP	Ventral Intra Parietal Complex
R, L MIP	Medial Intra Parietal Area
R, L AIP	Anterior Intra Parietal Area
R, L PGp	Area PGp
R, L IP2	Area Intraparietal 2
R, L IP1	Area Intraparietal 1
R, L IP0	Area Intraparietal 0
R, L PFop	Area PF opercular

PROJECT II:

ALPHA-MEDIATED LONG-RANGE CONNECTIVITY DURING RHYTHMIC VISUAL STIMULATION IN CONCURRENT EEG-FMRI STUDY

Abstract:

Neural oscillations play a prominent role in coordinating communication across distributed brain regions during cognition. Specifically, the posterior alpha oscillation is thought to modulate visual information processing by gaiting sensory neural activity through inhibition. Evidence from anticipatory attention studies suggests the behavioral relevance of modulatory changes in the alpha rhythm. However, it is not known whether long-range modulations in the alpha rhythm occur through cortico-cortical or thalamo-cortical connections. This study, uses a novel rhythmic light stimulation paradigm, previously shown to induce entrainment of the intrinsic alpha frequency, to spatially localize alpha-modulated long-range connectivity in a concurrent EEG-fMRI study. In the EEG, increased alpha coherency for rhythmic stimulation at the intrinsic alpha frequency (IAF) was observed between inferior frontal regions and occipital and parietal regions. While the fMRI revealed strong connectivity between the occipital thalamus and inferior and medial frontal cortex. Most notably, an analysis of covariation in trial-based EEG and fMRI connectivity revealed alpha-modulated connectivity varies along occipital-thalamic-frontal connections with the occipital thalamus having the highest degree centrality. In line with structural connectivity studies and intracranial electrophysiology studies, these results stress the relevance of functional modulation of the alpha rhythm through long-range cortico-thalamic connections. This study also employs a novel application of concurrent EEG-fMRI data to study task-based connectivity.

KEY WORDS: Visual stimulation, concurrent EEG-fMRI, alpha oscillation, functional connectivity, phase coherency, electrophysiological connectome

3.1 Introduction:

The brain's ability to coordinate parallel processing of sensory input and selective integration of context-relevant information into a continuous thought process is crucial for cognitive function.[1,2] Neural oscillations, composed of fluctuations in excitability states, are thought to regulate interareal neural communication by facilitating the coupling of excitability states across neural assemblies.[3–5] Similarly in fMRI, the statistical co-fluctuations of spatially distinct neurophysiological events are thought to reflect the integration of functionally segregated brain networks into common cognitive processes.[6,7] Dynamic jointly-derived electrophysiologic and fMRI network analyses during rest have shown that changes in neural oscillations in specific frequency bands correlate with dynamic organization of functional networks[8–10] and provide a putative framework for studying the hierarchical organization of the brain.[5,11] Yet it remains unclear whether dynamic changes in distinct neural oscillations spatially correlate with BOLD functional connectivity during active processing.

In vision, the posterior alpha oscillation (7-12Hz) is thought to coordinate visual information processing through selective inhibition of cortical excitability in local sensory areas.[3,12] The reduction of alpha power through sensory stimulation or directed spatial attention in targeted sensory areas and converse enhancement of alpha power in task-unrelated brain regions suggests active inhibition of cortical excitability due to high alpha power.[13–17] Inhibition is rhythmically modulated by the alpha oscillations as reflected by fluctuations in visual detection performance correlating with alpha phase.[18,19] Evidence from concurrent EEG-fMRI visual processing studies have also shown local occipital alpha power to correlate with a reduced BOLD amplitude response in the unattended hemisphere[20] and pre-stimulus alpha phase to modulate the BOLD amplitude in the visual cortex.[21]

Attentionally-driven modulation of alpha power and phase suggest the alpha rhythm lies under top-down control.[15,22–24] Concurrent EEG-fMRI studies showing increased functional connectivity between V1 and the thalamus during high alpha power [25] and increased functional connectivity in frontoparietal regions during high alpha phase synchronicity[26] support that context-dependent synchronization of neural populations through the alpha rhythm lies under top-down control.[27,28] Invasive electrophysiological recordings in animals have reported the correlation between thalamic spiking activity and sensory alpha phase coherency to increase with attention,[29] suggesting modulations of the alpha rhythm in sensory

areas occurs through thalamic connections. However, it remains unclear how cortical and thalamic interactions coordinate alpha coherence across the cortex and subsequent functional neural networks. Whole-brain connectivity measured from concurrent EEG-fMRI would elucidate the localization of long-range alpha connections and give insight into the modulation of long-range interactions through higher-order cognitive functions such as anticipatory attention.

Since the phase of the alpha oscillation is thought to regulate cortical excitability and subsequent interareal neural communication,[3,12] phase coupling provides a putative measure for studying long-range neural synchronization and connectivity of the alpha oscillation.[11,30] Yet only few studies have looked at the spatial localization of alpha phase coupling between cortical sources in EEG due to the low spatial resolution of EEG. However, the high spatial resolution of fMRI proves beneficial for overcoming the volume conductance problem in localizing EEG sources.[31,32] Significant spatial and temporal overlap has been found between alpha phase-coherency networks and fMRI-functional derived connectivity networks. Spontaneous changes in alpha-phase coherency have shown to covary with connectivity between the visual network and somatosensory network,[9] dorsal regions of the default mode network,[8] and the frontoparietal network.[26] Yet spontaneous modulations of the alpha rhythm in resting state studies are insufficient to study the dynamic relaying of information between higher order and sensory areas during visual processing as these processes are driven by sensory input.

Previous evidence has demonstrated intrinsic alpha oscillation can be entrained by external rhythmic light stimulation.[33–35] Furthermore, targeted entrainment of the intrinsic alpha frequency resulted in increased alpha phase coherency and BOLD connectivity in the occipitoparietal cortex.[35] We propose external modulations of the intrinsic alpha oscillation with rhythmic light stimulation activates stimulus-driven brain networks involved in visual perceptual processing and provide further insight into long-range, alpha-mediated communication processes. In this study, a modified entrainment paradigm from Jaeger and colleagues (*submitted)* was implemented to study changes in covarying EEG-fMRI whole-brain alpha connectivity networks during visual stimulation. We aim to show how the comparison of EEG-specific and fMRI-specific connectivity provide complementary findings in a trial-by-trial covariation analysis that gives new insight into functional role of alpha in mediating long range communication.

3.2 Methods:

3.2.1 Subjects:

34 (20 females, mean age 26.65, age range 19-37) healthy subjects with normal or corrected-to-normal vision and no history of neurological or psychiatric illness were recruited for this study. Three subjects discontinued the study preemptively during data acquisition and were excluded. Six subjects that did not have a definite alpha peak (alpha band-limited power below a threshold of 0.8 µV) during the resting state, eyes-closed, EEG only measure (used to determine the IAF) were also excluded from the study. Furthermore, subjects that had more than 30% movement-related artifacts in the EEG recordings either during the resting state session or the stimulation study were excluded from the study. Five subjects were excluded due to excessive movement. Data analyses was performed on 20 subjects (12 females, mean age 27.32, age range 19 -37). All subjects provided written consent prior to participating. Ethical approval was granted by an in-house ethics committee at TUM School of Medicine at the Technical University Munich.

3.2.2 *Data acquisition*

One concurrent EEG-fMRI session was acquired consisting of one five-minute eyes-closed, resting state run, followed by four fifteen-minute stimulation runs. fMRI data was acquired on a 3 Tesla Phillips Ingenia scanner with a 32-channel head coil. 150 and 450 echoplanar imaging (EPI) scans were acquired for the rest state run and the stimulation runs respectively (25 slices, TR = 2.0 seconds, voxel size = $3mm^3$, TE = 30ms, FOV = 192mm x 192mm x 82mm, matrix size = 64 x 62, flip angle = 70°, slice gap = 0.3mm). EEG data was acquired from 63 MR-compatible scalp electrodes (Easycap GmnH, Germany) with the online reference and ground electrode located at FCz and AFz respectively and an MR- compatible amplifier (BrainAmp MR, sampling rate 5kHz). One ECG electrode was placed between the shoulder blades. The scanner clock and amplifier clock were synchronized using a Sync Box (Brain Products, Germany). At the end of the study, an anatomical T1-weighted image was acquired (MPRAGE sequence, TE 3.3 ms, TR = 7.264 ms, flip angle = 8°, TI = 1060 ms, FoV = 240 mm x 240 mm x 170 mm, voxel size = $0.75mm^3$, matrix size = 320x320; 227 sagittal slices).

3.2.3 Determining individuals' intrinsic alpha frequency

Before placing participants into the MR scanner, subjects' intrinsic alpha frequency was determined in supine position in a separate testing room. Two minutes of resting-state, eyes-closed and resting-state eyes-open EEG data were acquired. EEG data was segmented into 4-second segments. Data was extracted from O1, O2, Oz, P1, P2, and Pz electrodes and baseline corrected to the average power of each segment. A fast-Fourier transform with 50% overlap between segments and a Hanning window taper was applied to calculate average power across segments. The most common peak frequency across all six electrodes was labeled as the intrinsic alpha frequency. Most previous studies used resting state, eyes-closed EEG measures to identify the IAF [33,36]. However, the peak alpha frequency has been shown to shift between rest and task.[37] Hence, an IAF value was determined separately for the eyes closed and eyes open EEG recordings to compare possible differences. If a subject's eyes-closed peak alpha power was less then 0.8 µV, the subject was excluded from the study. Six subjects were excluded from the study for having an alpha peak below the threshold.

3.2.4 Stimulation paradigm

Participants were cued to fixate on a red fixation cross and minimize blinking 2 – 6 seconds (randomized between trials) before presentation of a flickering radial checkerboard for 10 seconds. Four seconds after the end of the stimulation block participants were instructed to relax and allowed to blink. A variable rest period (30, 32, 34 seconds randomized across trials) ensued to allow the BOLD signal to return to baseline before presentation of the next stimulation condition. Presentation software (Neurobehavioral Systems, http://www.neurobs.com) and projected through a beamer onto a screen 1.5 meters from the participants head made visible to the participant by a mirror (visual angle 70°). Seven conditions were presented: no stimulation, rhythmic or arrhythmic stimulation at the IAF, 2 Hz below the IAF, and 2 Hz above the IAF. The flickering rate was determined through a custom-built LCD glass placed in front of a beamer. When a voltage is applied to the LCD glass, the glass darkens to a near opaque screen. The flickering rate was controlled through Arduino Microcontroller (Arduino Uno, Scarmagno, Italy) with a 50% duty cycle, denoting an opaque screen for half of the cycle and a transparent screen for the other half. A 25% jitter of the stimulation frequency was applied for the arrhythmic flicker conditions, maintaining the 50% duty cycle. Each stimulation condition was presented 3 times per session and 4 sessions of the stimulation paradigm were obtained resulting in 12 repetitions of each

flickering condition. The order of the flicker conditions was randomized across each session. Each scanning session lasted 15 minutes.

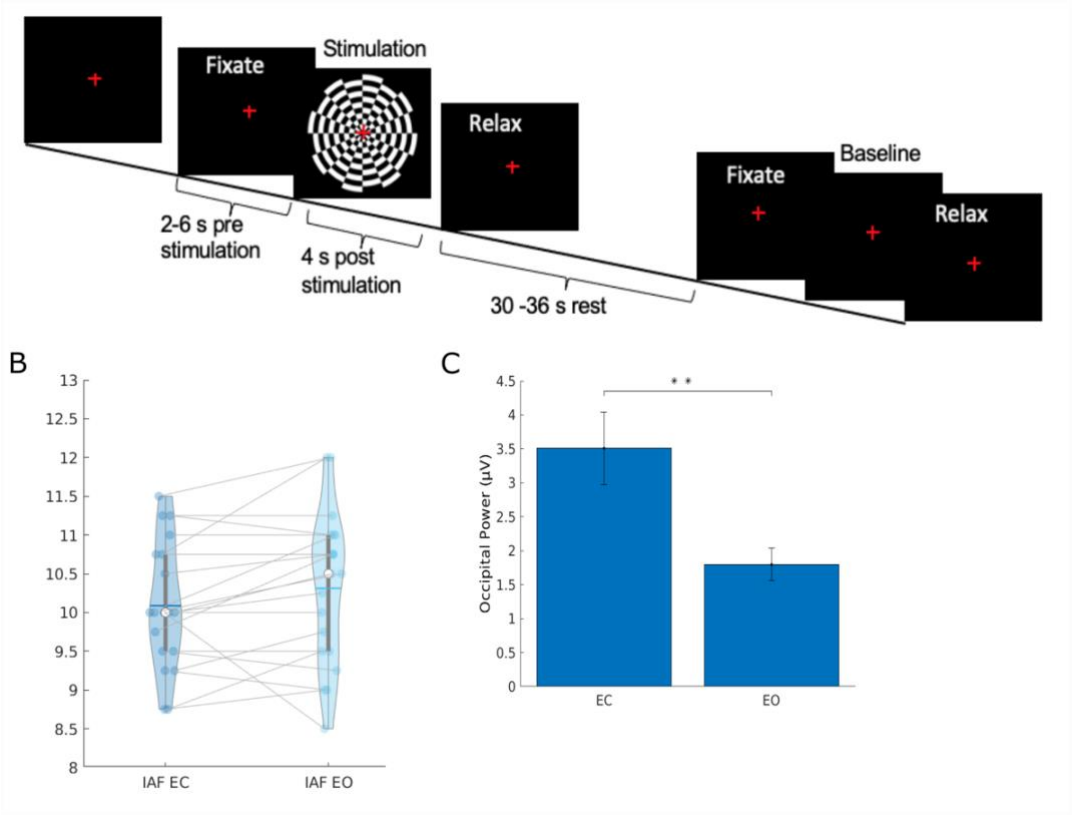

Figure 3.1: A) The stimulation paradigm consisted of seven conditions (rhythmic and arrhythmic stimulation at the IAF, two Hertz above the IAF and two Hertz below the IAF and a baseline condition. Participants were instructed to Fixate and not blink prior to stimulation onset. The fixation cue onset occurred randomly 2,4, ot 6 seconds to stimulation onset. Stimulation or the baseline condition occurred for 10 seconds followed by a clean four-second post-stimulation period. Participants were then instructed to relax and blink. The intertrial stimulation interval was either 30, 32, 34, or 36 seconds randomly assigned across trials. B) Variability in participants intrinsic alpha frequency. Participants eyes closed (EC) IAF ranged from 8.75 to 11.5 Hz (mean 10.1 Hz, median 10 Hz) and eyes open (EO) IAF ranged from 8.5 to 12 Hz (mean 10.3 Hz, median 10.5 Hz). C) Mean occipital power at the peak alpha frequency for eyes closed and eyes open across subjects. A paired t-test showed power at the eyes-closed IAF was significantly higher than the eyes-open IAF ($p = 0.000632$).

3.2.5 Data processing

3.2.5.1 Brainnetome Atlas

T1-weighted images normalized to MNI space were used to delineate brain regions into the 243 Brainnetome parcels.[38] To remain below the permitted average effective RF magnetic field value required for safe concurrent EEG-fMRI measurements, a smaller fMRI field of view was used which did not fully cover prefrontal and subcortical areas. Signal was

extracted from 203 regions with at least 70% of surface area within the field of view (see Supplementary Table 1 for a list of regions).

3.2.5.2 EEG data preprocessing

Scanner induced gradient artifacts were removed from the data using adaptive average artifact subtraction (AAS)[39] as implemented in BrainVision Analyzer. Cardioballistic artifacts were removed semi-automatically using the same method of average template subtraction. Further preprocessing was then carried out in EEGLAB.[40] Data was down sampled to 1000 Hz and bandpass filtered to range from 1 Hz to 30 Hz. Resting state data and the 10 seconds stimulation blocks from the four stimulation sessions were subsequently segmented to the fMRI TR time (2 second epochs). Data was re-referenced to the average. An independent component analysis was performed and components that were not labeled as brain by the ICLabel toolbox (Swartz Center for Computational Neuroscience, https://sccn.ucsd.edu/wiki/ICLabel) were removed. A maximum of 5 bad channels were re-interpolated into the data. Movement artifacts were further identified and removed using the Artifact Subspace Reconstruction algorithm in EEGLAB (timepoints exceeding 20 standard deviations of calibrated clean data or 25% of channels exceeded 7 standard deviation of average channel power). For the resting state EEG data, spectral content for ± 1Hz around the eyes-closed IAF was estimated for each epoch using a Fourier transform with a DPSS taper. The resting state data was subjected to a time-varying jackknife analysis (see supplementary methods) to assess spontaneous changes in alpha coherency. For the stimulation data, the spectral content was estimated for ± 1Hz around the stimulation frequency of interest or the eyes-open IAF for the baseline condition with cutoff. Tissue volume conductance was estimated from a template boundary element model as implemented in Fieldtrip.[41] EEG data was projected into source space using the partial canonical correlation (PCC) algorithm[42] with a regularize parameter set at 10% and averaged across regions of the Brainnetome atlas (excluding prefrontal and subcortical regions, see section 2.5.1). For the resting state session, spectral content was estimated around the eyes-closed IAF with a 2 Hz resolution using a Fourier transform with a DPSS filter. For the stimulation sessions, the spectral content was centered around the stimulation frequency or eyes-open IAF for the baseline condition, again with a 2 Hz resolution. The imaginary coherence between each parcel-pair was calculated from the complex part of the Fourier-transformed data for a given set of epochs as described in the connectivity analysis section. The imaginary coherence eliminates field spread of neighboring sources by removing zero-phase lag interactions.[43]

3.2.5.3 fMRI data preprocessing

FMRI preprocessing was performed using the CONN toolbox.[44] FMRI time series were slice-time corrected, motion-corrected through spatial realignment, and co-registered to the T1-weighted anatomical scan. The anatomical scan was segmented into six tissue probability maps and normalized to MNI space. The functional images were normalized to MNI space using the same transformations. The time series were then despiked using a brain-wavelet approach (Brain Wavelet Toolbox).[45] The time series were further denoised by using linear regression to regress out signal from white matter and cerebrospinal fluid (obtained from individual's masks in MNI space) as well as the Friston 24[46] movement parameters. The resting state data was subjected to a time-varying connectivity analysis (see supplementary methods for more details). For the stimulation sessions, a canonical hemodynamic response function was used to model visual stimulation onset and regress out the BOLD amplitude response in early visual areas in the fMRI time series. We assume the onset of high luminance would induce a strong BOLD amplitude response across all our stimulation conditions in early visual areas. As we were not interested in evoked visual responses, we regressed out luminance-induced BOLD changes. A temporal band-pass filter from 0.008 Hz to 0.09 Hz then applied to the residuals to mitigate non-hemodynamic influences on the BOLD signal. Subsequent time series were parcellated into the 203 regions of interest of the Brainnetome atlas, obtaining a mean time series per region.

3.2.5.4 Removal of motion artifacts

Any two-second epoch (corresponding to the TR duration) that contained movement artifacts either identified in EEG or fMRI were removed from both modalities. EEG-related artifacts were identified as mentioned in 2.5.2. For the fMRI data, the Artifact Detection Tools (ART) in the CONN toolbox was used to identify TR outliers that had an absolute value of threshold either 2 standard deviations away from the mean global signal or greater than 0.8mm translation or 0.034° rotation. Subjects that had more than 30% of movement related artifacts across the stimulation sessions were excluded from further data analysis. Eight subjects were excluded for having more than 30% noisy data.

3.2.6 Stimulation: connectivity analysis

3.2.6.1 EEG imaginary coherency

Imaginary coherency was calculated from the complex part of the Fourier-transformed data for a given set of epochs, which was used to obtain a value of phase coupling between each parcel-pair. Imaginary coherence eliminates field spread of neighboring sources by removing zero-phase lag interactions.[43] Imaginary coherence was calculated across trials for each stimulation condition across each region pair for each subject. For all subjects, the resulting seven coherency matrices [baseline, rhythmic IAF, arrhythmic IAF, rhythmic IAF +2 Hz, arrhythmic IAF + 2hZ, rhythmic IAF – 2Hz, arrhythmic IAF -2Hz] were Fisher Z-transformed and incorporated into an ANOVA. T-contrasts were then set on a given condition such as rhythmic IAF vs rhythmic all other frequencies to test for significant difference at each connection. Significant connections from resulting thresholded connectivity matrices were corrected for multiple comparisons using network-based statistics (NBS).[47]NBS statistic uses a non-parametric cluster-based approach that corrects for family-wise error rate (FWER) for mass univariate testing at each connection. 1000 permutations were performed to calculate an FWER-p-value to test for clusters of significantly connected nodes from the thresholded connectivity matrices. Degree centrality of resulting connectivity matrices was calculated by taking the sum of the number of direct connections for a given node to all other nodes that were above a given significance threshold.

3.2.6.2 fMRI connectivity

Pearson R correlation matrices were calculated from the denoised time series for each stimulation block and averaged across stimulation conditions for each subject. For all subjects, R-values in the resulting 7 connectivity matrices were Fischer Z-transformed and were subject to network-based statistics testing for significant difference in connectivity across stimulation conditions as described in section 3.2.6.1. Degree centrality was evaluated as described in section 3.2.6.1

3.2.6.3 Trial-by-trial EEG-fMRI covariation correlation

The fMRI-derived correlation matrices and EEG-coherency matrices were extracted for each stimulation trial. Covariation in EEG-derived and fMRI-derived connectivity was then assessed through R Pearson correlation of EEG coherency and fMRI connectivity matrices across trials for each stimulation condition. This resulted in seven covariation matrices corresponding to each flicker conditions. Network-based statistics was again performed to test for significant difference across subjects in connectivity across stimulation sections.

3.3 Results:

Individual variability in intrinsic alpha frequency

To ensure, the flicker frequency set for stimulation at the IAF conditions was within proximity of the true intrinsic rhythmic IAF, the IAF was determined for both eyes open and eyes closed. The alpha peak frequency measured from eyes-closed, resting-state, EEG only data varied across subjects ranging from 8.75 Hz to 11.5 Hz with mean of 10.1 Hz (Figure 1B). The alpha peak frequency measured during eyes-open, resting-state, EEG only measurement was on average slightly higher across subjects (range: range = 8.5 – 12 Hz, mean = 10.3 Hz). A paired t-test revealed alpha power (averaged across the electrodes O1, O2, Oz, P1, P2, and Pz) was significantly higher during eyes closed ($p = 0.000632$, Figure 1C), which suggests that more neural populations inherently synchronize at this frequency. A previous study also showed that stimulation at flicker frequencies within 1 Hz of the IAF seem drive entrainment.[35] For these reasons, the eyes closed peak alpha frequency was used as the IAF stimulation frequency. However, the baseline, eyes-open condition during the stimulation sessions was evaluated at the eyes open peak frequency.

Whole-brain EEG connectivity

Imaginary phase coherency between source pairs was used to evaluate source-reconstructed whole brain connectivity. Significant difference in connectivity across stimulation frequency was tested across subjects with network-based statistics[47] (significance threshold at $p < 0.05$), correcting for family-wise error rate through random permutation testing (1000 permutations, $p < 0.05$). Significant difference in connectivity between occipital parietal regions and frontal regions was observed for rhythmic stimulation at the IAF as compared to rhythmic stimulation of all other flicker frequencies (Figure 2). Interestingly, area 45 in the right inferior frontal gyrus (IFG) portrayed the highest degree centrality (11 connections) and was significantly connected with nodes in the postcentral, parietal and occipital cortex. The comparison of rhythmic stimulation at the IAF as compared to arrhythmic stimulation at the IAF resulted in connections trending towards significance ($p = 0.087$) between the left superior parietal lobe (SPL) and left and right superior frontal gyrus (SFG) and left IFG (Supplementary Figure 1). No significance was found for the comparison rhythmic stimulation at either 2Hz above or below the IAF frequencies greater than rhythmic stimulation at the IAF or the comparison arrhythmic stimulation greater than rhythmic stimulation at the IAF.

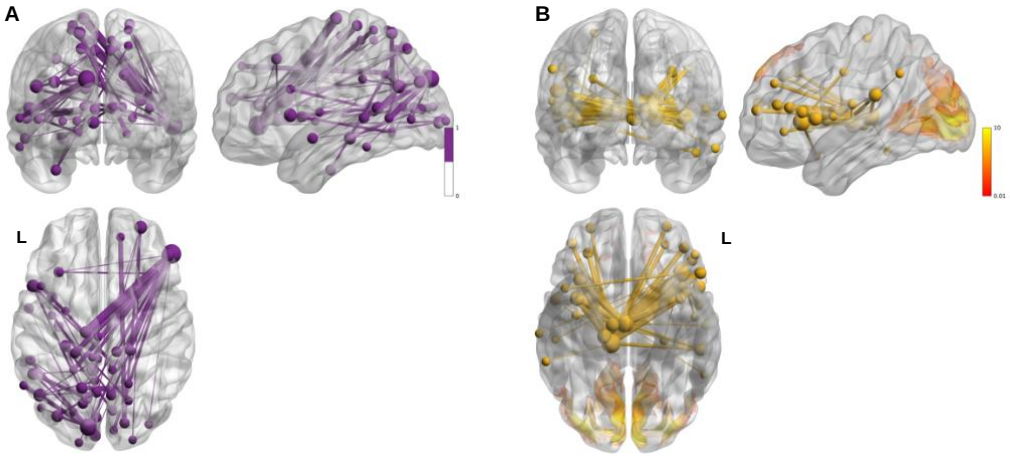

Figure 3.2: A) Significant connectivity in EEG. Significant difference in EEG coherency for rhythmic stimulation greater than rhythmic stimulation at the control frequencies (mass univariate testing at each connection, $p < 0.05$), family-wise error-corrected through random permutation testing (1000 permutations, $p < 0.05$). The node with the highest degree of centrality (11 connections) was in the right inferior gyrus B) Significant connectivity in fMRI. Significant difference in fMRI connectivity for rhythmic stimulation greater than rhythmic stimulation all other flicker frequencies (mass univariate testing at each connection, $p < 0.001$), family-wise error-corrected through random permutation testing (1000 permutations, $p < 0.05$). Task-activation statistical parameter maps were calculated for luminance-induced evoked BOLD response across all flicker conditions compared to baseline. Significant clusters ($p_{FWE} < 0.05$) are overlayed on the connectivity networks.

Whole-brain fMRI connectivity

Significant difference in connectivity across stimulation frequency was tested across subjects (significant threshold at $p < 0.001$), correcting for family-wise error rate through random permutation testing (1000 permutations, $p < 0.05$). Significant difference in connectivity between rhythmic stimulation at the IAF as compared to rhythmic stimulation at control flanker frequencies was observed between the right thalamus and inferior and middle frontal gyrus. Most notably, the node representing the highest degree centrality was the right occipital thalamus (15 connections), which was significantly connected with the left IFG and middle frontal gyrus (MFG) (Figure 2). Surprisingly, no significant connections were observed in the occipital cortex for rhythmic stimulation at the IAF. In a previous study,[35] increased connectivity was observed in the occipital cortex during rhythmic stimulation at the IAF, indicating a higher degree of synchronicity modulated by the alpha rhythm. However, in contrast to the previous study, the current study had shorter stimulation periods. A GLM analysis modeling significant activation with the canonical hemodynamic response function, showed significant task activation as compared to baseline for all stimulation frequencies in

occipital areas (Figure 1B) with no significant difference in activation between stimulation conditions (Supplementary Figure 2). Across all stimulation conditions, a high degree of synchronicity was observed in the visual network (Supplementary Figure 3). This suggests that the onset of the slow hemodynamic response, caused by sudden increase in luminance evoked by the flickering checkerboard, is similar across flicker conditions, which is further supported by no significant difference in BOLD amplitude between rhythmic IAF and other flicker frequencies (see supplementary information). The comparison greater connectivity for rhythmic stimulation versus arrhythmic stimulation at the IAF again yielded a trend towards significance ($p = 0.077$) within the precuneus, temporal gyrus, and pre- and post-central Gyrus (Supplementary Figure 1).

Significant covariation between EEG- and fMRI-derived connectivity

To spatially localize similarity in EEG- and fMRI-derived connectivity, we correlated variance in connectivity across trials between the two modalities for each stimulation condition. Significant covariation in connectivity was assessed through network-based statistics (significance: $p < 0.05$, 1000 permutations). Fluctuations in connectivity was significantly more correlated between EEG and fMRI during rhythmic stimulation at the IAF as compared to arrhythmic stimulation at IAF ($p = 0.011$) (Figure 3a). Interestingly, EEG-derived and fMRI-derived connectivity co-fluctuated significantly through thalamic connections projecting to the mid occipital and frontal cortex (Figure 3b). The number of significant connections that covaried were assigned to the YEO atlas intrinsic resting state networks.[48] A random permutation test was performed to test for significant number of between and within connections across the six pre-defined YEO atlas resting state networks (visual, default mode, somatosensory, ventral attention, dorsal attention and frontoparietal network) to associate the stimulation-based connectivity networks to known resting state networks. Connectivity significantly covaried between regions of the ventral attention and frontoparietal network (p-value = 0.0004, Supplementary Figure 6). Covarying connectivity for the comparison of rhythmic versus arrhythmic stimulation at the IAF was significantly greater than rhythmic versus arrhythmic stimulation at control frequencies between regions of the ventral attention and frontoparietal network as well as the left thalamus (Supplementary Figure 5A). The difference in correlation in covariance between rhythmic stimulation at the IAF versus rhythmic stimulation at other flicker frequencies trended toward significance ($p = 0.081$) with the highest degree centrality occurring in the thalamus (Supplementary Figure 5B).

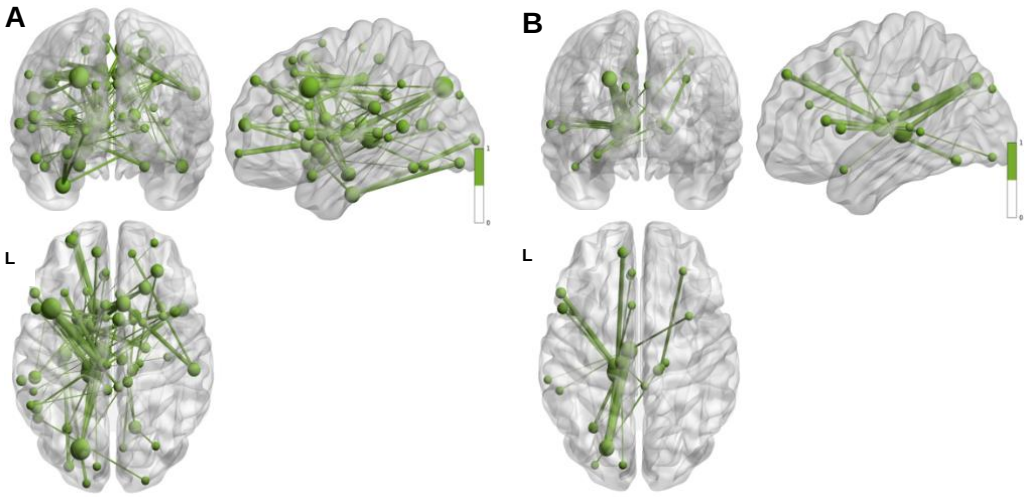

Figure 3.3: Trial-by-trial covariance between EEG-derived and fMRI-derived connectivity. A) Significant covariance between connectivity in EEG and fMRI for the comparison rhythmic stimulation at the IAF as compared to arrhythmic stimulation at the IAF (mass univariate testing at $p < 0.05$, 1000 permutations, $p_{FWER} < 0.05$). B) Visualizes only those significant connections that are directly connected with the thalamus.

3.4 Discussion:

This study implements a novel application of a visual entrainment paradigm to investigate covarying EEG- and fMRI-derived functional connectivity changes specific to modulations in the alpha oscillation. We found increased alpha phase coherency between the occipitoparietal cortex and frontal cortex in the EEG data during rhythmic stimulation of the IAF in comparison to rhythmic stimulation at neighboring frequencies. Whereas in the fMRI data, functional connectivity strongly correlated between the right thalamus, specifically the occipital thalamus, and frontal regions during rhythmic stimulation of the IAF. Interestingly when correlating trial-by-trial covariance between the two modalities, co-fluctuations in connectivity between the occipitoparietal cortex and frontal regions were mediated by thalamic connections during rhythmic stimulation of the IAF, suggesting alpha-mediated connectivity occurs through thalamocortical connections.

The high degree of functional connectivity emanating from the inferior frontal gyrus observed in both the EEG-derived and fMRI-derived connectivity (Figure 2) is in line with task-based studies. A granger causality analysis demonstrated occipital alpha modulations were driven by top-down influence of the right inferior frontal gyrus and the frontal eye field

during visual spatial attention EEG study.[49] Another EEG study found increase alpha power in frontal and parietal areas during top-down modulations of attention.[50] In the current study, strong alpha coherency was observed between the right IFG and parietal and occipital areas during rhythmic stimulation of the IAF. In the fMRI, connectivity in the IFG strongly connected with right thalamus during rhythmic stimulation of the IAF. Previous concurrent EEG-fMRI study also observed a positive correlation between alpha power and decision-related BOLD amplitude in IFG and MFG.[51] Furthermore, alpha phase correlated with BOLD activity in the thalamus.[51] In our results, covariation in connectivity between the two modalities in occipitoparietal and frontal nodes strongly correlated with the thalamus (Figure 3) and unifies previous EEG and fMRI findings.

The combined covariation results also provide functional evidence for thalamic structural projections. The pulvinar is a high-order thalamic nucleus thought to regulate information flow in higher-order visual processing along structural fiber tracts projecting to the frontal and occipital cortex.[52–54] The pulvinar relays feedforward information from layer 5 projections to layer 4 projections in higher order cortical areas,[55] whereas feedback projections originating in layer 6 are relayed through the pulvinar to layer 1 in lower cortical areas.[56,57] Invasive electrophysiological recordings in animals provide evidence that increase in cortical synchronization of the alpha oscillation is mediated through pulvino-cortical projections.[53,58] Together with task-based, electrophysiology, and structural findings our results suggest cortical alpha coherency is mediated through thalamic connections most likely localized in the pulvinar and involved in higher-order visual processing.[53,54] We note that we cannot determine whether the resulting long-range functional connectivity in our study was driven by feedforward or feedback processes. However, most likely sensory stimulation activates frontal connections that also reverberate back to sensory areas. The cortico-thalamic connections observed in the covariation connectivity spatially mapped to regions associated with higher-order ventral attention and frontoparietal network (SI Figure 6).

Only recently have scientist began to use dynamic multimodal functional connectivity analyses to explore how the temporal and spatial overlap of electrophysiology and fMRI-derived connectomes contribute to the functional relevance of brain connectomes in cognition. Resting state studies investigating spontaneous changes in alpha phase coherency and BOLD connectivity have found functional connectivity in both modalities to correlate with visual network and somatosensory network[9] and the posterior default mode network.[59]

Spatial correlation between increased alpha power and functional connectivity in the visual network[60,61] and default mode network[59,62,63] as well as reduced connectivity between the DMN and dorsal attention network.[64] Electrophysiology connectomes derived from frequency-specific phase or power measures may dissociate and indicate different neurophysiological processes.[65] We also analyzed time-varying co-fluctuations in spontaneous alpha coherency and BOLD functional connectivity during rest and found the strongest covariation across nodes spatially associated with the default mode network and visual and frontoparietal network (Supplementary Figure 7). The different distribution of covarying connectivity during rest and visual stimulation observed in our results support that frequency-specific neural oscillations inform about dynamic, state-dependent reorganization of functional networks.[66,67] FMRI-derived functional networks are relatively stable across rest and task[68] with only moderate task-specific, network reconfiguration occurring[69–71] with the thalamus thought to be implicated in governing these changes.[72,73] Furthermore, electrophysiological connectomes are spatially stable across time.[74,75] Yet frequency-specific functional networks reorganization occur on separate time scales independent from the canonical resting state network reorganization[75] and are thought to serve frequency-specific information processing.[66,76] Therefore frequency-specific EEG-derived connectomes can provide a better mechanistic understanding of long-range information exchange in context of distinct cognitive processes.[66,77]

In a previous study, rhythmic stimulation at the IAF resulted in increased occipital parietal phase coherency and BOLD functional connectivity as compared to rhythmic stimulation at other frequencies.[35] In the current study, occipitoparietal regions still showed increased alpha coherency for rhythmic stimulation at the IAF as compared to control frequencies. However alpha phase coherency was stronger between the inferior frontal cortex and posterior regions. There was also strong BOLD connectivity between the inferior frontal cortex and the thalamus (Figure 2). Yet no significant connectivity was observed for rhythmic stimulation at the IAF in the visual cortex. This was surprising because this study implemented more trials and used control frequencies that were equidistant from the IAF for all subjects. However, the duration of stimulation was shortened in the current study to increase trial number and reduce eye blinking during visual stimulation, which may corroborate alpha phase coherency.[78] The slow hemodynamic response evoked by the onset of the presentation of a visual stimulus was spatially similar across all flicker conditions (Supplementary Figure 2) and resulted in increased connectivity across visual areas across all conditions (Supplementary Figure 3).

This suggests on the one hand that the increased occipitoparietal connectivity observed for rhythmic stimulation at the IAF in the previous study occurred during the latter portion of the stimulation block (Supplementary Figure 4), but also that visual stimulation at the IAF entrains long-range alpha quickly.

We also note that the comparison rhythmic stimulation at the IAF greater than rhythmic stimulation at other control frequencies elicited significant connectivity in the separate EEG and fMRI analyses, but only trended towards significance in the covariation analysis (Supplementary Figure 5B). When rhythmic stimulation is compared to arrhythmic stimulation, stimulation at the IAF still exhibits significantly more correlation in co-fluctuating connectivity as compared to stimulation at the control frequencies (Supplementary Figure 5A). This suggests that although the variance only significantly correlates for stimulation at the IAF, rhythmic stimulation at any frequency may evoke synchronous neural activity that may also induce rhythmic co-fluctuations in both EEG and fMRI. However, the correlation in connectivity between the modalities is much weaker as the comparison rhythmic versus arrhythmic stimulation at a given control frequency resulted in no significant joint connectivity.

In conclusion, we used visual stimulation to modulate individual's alpha frequency and assessed subsequent electrophysiological and fMRI functional connectivity. We show that modulations to the alpha frequency result in increased frontal-posterior alpha coherency. Results from fMRI-derived connectivity and trial-by-trial correlation between the two modalities suggest that cortical alpha coherency are established through thalamic connections, suggesting alpha communication occurs through cortico-thalamic connections. These results are in line with electrophysiology studies that suggest sensory alpha-mediated modulations occur through cortico-thalamic projections. Furthermore, we show external sensory stimulation can be used to study frequency-specific network reorganization in concurrent EEG-fMRI in a brain state that more resembles task-based sensory processing. This application has the potential to be applied to other canonical frequency bands. Along with behavioral performance studies performed under entrainment and effective connectivity studies, this method has the potential to be applied in the future to study frequency-specific networks involved in distinct cognitive process.

3.5 References:

1. Crick, F. & Koch, C. A framework for consciousness. *Nat. Neurosci.* **6**, 119–126 (2003).
2. Varela, F., Lachaux, J. P., Rodriguez, E. & Martinerie, J. The brainweb: Phase synchronization and large-scale integration. *Nat. Rev. Neurosci. 2001 24* **2**, 229–239 (2001).
3. Fries, P. Rhythms For Cognition: Communication Through Coherence. *Neuron* **88**, 220 (2015).
4. Siegel, M., Donner, T. H. & Engel, A. K. *Spectral fingerprints of large-scale neuronal interactions*. (2012).
5. Bastos, A. M. *et al.* Visual Areas Exert Feedforward and Feedback Influences through Distinct Frequency Channels. *Neuron* **85**, 390–401 (2015).
6. Fox, M. D. *et al.* The human brain is intrinsically organized into dynamic, anticorrelated functional networks. *Proc. Natl. Acad. Sci.* **102**, 9673–9678 (2005).
7. Raichle, M. E. The restless brain: How intrinsic activity organizes brain function. *Philosophical Transactions of the Royal Society B: Biological Sciences* (2015) doi:10.1098/rstb.2014.0172.
8. Vidaurre, D. *et al.* Spontaneous cortical activity transiently organises into frequency specific phase-coupling networks. *Nat. Commun.* **9**, (2018).
9. Wirsich, J., Giraud, A. L. & Sadaghiani, S. Concurrent EEG- and fMRI-derived functional connectomes exhibit linked dynamics. *Neuroimage* **219**, (2020).
10. Sadaghiani, S. & Wirsich, J. Intrinsic connectome organization across temporal scales: New insights from cross-modal approaches. *Netw. Neurosci.* **4**, 1 (2020).
11. Sadaghiani, S., Brookes, M. J. & Baillet, S. Connectomics of human electrophysiology. *Neuroimage* **247**, 118788 (2022).
12. Jensen, O. & Mazaheri, A. Shaping Functional Architecture by Oscillatory Alpha Activity: Gating by Inhibition. *Front. Hum. Neurosci.* (2010) doi:10.3389/fnhum.2010.00186.
13. Ergenoglu, T. *et al.* Alpha rhythm of the EEG modulates visual detection performance in humans. *Brain Res. Cogn. Brain Res.* **20**, 376–383 (2004).
14. Van Dijk, H., Schoffelen, J. M., Oostenveld, R. & Jensen, O. Prestimulus Oscillatory Activity in the Alpha Band Predicts Visual Discrimination Ability. *J. Neurosci.* **28**, 1816–1823 (2008).

15. Thut, G., Nietzel, A., Brandt, S. A. & Pascual-Leone, A. α-Band Electroencephalographic Activity over Occipital Cortex Indexes Visuospatial Attention Bias and Predicts Visual Target Detection. *J. Neurosci.* **26**, 9494 (2006).
16. Hanslmayr, S. *et al.* Visual discrimination performance is related to decreased alpha amplitude but increased phase locking. *Neurosci. Lett.* **375**, 64–68 (2005).
17. Sauseng, P. *et al.* EEG alpha synchronization and functional coupling during top-down processing in a working memory task. *Hum. Brain Mapp.* (2005) doi:10.1002/hbm.20150.
18. Busch, N. A., Dubois, J. & VanRullen, R. The Phase of Ongoing EEG Oscillations Predicts Visual Perception. *J. Neurosci.* **29**, 7869–7876 (2009).
19. Mathewson, K. E., Gratton, G., Fabiani, M., Beck, D. M. & Ro, T. To See or Not to See: Prestimulus α Phase Predicts Visual Awareness. *J. Neurosci.* **29**, 2725–2732 (2009).
20. Zumer, J. M., Scheeringa, R., Schoffelen, J. M., Norris, D. G. & Jensen, O. Occipital Alpha Activity during Stimulus Processing Gates the Information Flow to Object-Selective Cortex. *PLOS Biol.* **12**, e1001965 (2014).
21. Scheeringa, R., Mazaheri, A., Bojak, I., Norris, D. G. & Kleinschmidt, A. Modulation of Visually Evoked Cortical fMRI Responses by Phase of Ongoing Occipital Alpha Oscillations. *J. Neurosci.* (2011) doi:10.1523/JNEUROSCI.4697-10.2011.
22. Worden, M. S., Foxe, J. J., Wang, N. & Simpson, G. V. *Anticipatory Biasing of Visuospatial Attention Indexed by Retinotopically Specific-Band Electroencephalography Increases over Occipital Cortex*. http://www.jneurosci.org/cgi/content/full/4016 (2000).
23. Foxe, J. J. & Snyder, A. C. The role of alpha-band brain oscillations as a sensory suppression mechanism during selective attention. *Front. Psychol.* **2**, 154 (2011).
24. Hanslmayr, S., Gross, J., Klimesch, W. & Shapiro, K. L. The role of alpha oscillations in temporal attention. *Brain Research Reviews* (2011) doi:10.1016/j.brainresrev.2011.04.002.
25. Scheeringa, R., Petersson, K. M., Kleinschmidt, A., Jensen, O. & Bastiaansen, M. C. m. EEG Alpha Power Modulation of fMRI Resting-State Connectivity. *Brain Connect.* **2**, 254–264 (2012).
26. Sadaghiani, S. *et al.* Alpha-Band Phase Synchrony Is Related to Activity in the Fronto-Parietal Adaptive Control Network. *J. Neurosci.* (2012) doi:10.1523/JNEUROSCI.1358-12.2012.

27. Wang, C., Rajagovindan, R., Han, S. M. & Ding, M. Top-Down Control of Visual Alpha Oscillations: Sources of Control Signals and Their Mechanisms of Action. *Front. Hum. Neurosci.* **10**, (2016).
28. Samaha, J., Bauer, P., Cimaroli, S. & Postle, B. R. Top-down control of the phase of alpha-band oscillations as a mechanism for temporal prediction. *Proc. Natl. Acad. Sci.* (2015) doi:10.1073/pnas.1503686112.
29. Saalmann, Y. B., Pinsk, M. A., Wang, L., Li, X. & Kastner, S. The pulvinar regulates information transmission between cortical areas based on attention demands. *Science (80-.).* (2012) doi:10.1126/science.1223082.
30. Marzetti, L. *et al.* Brain Functional Connectivity Through Phase Coupling of Neuronal Oscillations: A Perspective From Magnetoencephalography. *Front. Neurosci.* **13**, (2019).
31. Laufs, H. A personalized history of EEG–fMRI integration. *Neuroimage* **62**, 1056–1067 (2012).
32. Tagliazucchi, E. & Laufs, H. Multimodal imaging of dynamic functional connectivity. *Front. Neurol.* **6**, 10 (2015).
33. Notbohm, A., Kurths, J. & Herrmann, C. S. Modification of Brain Oscillations via Rhythmic Light Stimulation Provides Evidence for Entrainment but Not for Superposition of Event-Related Responses. *Front. Hum. Neurosci.* (2016) doi:10.3389/fnhum.2016.00010.
34. Mathewson, K. E. *et al. Making Waves in the Stream of Consciousness: Entraining Oscillations in EEG Alpha and Fluctuations in Visual Awareness with Rhythmic Visual Stimulation*. (2012).
35. Jaeger, C. *et al.* Targeted rhythmic visual stimulation at individual subjects' intrinsic alpha frequency causes selective increase of occipitoparietal BOLD-fMRI and EEG functional connectivity. *submitted* (2022).
36. Barzegaran, E., Vildavski, V. Y. & Knyazeva, M. G. Fine Structure of Posterior Alpha Rhythm in Human EEG: Frequency Components, Their Cortical Sources, and Temporal Behavior. *undefined* **7**, (2017).
37. Haegens, S., Cousijn, H., Wallis, G., Harrison, P. J. & Nobre, A. C. Inter- and intra-individual variability in alpha peak frequency. *Neuroimage* **92**, 46–55 (2014).
38. Fan, L. *et al.* The Human Brainnetome Atlas: A New Brain Atlas Based on Connectional Architecture. *Cereb. Cortex* **26**, 3508–3526 (2016).
39. Allen, P. J., Josephs, O. & Turner, R. A Method for Removing Imaging Artifact from

Continuous EEG Recorded during Functional MRI. *Neuroimage* **12**, 230–239 (2000).

40. Delorme, A. & Makeig, S. EEGLAB: an open source toolbox for analysis of single-trial EEG dynamics including independent component analysis. *J. Neurosci. Methods* **134**, 9–21 (2004).
41. Oostenveld, R., Fries, P., Maris, E. & Schoffelen, J. M. FieldTrip: Open source software for advanced analysis of MEG, EEG, and invasive electrophysiological data. *Comput. Intell. Neurosci.* **2011**, (2011).
42. Zhuang, X., Yang, Z. & Cordes, D. A technical review of canonical correlation analysis for neuroscience applications. *Hum. Brain Mapp.* **41**, 3807–3833 (2020).
43. Nolte, G. *et al.* Identifying true brain interaction from EEG data using the imaginary part of coherency. *Clin. Neurophysiol.* **115**, 2292–2307 (2004).
44. Whitfield-Gabrieli, S. & Nieto-Castanon, A. Conn: a functional connectivity toolbox for correlated and anticorrelated brain networks. *Brain Connect.* **2**, 125–141 (2012).
45. Patel, A. X. *et al.* A wavelet method for modeling and despiking motion artifacts from resting-state fMRI time series. *Neuroimage* **95**, 287–304 (2014).
46. Friston, K. J., Williams, S., Howard, R., Frackowiak, R. S. J. & Turner, R. Movement-related effects in fMRI time-series. *Magn. Reson. Med.* **35**, 346–355 (1996).
47. Zalesky, A., Fornito, A. & Bullmore, E. T. Network-based statistic: identifying differences in brain networks. *Neuroimage* **53**, 1197–1207 (2010).
48. Thomas Yeo, B. T. *et al.* The organization of the human cerebral cortex estimated by intrinsic functional connectivity. *J. Neurophysiol.* **106**, 1125–1165 (2011).
49. Wang, C., Rajagovindan, R., Han, S. M. & Ding, M. Top-down control of visual alpha oscillations: Sources of control signals and their mechanisms of action. *Front. Hum. Neurosci.* **10**, 15 (2016).
50. Misselhorn, J., Friese, U. & Engel, A. K. Frontal and parietal alpha oscillations reflect attentional modulation of cross-modal matching. *Sci. Reports 2019 91* **9**, 1–11 (2019).
51. Walz, J. M. *et al.* Prestimulus EEG Alpha Oscillations Modulate Task-Related fMRI BOLD Responses to Auditory Stimuli. *Neuroimage* **113**, 153 (2015).
52. Leh, S. E., Chakravarty, M. M. & Ptito, A. The connectivity of the human pulvinar: a diffusion tensor imaging tractography study. *Int. J. Biomed. Imaging* **2008**, (2008).
53. Saalmann, Y. B., Pinsk, M. A., Wang, L., Li, X. & Kastner, S. The pulvinar regulates information transmission between cortical areas based on attention demands. *Science* **337**, 753–756 (2012).
54. Guedj, C. & Vuilleumier, P. Functional connectivity fingerprints of the human

pulvinar: Decoding its role in cognition. *Neuroimage* **221**, 117162 (2020).

55. Felleman, D. J. & Van Essen, D. C. Distributed hierarchical processing in the primate cerebral cortex. *Cereb. Cortex* **1**, 1–47 (1991).
56. Benevento, L. A. & Rezak, M. The cortical projections of the inferior pulvinar and adjacent lateral pulvinar in the rhesus monkey (Macaca mulatta): an autoradiographic study. *Brain Res.* **108**, 1–24 (1976).
57. Shipp, S. The functional logic of cortico-pulvinar connections. *Philos. Trans. R. Soc. B Biol. Sci.* **358**, 1605 (2003).
58. Cortes, N., Abbas Farishta, R., Ladret, H. J. & Casanova, C. Corticothalamic Projections Gate Alpha Rhythms in the Pulvinar. *Front. Cell. Neurosci.* **15**, 487 (2021).
59. Vidaurre, D. *et al.* Spontaneous cortical activity transiently organises into frequency specific phase-coupling networks. *Nat. Commun. 2018 91* **9**, 1–13 (2018).
60. Hillebrand, A., Barnes, G. R., Bosboom, J. L., Berendse, H. W. & Stam, C. J. Frequency-dependent functional connectivity within resting-state networks: an atlas-based MEG beamformer solution. *Neuroimage* **59**, 3909–3921 (2012).
61. Hipp, J. F., Hawellek, D. J., Corbetta, M., Siegel, M. & Engel, A. K. Large-scale cortical correlation structure of spontaneous oscillatory activity. *Nat. Neurosci. 2012 156* **15**, 884–890 (2012).
62. Brookes, M. J. *et al.* Investigating the electrophysiological basis of resting state networks using magnetoencephalography. *Proc. Natl. Acad. Sci. U. S. A.* **108**, 16783–16788 (2011).
63. Clancy, K. J. *et al.* Transcranial stimulation of alpha oscillations up-regulates the default mode network. *Proc. Natl. Acad. Sci. U. S. A.* **119**, (2022).
64. Chang, C., Liu, Z., Chen, M. C., Liu, X. & Duyn, J. H. EEG correlates of time-varying BOLD functional connectivity. *Neuroimage* **72**, 227–236 (2013).
65. Siems, M. & Siegel, M. Dissociated neuronal phase- and amplitude-coupling patterns in the human brain. *Neuroimage* **209**, 116538 (2020).
66. Sadaghiani, S., Brookes, M. J. & Baillet, S. Connectomics of human electrophysiology. *Neuroimage* **247**, 118788 (2022).
67. Siegel, M., Donner, T. H. & Engel, A. K. Spectral fingerprints of large-scale neuronal interactions. *Nat. Rev. Neurosci. 2012 132* **13**, 121–134 (2012).
68. Cole, M. W., Bassett, D. S., Power, J. D., Braver, T. S. & Petersen, S. E. Intrinsic and task-evoked network architectures of the human brain. *Neuron* **83**, 238–251 (2014).

69. Hearne, L. J., Cocchi, L., Zalesky, A. & Mattingley, J. B. Reconfiguration of Brain Network Architectures between Resting-State and Complexity-Dependent Cognitive Reasoning. *J. Neurosci.* **37**, 8399–8411 (2017).
70. Jung, K. *et al.* Effective connectivity during working memory and resting states: A DCM study. *Neuroimage* **169**, 485–495 (2018).
71. Kraus, B. T. *et al.* Network variants are similar between task and rest states. *Neuroimage* **229**, 117743 (2021).
72. Di, X., Gohel, S., Kim, E. H. & Biswal, B. B. Task vs. rest-different network configurations between the coactivation and the resting-state brain networks. *Front. Hum. Neurosci.* **0**, 493 (2013).
73. Nakajima, M. & Halassa, M. M. Thalamic control of functional cortical connectivity. *Curr. Opin. Neurobiol.* **44**, 127–131 (2017).
74. Nentwich, M. *et al.* Functional connectivity of EEG is subject-specific, associated with phenotype, and different from fMRI. *Neuroimage* **218**, 117001 (2020).
75. Mostame, P. & Sadaghiani, S. Oscillation-Based Connectivity Architecture Is Dominated by an Intrinsic Spatial Organization, Not Cognitive State or Frequency. *J. Neurosci.* **41**, 179–192 (2021).
76. Florin, E. & Baillet, S. The brain's resting-state activity is shaped by synchronized cross-frequency coupling of neural oscillations. *Neuroimage* **111**, 26–35 (2015).
77. Hari, R. & Parkkonen, L. The brain timewise: how timing shapes and supports brain function. *Philos. Trans. R. Soc. B Biol. Sci.* **370**, (2015).
78. Bonfiglio, L. *et al.* Reciprocal dynamics of EEG alpha and delta oscillations during spontaneous blinking at rest: a survey on a default mode-based visuo-spatial awareness. *Int. J. Psychophysiol.* **80**, 44–53 (2011).

Appendices:

Appendix A: Supplementary Methods:

Dynamic resting state functional connectivity

To analyze the time-varying co-fluctuations in synchronicity between EEG and fMRI, a jackknife correlation approach was used. The jackknife correlation approach has a finer-grained temporal resolution and more accurately detects fluctuations in signal covariance than more common sliding window approach (Fransson 2018, Thompson 2018). For the EEG data, imaginary coherency was averaged across two second epochs for each region pair,

iteratively leaving out one epoch each time. FMRI connectivity was calculated using Pearson correlations across time points again iteratively leaving out one time point. This resulted in an EEG and fMRI jackknife connectivity (JC) matrix of length (epochs/timepoints – 1). The EEG and fMRI JC matrices were Fischer Z-transformed. Pearson R correlation matrices were calculated per node pair between the EEG and fMRI JC matrices. We note the hemodynamic response to neural activity is delayed by about six seconds (Liao 2002, Soon 2003). Therefore, a time lag of 3 epochs, corresponding to six seconds, was incorporated into the EEG data. This resulted in a joint EEG-fMRI correlation matrix, in which strength of correlation between connectivity in EEG and fMRI data is captured.

Non-parametric significance testing of resting state covariation connectivity matrix

Statistical significance of covariation connectivity matrices for each connection was assessed by comparing the joint EEG-fMRI correlation matrix to a null model. Creation of the null model was adapted from Wirsich et al. (2020), in which the temporally phase-randomized fMRI time series are used to create null-model correlation matrices. The phase-randomized time series were created based on the method implemented by Dolan & Spano (2001). For each connection, the Fourier transform of the jackknife time series was taken. The phases of the transformed time series were then randomly shuffled before taking the inverse Fourier transform to obtain fMRI phase-randomized jackknife time series. FMRI correlation matrices were then calculated for each phase-randomized jackknife time course. Subsequent pearson R correlation matrices were then calculated between the real EEG coherency data and the phase-randomized fMRI connectivity matrices. Because we were interested in the dynamic connectivity between modalities, only the fMRI modality was phase randomized. The phase-randomization of the jackknife fMRI time series and calculation of Pearson R correlation matrices between randomized fMRI connectivity time series and unaltered EEG coherency time series was carried out 50 times for each connection and each subject. To create a null correlation model, the phase-randomized correlation matrices were average across iterations for each subject. On a group level, a connection-wise pair t-test was performed across subjects between the actual covariation correlation matrix and the null model. The resulting p-values were Bonferroni-corrected for the number of connections.

Intrinsic functional connectivity maps

The top 200 significant connections for the joint EEG-fMRI resting state and stimulation correlation matrices were mapped to the 7 canonical ICNs defined by the Yeo Atlas (Yeo

2011). Significant number of connections between and within a network was tested by randomly selecting 200 connections and assigning them to the corresponding networks. This was repeated 100,000 times. The number of times the random connections exceeded the actual significant value was counted and divided by number of iterations to attain a p-value. All connections below a p-value of 0.00025, Bonferroni-corrected for number of comparisons, for a given contrast of interest are shown.

BOLD activation GLM Analysis

To ensure BOLD activity increased in occipital regions during the stimulation blocks, a GLM analysis was performed. The normalized and preprocessed functional images were smoothened with an 8mm Gaussian kernel. On the subject level, a GLM was implemented using a canonical hemodynamic response function was used model BOLD amplitude changes for each flicker condition and the baseline condition. The six head motion parameters were also included into the design matrix as nuisance regressors. A high pass filter of 0.0078 Hz (128 sec) was applied to remove slow scanner drifts. Statistical parametric maps were calculated for each stimulation condition compared to baseline condition as well as all task activation (i.e., all flicker conditions) compared to baseline. The threshold of significance was set at $p_{cc} < 0.05$, cluster-corrected for multiple comparisons on the voxel uncorrected level ($p_u < 0.001$).

Occipitoparietal fMRI connectivity varying with duration of stimulation block

Alpha-mediated occipitoparietal functional connectivity, elicited through rhythmic stimulation of the IAF, was previously investigated in Jaeger and others (*submitted)*. The previous study had stimulated for 20 second duration. The parcellated fMRI time series, delineated into regions from the Glasser atlas, (Glasser 2016) were taken from that study and segmented into two 10 second segments. fMRI Pearson R correlations were then performed for all occipitoparietal regions (see Jaeger et al. *submitted* for list of regions) either across the first 10 second block or the last 10 second block for each stimulation condition and averaged across the two scanning sessions. The resulting fourteen correlation matrices corresponding to rhythmic and arrhythmic stimulation at the IAF, 7, 8, 9, 10, 11 and 12 Hz were subjected to ANOVA. Network-based statistics (Zalesky 2010) were performed for the contrast rhythmic stimulation at the IAF more significant than rhythmic stimulation at all other frequencies. No significant connectivity was found in the first 10 second segments for

rhythmic stimulation at the IAF. Significant increase in fMRI connectivity was observed in occipitoparietal regions during the latter half of the stimulation block for rhythmic stimulation at the IAF.

Appendix B: Supplementary Figures

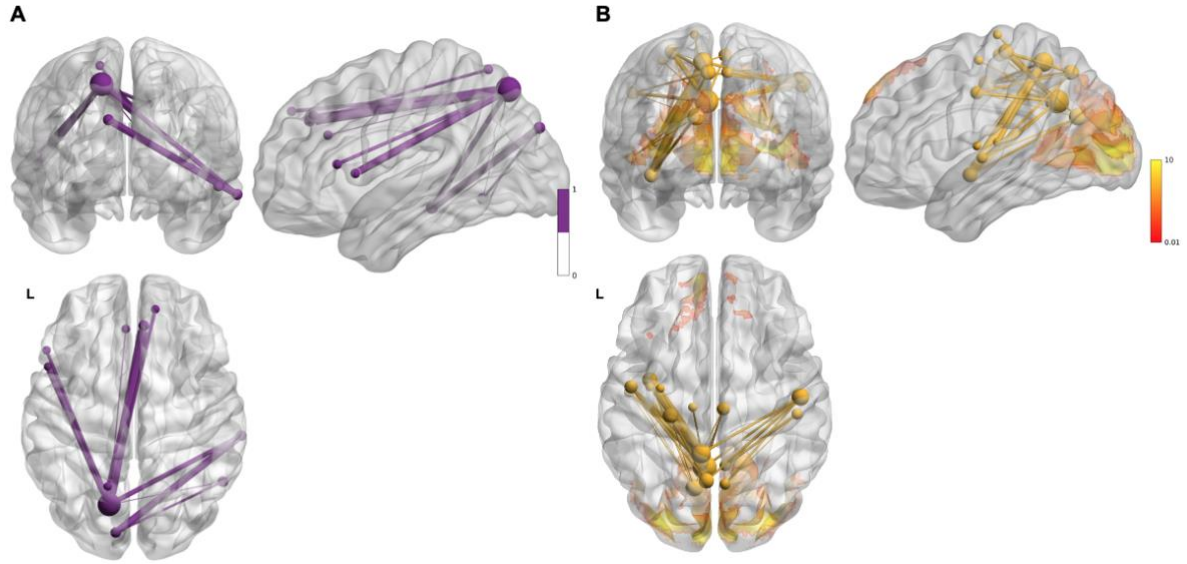

Supplementary Figure 1: A) In the EEG, the comparison of alpha coherency at rhythmic versus arrhythmic stimulation at the IAF trended towards significance after family-wise error rate correction ($p = 0.087$). The left superior parietal region had the largest degree centrality with 8 connections. B) In the fMRI data, the comparison of connectivity between rhythmic versus arrhythmic stimulation at the IAF trended towards significance after family-wise error rate correction ($p = 0.07$). Again, the stimulation-activation statistical parameter map of the evoked BOLD response averaged across all flicker conditions compared to baseline ($p_{FWER} < 0.05$) is overlayed on the connectivity network.

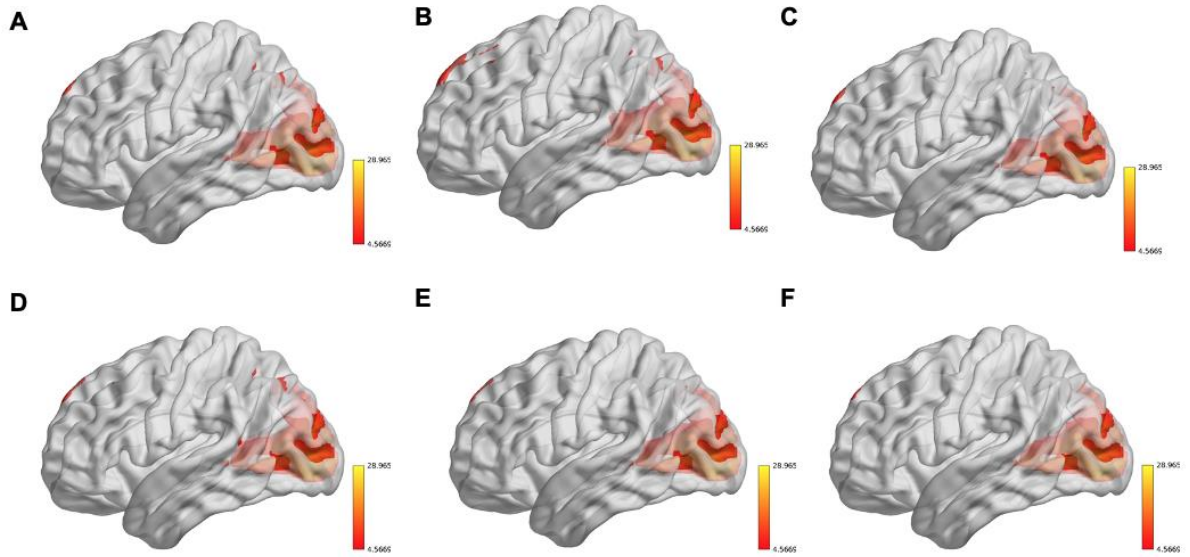

Supplementary Figure 2: Significant BOLD activation elicited by flicker frequency. Statistical parameter maps were thresholded for voxel-wise family error correction ($p_{FWER} < 0.05$). Significant activation for stimulation at A) rhythmic IAF, B) arrhythmic IAF, C) rhythmic 2Hz above the IAF, D) arrhythmic 2 Hz above the IAF, E) rhythmic 2 Hz below the IAF, and F) arrhythmic 2 Hz below the IAF.

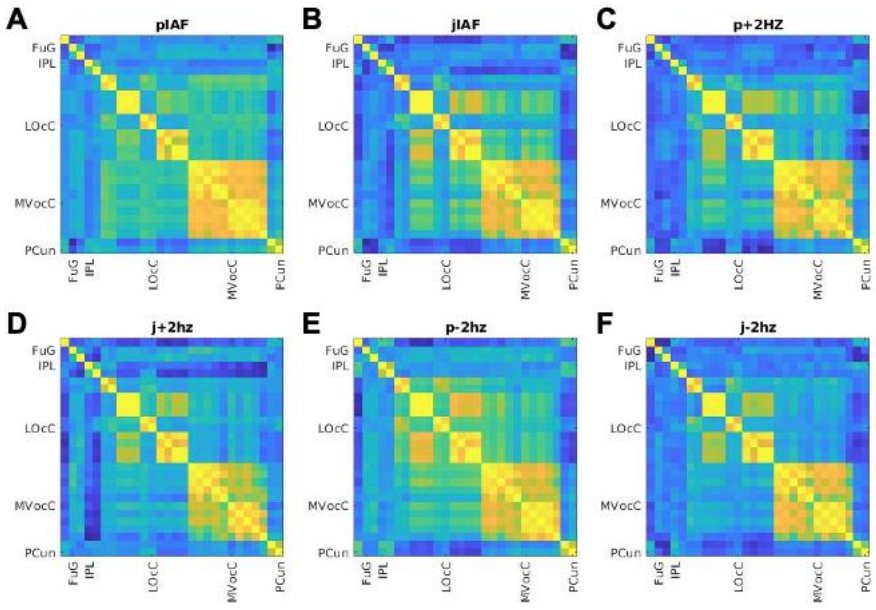

Supplementary Figure 3: Average fMRI Pearson correlation matrices for areas mapped to the YEO visual intrinsic connectivity network. Correlation matrices are shown for stimulation at A) rhythmic IAF, B) arrhythmic IAF, C) rhythmic 2Hz above the IAF, D) arrhythmic 2 Hz above the IAF, E) rhythmic 2 Hz below the IAF, and F) arrhythmic 2 Hz below the IAF.

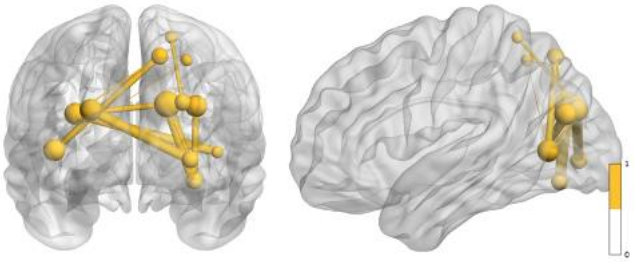

Supplementary Figure 4: Reanalysis of significant fMRI-derived connectivity of data from previous study in Jaeger et al. (*submitted)*. Data was segmented into either the first 10 seconds of stimulation or the last 10 seconds of stimulation. The comparison of connectivity for rhythmic stimulation at the IAF greater than rhythmic stimulation of all other control frequencies resulted in no significant connectivity in the occipital parietal cortex during the first 10 seconds of stimulation. However, the last 10 seconds of the stimulation block resulted in significant connectivity ($p < 0.001$, 5000 iterations) for rhythmic stimulation at the IAF as compared to rhythmic stimulation at all other control frequencies.

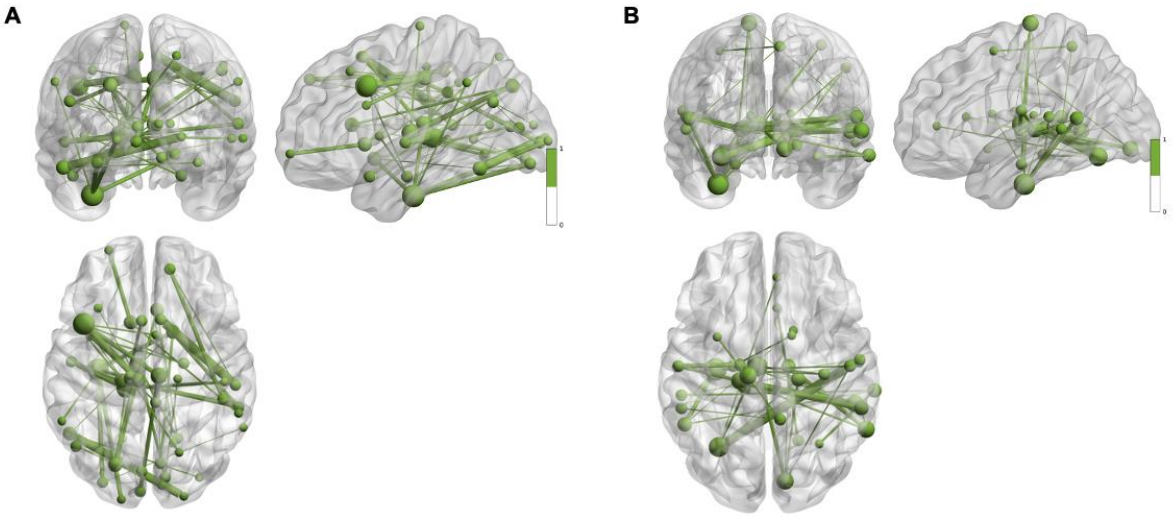

Supplementary Figure 5: Covariation between EEG-derived and fMRI-derived connectivity A) for the comparison rhythmic – arrhythmic stimulation at the IAF significantly correlated in comparison to rhythmic – arrhythmic stimulation all other flicker frequencies ($p = 0.049$, 1000 iterations, $p < 0.05$). B) The comparison rhythmic versus arrhythmic stimulation at the IAF trended towards significance ($p = 0.081$) after correcting for family-wise error rate through random permutation testing (1000 iterations, $p < 0.05$).

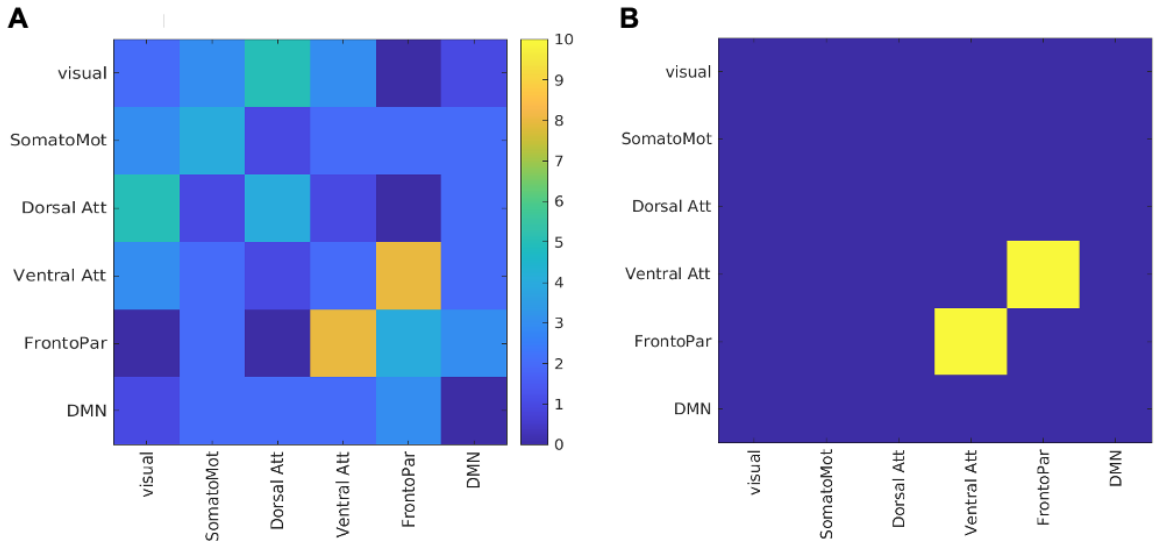

Supplementary Figure 6: The connections showing significant covariation between EEG and fMRI for rhythmic stimulation at the IAF as compared to arrhythmic stimulation were mapped to known intrinsic connectivity networks as defined by the Yeo atlas. B) The number of connections per intrinsic connectivity network were then tested for significance through non-parametric permutation testing. Significant connections between networks ($p = 3 \times 10^{-5}$) are shown in yellow.

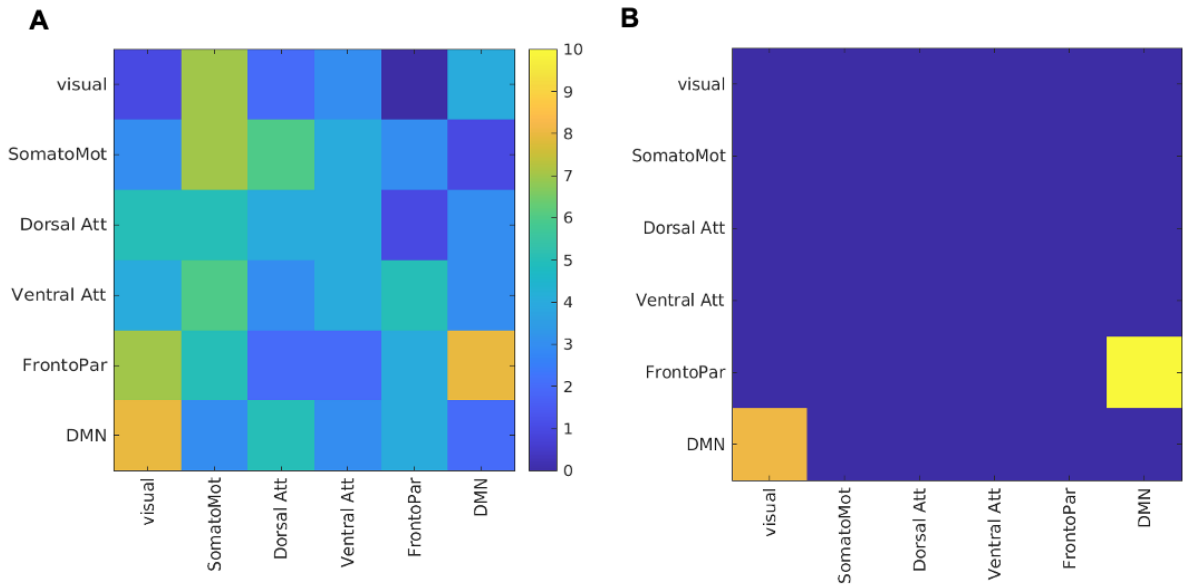

Supplementary Figure 7: A) Distribution of top 200 connections showing significant covariation between EEG and fMRI time-varying resting state connectivity within Yeo Atlas canonical resting state networks. B) The number of connections per intrinsic connectivity network were then tested for significance through non-parametric permutation testing. Significant connections between networks ($p < 0.00025$) are shown in yellow.

Appendix C: Supplementary Tables

Supplementary Table 1: List of Brainnetome regions included in the brain parcellations

L, R SFG_7_1	L, R STG_ 6_6	L, R INS_6_4	L, R Tha_8_4
L, R SFG_7_2	L, R MTG_ 4_1	L, R INS_6_5	L, R Tha_8_5
L, R SFG_7_3	L, R MTG_4_3	L, R INS_6_5	L, R Tha_8_6
L, R SFG_7_4	L, R ITG_7_2	L, R CG_7_1	L, R Tha_8_7
L, R SFG_7_5	L R ITG_7_5	L, R CG_7_2	
L, R SFG_7_6	L, R ITG_7_6	L, R CG_7_3	
L, R SFG_7_7	L, R, FuG_3_1	L, R CG_7_4	
L, R MFG_7_1	L, R, FuG_3_2	L, R CG_7_5	
L, R MFG_7_2	L, R, FuG_3_3	L, R CG_7_6	
L, R MFG_7_3	L, R pSTS_2_1	L, R CG_7_7	
L, R MFG_7_4	L, R pSTS_2_2	L, R MVOcC_5_1	
L, R MFG_7_5	L, R SPL_5_1	L, R MVOcC_5_2	
L, R MFG_7_6	L, R SPL_5_2	L, R MVOcC_5_3	
L, R MFG_7_7	L, R SPL_5_3	L, R MVOcC_5_4	
L, R IFG_6_1	L, R SPL_5_4	L, R MVOcC_5_5	
L, R IFG_6_2	L, R SPL_5_5	L, R MVOcC_5_6	
L, R IFG_6_3	L, R IPL_6_1	L, R LOcC_2_1	
L, R IFG_6_4	L, R IPL_6_2	L, R LOcC_2_2	
L, R IFG_6_5	L, R IPL_6_3	L, R LOcC_4_1	
L, R IFG_6_6	L, R IPL_6_4	L, R LOcC_4_2	
L, R PrG_6_1	L, R IPL_6_5	L, R LOcC_4_3	
L, R PrG_6_2	L, R IPL_6_6	L, R LOcC_4_4	
L, R PrG_6_3	L, R Pcun_4_1	L, R Hipp_2_1	
L, R PrG_6_4	L, R Pcun_4_2	L, R Hipp_2_2	
L, R PrG_6_5	L, R Pcun_4_3	L, R BG_6_1	
L, R PrG_6_6	L, R Pcun_4_4	L, R BG_6_2	
L, R PCL_ 2_1	L, R PoG_4_1	L, R BG_6_3	
L, R PCL_2_2	L, R PoG_4_2	L, R BG_6_4	
L, R STG_ 6_1	L, R PoG_4_3	L, R BG_6_5	
L, R STG_ 6_2	L, R PoG_4_4	L, R BG_6_6	
L, R STG_ 6_3	L, R INS_6_1	L, R Tha_8_1	
L, R STG_ 6_4	L, R INS_6_2	L, R Tha_8_2	
L, R STG_ 6_5	L, R INS_6_3	L, R Tha_8_3	

Supplementary Table 2: Degree centrality for nodes in EEG coherency network for rhythmic stimulation at the IAF greater than rhythmic stimulation at control frequencies

Yeo atlas Region	Degree centrality
SPL_R_5_3	11
CG_R_7_1	4
FuG_R_3_3	4
IFG_L_6_2	4
IFG_L_6_5	4
MVOcC_L_5_1	4
PrG_R_6_1	4
PrG_R_6_2	4
INS_L_6_1	3
LOcC_R_4_3	3
MFG_L_7_1	3
MFG_R_7_4	3
MVOcC_R_5_4	3
SFG_R_7_1	3
STG_L_6_4	3
CG_R_7_6	2
INS_L_6_6	2
IPL_R_6_3	2
LOcC_L_4_1	2
LOcC_R_4_1	2
MFG_L_7_3	2
MVOcC_L_5_4	2
MVOcC_L_5_5	2
PCun_L_4_4	2
PCun_R_4_1	2
PrG_L_6_1	2
SFG_L_7_5	2
SFG_L_7_6	2
SPL_R_5_2	2
BG_L_6_5	1
MFG_L_7_2	1
MFG_L_7_7	1
MVOcC_R_5_1	1
PCL_L_2_1	1
PoG_R_4_3	1
PrG_L_6_3	1

Supplementary Table 3: Degree centrality for nodes in fMRI connectivity network for rhythmic stimulation at the IAF greater than rhythmic stimulation at control frequencies

Yeo atlas region	Degree Centrality
Tha_R_8_6	15
Tha_R_8_7	12
IFG_L_6_5	11
Tha_R_8_4	11
INS_R_6_6	6
Tha_R_8_3	5
IFG_L_6_6	4
INS_R_6_3	4
IPL_L_6_6	4
Tha_R_8_2	4
IFG_L_6_3	3
Tha_R_8_1	3
IFG_L_6_2	2
INS_L_6_6	2
MFG_L_7_3	2
MFG_L_7_4	2
MFG_R_7_1	2
MFG_R_7_3	2
MFG_R_7_4	2
MFG_R_7_5	2
PrG_R_6_5	2
IFG_L_6_4	1
INS_R_6_5	1
IPL_L_6_4	1
ITG_R_7_6	1
MFG_L_7_1	1
PoG_L_4_2	1
PrG_L_6_1	1
PrG_L_6_3	1
PrG_L_6_5	1
STG_R_6_2	1
STG_R_6_4	1
STG_R_6_5	1

Supplementary Table 4: Degree centrality for nodes in trial-by-trial covariation analysis for rhythmic stimulation at the IAF greater than arrhythmic stimulation at the IAF.

Yeo Atlas Regions	Degree Centrality
LOcC_L_2_2	6
MFG_L_7_2	6
Tha_L_8_6	6
Tha_L_8_4	5
BG_L_6_1	4
BG_L_6_4	4
FuG_L_3_1	4
SFG_R_7_1	4
Tha_L_8_5	4
BG_L_6_3	3
BG_L_6_5	3
BG_R_6_3	3
CG_L_7_6	3
CG_R_7_5	3
Hipp_L_2_1	3
IPL_L_6_6	3
IPL_R_6_6	3
MFG_L_7_3	3
MFG_R_7_1	3
MVOcC_R_5_5	3
SFG_R_7_2	3
STG_R_6_5	3
Tha_L_8_7	3
pSTS_L_2_2	3
BG_L_6_2	2
CG_L_7_1	2
CG_L_7_3	2
CG_R_7_1	2
CG_R_7_2	2
CG_R_7_6	2

Appendix D: Supplementary References

Fransson, Peter Schiffler, Björn C. Thompson, William Hedley. 2018. "Brain network segregation and integration during an epoch-related working memory fMRI experiment." *NeuroImage* 178: 147-161.

Thompson, William Hedley Richter, Craig Geoffrey Plavén-Sigray, Pontus Fransson, Peter. 2018. "Simulations to benchmark time-varying connectivity methods for fMRI." *PLoS Computational Biology* 14 (5).

Liao, C. H. Worsley, K. J. Poline, J. B. Aston, J. A.D. Duncan, G. H. Evans, A. C. 2002. "Estimating the delay of the fMRI response." *NeuroImage* 16 (3 Pt 1): 593-606.

Soon, Chun Siong Venkatraman, Vinod Chee, Michael W.L. 2003. "Stimulus repetition and hemodynamic response refractoriness in event-related fMRI." *Human Brain Mapping* 20 (1): 1.

Wirsich, Jonathan Giraud, Anne Lise Sadaghiani, Sepideh. 2020. "Concurrent EEG- and fMRI-derived functional connectomes exhibit linked dynamics." *NeuroImage* 219.

Dolan, Kevin T Spano, Mark L. 2001. "Surrogate for nonlinear time series analysis." *Phys. Rev. E* 64 (4).

Thomas Yeo, B. T. Krienen, Fenna M. Sepulcre, Jorge Sabuncu, Mert R. Lashkari, Danial Hollinshead, Marisa Roffman, Joshua L. Smoller, Jordan W. Zöllei, Lilla Polimeni, Jonathan R. Fisch, Bruce Liu, Hesheng Buckner, Randy L. 2011. "he organization of the human cerebral cortex estimated by intrinsic functional connectivity." *Journal of Neurophysiology* 106 (3): 1125-1165.

Glasser, Matthew F. Coalson, Timothy S. Robinson, Emma C. Hacker, Carl D. Harwell, John Yacoub, Essa Ugurbil, Kamil Andersson, Jesper Beckmann, Christian F. Jenkinson, Mark Smith, Stephen M. Van Essen, David C. 2016. "A multi-modal parcellation of human cerebral cortex." *Nature* 536 (7615): 171.

Zalesky, Andrew Fornito, Alex Bullmore, Edward T. 2010. "Network-based statistic: identifying differences in brain networks." *NeuroImage* 53 (4): 1197-1207.

GENERAL DISCUSSION:

4.1 Summary

In summary, I established a method for analyzing alpha-specific connectivity changes in concurrent EEG and fMRI considering individual variability in the peak alpha frequency. In my first project, I tested the efficacy of rhythmic light stimulation as a tool to drive entrainment and subsequent modulation of individual's intrinsic alpha frequency. I showed that targeted rhythmic stimulation at the IAF increases occipitoparietal alpha coherency in EEG and functional connectivity in fMRI, which serve as a proxy for increased neural synchrony. In project two, I implemented my entrainment paradigm in concurrent EEG-fMRI to study how changes in alpha and BOLD connectivity covary. Interestingly, external stimulation at the IAF drove increased connectivity along visual connections through the thalamus and into frontal regions in line with findings previously only derived from structural connectivity and electrophysiology in primates. In the following sections, I will first discuss the limitations of entrainment and how to address these in future behavioral studies. I will then put my results in context of ongoing oscillatory research focusing on the role of cross-frequency coupling in the hierarchical organization of neural communication during cognition and the impact of aberrant coupling in neuropsychiatric illness. I will end my discussion on advances in multimodal imaging techniques and how multimodal approaches can be applied to answer remaining questions.

4.2 Limitations and future applications of alpha entrainment

Although I successfully showed the intrinsic alpha frequency can be entrained, there are some assumptions that should be mentioned. To begin, the fMRI connectivity findings diverged in my two projects. Although fMRI connectivity was high in visual areas for stimulation at the IAF, no significant increase in connectivity was observed as compared to control frequencies in visual areas in the second project. The stimulation blocks were shortened to a duration of 10 seconds in the second project. From the task-based evoked BOLD response in visual areas, I assume the increase in luminance at the onset of stimulation evoked a slow hemodynamic response that induced similar increases in visual connectivity across stimulation conditions. Indeed in the first project, the connectivity for the IAF differed most

significantly for the latter ten seconds of stimulation. However, I chose to shorten the stimulation block in the second study to increase trial number and reduce eye blinking during stimulation, as this appears to influence alpha rhythm. Furthermore, shorter entrainment periods are also more plausible in study designs integrating visual stimulation with task-based paradigms.

An increase in trial number in both studies would have helped increase statistical power. EEG is very artifact prone, especially during the acquisition of fMRI. Phase angles in EEG are very sensitive to movement artifacts and may be artificially biased. However, I tried to use control conditions to control for phase-related biases as these would have been present across all flicker conditions. Nevertheless, an increase in trial number and statistical power may have resulted in more robust connectivity networks.

Although my results provided novel evidence that alpha-mediated information flow in visual processing occurs through thalamocortical connections and alludes to the top-down control of the alpha rhythm. It remains to be behaviorally verified whether the modulations in the alpha rhythm lie under top-down control. Implementing visual perception and attentional cueing paradigms during different visual stimulation conditions will elucidate the systematic role of the alpha oscillation during behavior. It is not known how long the entrainment effect lasts (Otero et al., 2020). Therefore, I propose implementing task-based paradigms during sustained visual stimulation. This poses the problem of visual stimuli being missed during dimming of the shutter glasses. However, this challenge can be overcome by implementing flicker shutters that only cover part of the visual field. For example, using flickering concentric circles in the outer visual field, while presenting the task paradigm in the center of the visual field would allow the presentation of stimuli during a given phase of the alpha cycle. Furthermore, implementing an attentional cueing paradigm will further illuminate whether sensory driven neural modulations can be overridden by top-down processes.

4.3 Cross-frequency coupling

The alpha oscillation interacts with other neural frequencies and can be modulated by intrinsic rhythms. It is important to consider the spatial underpinnings of other frequencies as well as cross-frequency interactions with the alpha oscillation to build a cohesive

representation of hierarchical brain organization and the individually contributing processes during cognition. Cross-frequency coupling between neural oscillations has also been proposed to coordinate neural communication by integrating local cortical processing and functional systems across multiple spatiotemporal scales. Initial research focused on phase-amplitude coupling between low frequency oscillations and high frequency gamma oscillations. Gamma amplitude has been shown to correlate with the phase of alpha in occipital regions (Osipova et al., 2008; Voytek & Knight, 2010). Gamma amplitude has also been demonstrated to be phase-locked to the delta frequency in the occipital cortex (Händel & Haarmeier, 2009). The phase of delta has shown to modulate the amplitude of the alpha rhythm in the medial frontal cortex with the differences in cross-frequency coupling strength correlating with performance on a decision-making task (Cohen et al., 2009). These studies suggest communication is organized in a hierarchy where fast oscillations are modulated by slow oscillations, which may be even modulated by slower ones. The cross-frequency coupling strength across different oscillations is therefore thought to serve as a functional mechanism for multi-scale integration of sensory information in a fast and computationally efficient manner. Specifically, information from local, segregated cortical processing occurs on fast time scales and gets regulated by distributed brain networks operating on a slower, behavioral time scale. Modulation of low frequencies in frontal areas serves as a mechanism for the brain to make active inferences about incoming signals. Simultaneous updating of internal representations with incoming sensory information in context-dependent manner occurs through coupled low-frequency modulations in cortical excitability in sensory areas (Canolty & Knight, 2010; Fries, 2015; Siegel et al., 2012).

Audiovisual speech processing studies provide exemplary evidence for the complex coupling between oscillations during multi-sensory processing and integration. Experimental studies implementing the McGurk effect in which visual input of mouth movement is incongruent with auditory speech signals, have shown the dynamic cross-frequency coupling between congruent and incongruent sensory signals. Segregated, processed signal from each modality is integrated in higher-order areas where signal congruence is compared through feedforward-feedback connections (Stein et al., 1993). Propagation of gamma power has been shown to go from sensory areas to higher order areas, whereas phase modulations in the alpha-beta range propagate from higher order areas in auditory and visual processing (Fontolan et al., 2014; Michalareas et al., 2016; Schroeder & Lakatos, 2009; Simon et al., 2017). Increased theta and delta coherency were observed between frontal and temporal

regions when participants saw the speaker's mouth (Giordano et al., 2017). Coupling between the delta phase and beta-power also correlated with temporal alignment of auditory and visual inputs (Ohki et al., 2016). These results suggest that integration between the two modalities occurs through phase coherency in the theta and delta (Bauer et al., 2020; Keil & Senkowski, 2018). The brain is thought to speed up information processing, by generating predictions from one modality about the other (Arnal et al., 2015). However, when incongruent information is processed, which violates predictions, top-down modulation redirects attention to incoming sensory input (Smout et al., 2019; Wills et al., 2007). Comparison of congruent and incongruent audiovisual speech stimuli revealed increases in temporal-parietal gamma and beta-band power during congruent trials and increases in alpha power during incongruent trials (Lange et al., 2013). In line with these findings, the alpha oscillation has been associated with shifts of spatial attention (Snyder & Foxe, 2010; Van Diepen & Mazaheri, 2018) and intersensory attention (Pomper et al 2015) by inhibiting task-irrelevant areas. Asynchronous presentation of audiovisual stimulus has also been correlated with shifts in gamma activity nested within the phase of the alpha cycle, suggesting top-down phase resetting of the alpha oscillation can shift sensory processing of sensory stimuli (Lennert et al 2021).

Yet expectation of presentation of stimuli seems to be influenced by the phase of the delta rhythm. A study by Helfrich and colleagues (2017) using rhythmic and arrhythmic presentation of visual stimuli to entrain the alpha rhythm during a predictive coding experiment observed that the phase of the delta rhythm modulated posterior alpha during predictive trials and reduced the bottom-up alpha entrainment effect on behavioral outcome. Furthermore, intersensory attention paradigm studies found reduced alpha power when participants focused on visual stimuli (Pomper et al., 2015) and correlations between delta- and beta-modulations and temporal expectation (Keil et al., 2016). A novel entrainment study entrained both the alpha rhythm (through rhythmic or arrhythmic stimulus presentation at 10Hz) and delta rhythm (through contextual background changes such as color, pitch, and motion at 2.5Hz) (Yuan et al., 2021). Yuan and colleagues (2021) observed contextual modulations in the delta band diminished the alpha-entrainment effect by modulating alpha power and behavioral performance. All in all, these studies suggest that feedforward processing of information occur through fast neural oscillations in the gamma, while simultaneous feedback modulations of sensory information processing occurs through lower frequencies in the alpha and beta band (Florin & Baillet, 2015; Keil & Senkowski, 2018;

Sedley et al., 2016). Finally multimodal integration of sensory information and predictive inferences about incoming sensory information may be governed by even slower frequencies such as the delta oscillation (Breska & Deouell, 2017; Keil & Senkowski, 2018; Landau & Fries, 2012). Yet how exactly these frequencies couple across different cognitive tasks and with changing cognitive demand remain to be elucidated.

4.4 Hierarchical architecture of neural oscillations

Spatial evidence from concurrent EEG-fMRI studies supports the hypothesis of hierarchical organization of information processing through cross-frequency coupling as similar spatial overlap between frequency-specific functionally connectivity networks and resting state networks have been observed (Deligianni et al., 2014; Hipp & Siegel, 2015; Wirsich et al., 2017, 2020). The ultraslow fluctuations in BOLD signal that are observed in resting-state networks have been shown to be linked with phase-amplitude coupling of faster electrophysiological oscillations (Hunyadi et al., 2019; Murta et al., 2017). Somatomotor network, auditory network, and visual network correlate with beta and alpha band (Brookes et al., 2011; Hacker et al., 2017; Hipp et al., 2012). Power changes in the beta band have also been correlated with the frontoparietal network (Brookes et al., 2011). Posterior alpha power has also been shown to correlate with dorsal attention network (Hacker et al., 2017) and the dorsal part of a higher cognitive network (Vidaurre et al., 2018). Whereas the delta and theta band correlate with frontal apart of a higher order cognitive network (Vidaurre et al., 2018) and frontoparietal network (Hacker et al., 2017). Studies looking at phase-phase coupling across frequency-specific bands during rest show that concurrent EEG-fMRI connectivity maps better predict structural connectivity from function (Engel et al., 2013; Wirsich et al., 2017). In line with these findings, I showed that increased phase synchronization of the alpha rhythm leads to increased connectivity between visual areas and frontal areas mediated through the occipital thalamus, which are very similar to structural connections going from and to the pulvinar (Leh et al., 2008). Only few other studies have examined concurrent functional connectivity changes during task. One study examining replay of acquired information showed transient bursts of activity in the alpha parietal network correlated with activation in the default mode network (Higgins et al., 2021).

Improvements in the spatial resolution of imaging techniques, such as layer-specific fMRI, are giving novel insight into the cellular composition across cortical layers contributes to

neural activity along feedforward and feedback projections (Scheeringa & Fries, 2019). A study looking measuring concurrent layer-specific BOLD and EEG during a visual attention task found BOLD activity in the infragranular layers negatively correlated with beta and alpha power, while BOLD activity in the supragranular layers positively correlated with gamma power and negatively with alpha power during attended trials (Scheeringa et al., 2016). Taken together with evidence from cellular electrophysiology, Scheeringa and others argue feedback and feedforward projections are organized in different cortical layers with gamma-mediate feedforward projections ending in superficial layers and feedback alpha-beta mediated projections ending in deep layers in the sensory cortex (Bollimunta et al., 2011; Buffalo et al., 2011; Scheeringa et al., 2016; Spaak et al., 2012). Concurrent EEG and layer-specific fMRI studies may therefore also help segregate functional connectivity networks into feedforward- and feed-back driven networks (Scheeringa & Fries, 2019).

4.5 Adaptability of oscillations

Two aspects of neural oscillations add to the complexity of the role of neural oscillations in cognition: 1) the ability of oscillations to be entrained by endogenous or environmental rhythms and 2) shifts in the peak frequency of an oscillation. A natural example of neural entrainment to external rhythmic stimuli occurs during language processing. The intrinsic delta/theta rhythm synchronizes to the speech envelope during language processing with sharp speech edges correlating with phase resetting of the slow frequencies and coupled gamma amplitude modulations (Assaneo & Poeppel, 2018; Giraud & Poeppel, 2012; Gross et al., 2013; Lakatos et al., 2019a). However, this effect was attenuated when speech was presented backwards (Gross et al., 2013). Modulations in the neural oscillations below 7 Hz are thought to facilitate transmission of predictions about incoming sensory information by, for example, estimating syllabus presentation rate (Bourguignon et al., 2013; Kö et al., 2018). The alpha rhythm can also be entrained through external rhythmic stimuli, which may serve as a role for selective anticipation of future salient events (Clayton et al., 2018; Ronconi et al., 2018). Temporal expectation studies have shown that when stimuli are presented rhythmically, alpha power is reduced in the visual cortex even in the absence of stimulus presentation (Rohenkohl & Nobre, 2011). Furthermore, this only occurred during trials where stimuli were presented in a rhythmic sequence and the onset of a stimulus was predictable (Rohenkohl & Nobre, 2011). I showed in both of my studies that the alpha oscillation can be entrained by external visual stimuli. However, in the first study significant synchronicity was

also observed for the 10 Hz flicker condition in the EEG and the 9 Hz flicker in the fMRI. One explanation for these findings suggest that the intrinsic alpha frequency can slightly shift the peak frequency to adapt to environmental cues. Intraindividual shifts in the peak alpha frequency have been observed across the duration of a study (Babu Henry Samuel et al., 2018; Benwell et al., 2019) and have behavioral implications (Mierau et al., 2017). The speed of the IAF correlated with temporal resolution of visual perception where increase in the IAF frequency correlated with perceiving rapidly presented objects as two separate events rather than the same event (Samaha & Postle, 2015b). The alpha peak frequency has been observed to increase with cognitive load during an N-back task (Haegens et al., 2014b; Maurer et al., 2015).

State-dependent shifts in the alpha peak frequency may not only help with resolution of temporal sampling (Cecere et al., 2015; Samaha & Postle, 2015b), but also facilitate integration and segregation. A study by Ronconi and others (2018) used rhythmic flickering light to either entrain alpha slightly below or above the IAF while participants performed a segregation (identifying an odd element) or integration (locating a missing element) visual task. They observed decrease in the alpha peak frequency correlated with better performance on the integration task, while increase in alpha peak correlated with better performance in the segregation task (Ronconi et al., 2018). In my second study, I also observed a slight increase in the mean peak alpha frequency between eyes closed and eyes open resting state measures, which also supports that during lack of visual input the alpha frequency shifts to focus on more intrinsic neural processes. However, alpha peak power during eyes open was also significantly less.

It remains to be elucidated whether shifts in alpha peak frequency and power are the byproduct of local desynchronization of neural activity or whether a shift in peak frequency occurs (Mierau et al., 2017). Implementing novel techniques, such as calculating the instantaneous frequency (Cohen, 2014), as well as using entrainment to experimentally modulate the alpha peak frequency (Ronconi et al., 2018) are needed to study subsequent changes in source-localized alpha peak frequency. A study observing shifts in instantaneous resting state IAF observed that shifts in the IAF correlated with different source-localized components (Benwell et al., 2019). Furthermore, the frequency of canonical neural oscillations, BOLD fluctuations, and even body rhythms such as respiration rate are thought

to be coupled by a golden ratio (Wolfgang Klimesch, 2018) providing to motivation to study the effect of shifts in the IAF on cross-frequency coupling.

4.6 Clinical relevance: neural oscillations in the context of illness

My findings and many other studies suggest neural oscillations serve as a mechanism to coordinate the interaction of large ensembles of neurons across distributed specialized brain regions. Thus, allowing for the parallel processing of sensory input and selective integration of context- relevant information into a continuous thought process (Engel et al., 2001; Fries, 2005a). Aberrant patterns in synchronized activity across local and distributed brain regions can lead to impaired segregation and integration of sensory input and have been linked to many sensory and psychiatric illnesses (Uhlhaas & Singer, 2006). Disrupted balance between segregation and integration across functional networks has been linked to schizophrenia (Liu et al., 2008; Lynall et al., 2010; Wei et al., 2018) bipolar disorder (Wang et al 2016, Wei et al 2018), attention-deficit-hyperactivity disorder (ADHD, Lenartowicz et al., 2018), autism (Rudie et al., 2012), and major depressive disorder (Wei et al., 2018). These studies mainly arise from differential functional connectivity patters found between illness groups and healthy controls. For example, decrease in short-range connectivity and increase in medium to long range connectivity has been observed in schizophrenia, bipolar disorder, and major depressive disorder (Xia et al., 2019). Recently, findings of aberrant patterns in neural oscillations in illness groups, such as increased power in low frequencies (delta and theta) and decreased power in higher frequencies (alpha, beta, and gamma) in ADHD, schizophrenia, and obsessive-compulsive disorder (Newson & Thiagarajan, 2019), has sparked interest in using neural oscillations as biomarkers for classification of neuropsychiatric illness (Newson & Thiagarajan, 2019; Sargent et al., 2021). However, heterogeneity in resting state EEG analyses among healthy individuals and disease groups (Cox et al., 2018; Demuru & Fraschini, 2020; Kumral et al., 2020) and overlap of characteristic oscillatory patterns across illnesses (Newson & Thiagarajan, 2019) require further classification and spatial localization of oscillatory features. In the following section, I highlight findings in schizophrenia and ADHD linking alterations in the alpha rhythm and functional connectivity to impaired top-down regulation and subsequent impaired integration of sensory input. I also argue that external rhythmic stimulation can be used to study alterations in functional connectivity patterns in these patient groups and may serve as a better biomarker of studying altered alpha-related functional connectivity than comparing experimental groups in resting state studies.

Schizophrenia is a complex and debilitating neuropsychiatric disorder that is characterized by impaired integration of sensory input and subsequent perception (Ross et al., 2006). Abnormal spontaneous alpha activity and altered resting-state functional connectivity have been observed in patients with schizophrenia. Resting-state eyes closed studies analyzing alpha-related functional connectivity using phase lag index reported decreased connectivity in superior parietal, right temporal and left occipital brain regions (Liu et al., 2019), but decreased connectivity within the right frontoparietal network (Trajkovic et al., 2021). Decreased alpha power in occipitoparietal regions and frontal regions was observed in patients with schizophrenia as compared to healthy controls during rest and task (Thilakavathi et al., 2019). Impaired top-down regulation (Dima et al., 2009, 2010) and altered thalamo-cortical connectivity between the visual cortex and thalamus (Iwabuchi & Palaniyappan, 2017) have been reported and may explain impaired visual-processing in schizophrenia. Yet how abnormal hyperconnectivity and hypoconnectivity across functional connectivity networks lead to impaired cognitive function in schizophrenia remains unclear.

ADHD is accompanied with symptoms of ongoing inattention, hyperactivity and impulsivity and interferes with many cognitive functions (Barkley, 1997). Task-related studies implementing visuospatial attention paradigms have shown impaired lateralization of alpha power in response to cued and distractor items (Vollebregt et al., 2016). Increased suppression of alpha power in distractor areas and sensorimotor areas have also been observed during visuospatial attention tasks, suggesting an inability to suppress sensory information coming from irrelevant, distractor sources (Yordanova et al., 2013). During memory encoding in spatial working memory paradigm, event-related decrease in posterior alpha power was correlated with increased fMRI-derived activity between occipital and frontoparietal regions (Lenartowicz et al., 2016) in healthy controls. Whereas participants with ADHD had an attenuated event-related decrease in posterior alpha power during memory encoding (Lenartowicz et al., 2014; Mazaheri et al., 2014). Disrupted communication between frontal and visual areas, leads to impaired top-down regulation of attention and the inability to suppress sensory processing of distractor information (Lenartowicz et al., 2016; Mazaheri et al., 2010). Scientists believe disruption in thalamo-cortical circuitry (Liu et al., 2016; Saalmann & Kastner, 2011) or cortico-cortical connections through superior longitudinal fasciculus (Marshall et al., 2015) lead to dysregulation of top-down attention in ADHD (Lenartowicz et al., 2016). Only few alpha connectivity studies

have been performed in patient populations with ADHD (Lenartowicz et al., 2018). Future studies are needed to understand how alterations in the alpha band and functional connectivity patterns may lead to dysfunctional top-down regulation of attention.

Both ADHD and schizophrenia are characterized by impaired sensory integration and altered alpha activity mainly thought to arise from impaired long-range, top-down communication along thalamocortical and cortico-cortical pathways. Electrophysiological studies performed in animals suggest feedback loops between excitatory and inhibitory neurons in the thalamocortical pathway generate alpha oscillations (Jones, 2009; Steriade & Deschenes, 1984). The alpha rhythm propagates across distributed brain areas through short- and long-range cortico-cortical, cortico-thalamic and thalamo-cortical connections (Halgren et al., 2019; Ito et al., 2005). In line with electrophysiological findings, our results, which analyzed whole-brain connectivity, showed increased synchronicity between thalamus and frontal areas in the fMRI as well as increased fronto-parietal synchronicity in EEG during entrainment of the intrinsic alpha frequency. My findings not only support that communication between frontal and parietal regions along thalamo-cortical and cortico-cortical connections arise through synchronization of the intrinsic alpha rhythm, but also serves as a template for comparing alpha-functional connectivity and alterations in top-down communication in patient populations. I propose that modulation of the IAF, through a visual entrainment paradigm allows for better comparison of functional connectivity changes between healthy controls and groups, as it considers individual variability and compares changes in connectivity within an individual rather than making a composite comparison between two groups.

4.7 Advancements in multi-modal imaging techniques

The use of combined neuroimaging techniques is becoming increasingly more popular to gain a comprehensive understanding of the brain from activity in single cells to whole brain network level. Imaging techniques utilize specific physical principles to interact with neural tissue and produce a signal that serves as a proxy for neural activity. However, these signals have limitations in the amount of spatial and temporal information they can provide about neural activity. These limitations serve as the main motivation to combine neuroimaging techniques that spatio-temporally complement each other. The use of concurrent EEG-fMRI

has become increasingly popular to localize EEG features using the high spatial resolution of fMRI. However, discrepancies between the two modalities brings into question how the signals derived from these two imaging modalities complement each other on a biophysiological level. These discrepancies are driving scientists to reconsider the physical properties of neuroimaging signals and leading to novel insight and models of brain processes. Furthermore, the combination of trimodal imaging techniques such as the use of positron emission tomography with concurrent EEG-fMRI has the potential of elucidating unresolved questions.

Studies correlating frequency-specific changes in LFPs using electrocorticography (ECoG) measured in visual areas, have shown broadband power to correlate with BOLD amplitude changes (Hermes et al., 2017; Ojemann et al., 2013). Increase in broadband power changes have been correlated with increased spiking activity, which can be considered as representing total neural activity (Manning et al., 2009; Miller et al., 2009). In line with these findings and under the assumption BOLD indirectly reflects synaptic activity, changes in the BOLD amplitude serves as a proxy for total neural activity (Winawer et al., 2013). Whereas increases in amplitude of neural oscillations reflect the amount of synchronous activity. This interpretation brings insight into combined EEG-fMRI studies that have reported either correlations (Laufs et al., 2003; Scheeringa et al., 2009, 2012) or no correlations (Butler et al., 2017; Hermes et al., 2017; Portnova et al., 2018) between BOLD amplitude changes and distinct neural oscillations. In context of my thesis, this model serves as an explanation for the observed uncoupling of the BOLD amplitude response and entrainment response seen in both studies. When using external flickering light to stimulate neural activity, the change in luminance will increase overall neural activity, which may be asynchronous or synchronous in nature. The BOLD response in early visual areas increases with luminance (Liang et al., 2013; Vinke & Ling, 2018; Winawer et al., 2013). Whereas the flicker regularity, i.e. rhythmic or arrhythmic, will influence the degree of synchronicity of the neural activity (Notbohm & Herrmann, 2016). Since the mean luminance was kept constant across flicker conditions, no change in BOLD amplitude would be expected. Yet this interpretation of EEG and fMRI signal still fails to give insight into the neural composition of the visual cortex and how the interplay of excitatory and inhibitory synaptic activity relates to the role of neural oscillations.

The question of how the balance between excitatory and inhibitory activity affect changes in neural communication, neural oscillations and the BOLD signal remains unanswered. The combination of positron emission tomography (PET) imaging to measure metabolic energy consumption, and PET imaging and MR spectroscopy to measure neurotransmitter composition, have the potential in building a better understanding how excitatory and inhibitory neural activity contribute to global baseline activity and specific neural processes. In brief, fluorodeoxyglucose (FDG -PET) imaging measures the amount of glucose metabolism needed for cellular respiration during synaptic activity (Villien et al., 2014). A key study by Shah et al. (2017) used concurrent trimodal MR-PET-EEG imaging to relate metabolic demand, neuro-vascular coupling, and oscillatory neural activity to functional connectivity between the dorsal default mode network (DMN) and sensorimotor network (SMN). The study found increase in metabolic activity and mean BOLD signal intensity in the DMN as compared to the SMN. Although no frequency-specific oscillation correlated directly with the DMN, the spatial composition of the source-localized power within frequency bands varied between the DMN and SMN. No correlation was found between metabolic activity and spectral power across the two networks. In general, glucose metabolism is thought to correlate with BOLD amplitude and nonlinearly correlates with functional connectivity (Tomasi et al., 2013). Yet recent findings in concurrent PET-fMRI studies have revealed that energy efficiency varies across brain regions (Aiello et al., 2015; Bullmore & Sporns, 2012; Tomasi et al., 2013) bringing into question what causes differences in energy efficiency and how this changes neurovascular coupling. A different trimodal study using a radiotracer to study the binding availability of GABAergic and glutamatergic receptors found GABAergic metabolism was more tightly associated with spatial localization of EEG microstates and functional connectivity in the DMN than glutamatergic and glucose metabolism (Rajkumar et al., 2021). This study suggests that the composition of neural receptors leads to altered glucose metabolism and influences fMRI functional connectivity networks and EEG oscillations.

The excitatory/inhibitory balance gives rise to functional connectivity networks in fMRI and EEG oscillations and is crucial for normal cognitive function. Along with PET studies, single voxel spectroscopy can be used to assess GABA-to-creatine ratio and glutamate-glutamine to creatine ratio, thus giving insight to the amount of inhibitory and excitatory neurotransmitters in a given brain region (Finnema et al., 2015). A study comparing functional magnetic resonance spectroscopy in the visual cortex during visual stimulation found the BOLD signal

correlated with glutamate and lactate concentrations (Boillat et al., 2020)supporting BOLD amplitude reflects excitatory synaptic activity. Whereas another study found that the ratio of local-to-global $GABA_A$ binding potential correlated with increased functional connectivity in the visual cortex, suggesting GABAergic connections influence long-range synchronicity (Qin et al., 2012). Yet it remains to be answered how modulations in neural oscillations. Only few studies have correlated GABAergic concentration to neural oscillations, specifically the gamma oscillation (Kujala et al., 2015; Muthukumaraswamy et al., 2009). MR spectroscopy is not compatible with simultaneous EEG recording. However targeted modulation of neural oscillations would allow more direct inferences between neurotransmitter levels and neural oscillations.

One caveat of combination of PET, fMRI, MR spectroscopy, and EEG is the vast difference in temporal resolution across these modalities. Nonetheless, these study shows the richness of multi-modal data and its potential in building a comprehensive understanding of the complex brain. Future improvements in study designs, such as using entrainment paradigms to modulate specific neural oscillations over or sensory systems will help elucidate unanswered questions.

4.8 Conclusion and future outlook

In conclusion, neural oscillations' role in coordinating communication is hierarchical and highly complex. Neural oscillations are cross-modal, intermittently couple across frequencies, highly adaptable and vary across individuals making it difficult to parse apart their individual role in cognition. Controlled, experimental modulation of neural oscillation is crucial for correlating frequency-specific changes to behavior. I implemented a method for inducing and localizing alpha-modulated connectivity changes in concurrent EEG and fMRI. My results show alpha-mediated communication relays across thalamo-cortical connections between the visual and frontal areas and complement structural connectivity. My findings also show the advantage of combining EEG and fMRI to gain a more comprehensive insight on functional connectivity.

There is a current trend towards studying the functional relevance of spatially overlapping electrophysiological and fMRI-derived resting state networks. I show the benefit of using

visual stimulation to study the functional relevance of connectomes. I have also highlighted the benefit of using entrainment in future studies to investigate alterations in connectivity in disease as well as changes in metabolic demand and neural composition.

Although my experiment only investigated the effect of entrainment on the alpha band, entrainment can also be used to modulate oscillations in the other canonical frequency bands. A few studies have successfully entrained several frequencies across modalities to study the effect of cross-frequency coupling on behavior (Helfrich et al., 2017; Yuan et al., 2021). Yet I urge the scientific community to take individual differences into account and to implement task paradigms that entrain at targeted frequencies in future studies. Targeted modulation of intrinsic neural oscillations will clarify how shifts in frequency, phase coupling and power relate to behavioral outcomes across varied populations of individuals and will help build a distinguished and comprehensive picture of the role of neural oscillations in cognition.

REFERENCES:

Abreu, R., Leal, A., & Figueiredo, P. (2018). EEG-Informed fMRI: A Review of Data Analysis Methods. *Frontiers in Human Neuroscience*. https://doi.org/10.3389/fnhum.2018.00029

Aiello, M., Salvatore, E., Cachia, A., Pappatà, S., Cavaliere, C., Prinster, A., Nicolai, E., Salvatore, M., Baron, J. C., & Quarantelli, M. (2015). Relationship between simultaneously acquired resting-state regional cerebral glucose metabolism and functional MRI: a PET/MR hybrid scanner study. *NeuroImage*, *113*, 111–121. https://doi.org/10.1016/J.NEUROIMAGE.2015.03.017

Allen, P. J., Josephs, O., & Turner, R. (2000). A Method for Removing Imaging Artifact from Continuous EEG Recorded during Functional MRI. *NeuroImage*, *12*(2), 230–239. https://doi.org/10.1006/NIMG.2000.0599

Arnal, L. H., Doelling, K. B., & Poeppel, D. (2015). Delta-beta coupled oscillations underlie temporal prediction accuracy. *Cerebral Cortex*. https://doi.org/10.1093/cercor/bhu103

Assaneo, M. F., & Poeppel, D. (2018). The coupling between auditory and motor cortices is rate-restricted: Evidence for an intrinsic speech-motor rhythm. *Science Advances*, *4*(2). https://doi.org/10.1126/SCIADV.AAO3842

Attwell, D., & Iadecola, C. (2002). The neural basis of functional brain imaging signals. *Trends in Neurosciences*, *25*(12), 621–625. https://doi.org/10.1016/S0166-2236(02)02264-6

Babu Henry Samuel, I., Wang, C., Hu, Z., & Ding, M. (2018). The frequency of alpha oscillations: Task-dependent modulation and its functional significance. *NeuroImage*, *183*, 897. https://doi.org/10.1016/J.NEUROIMAGE.2018.08.063

Baker, A. P., Brookes, M. J., Rezek, I. A., Smith, S. M., Behrens, T., Smith, P. J. P., & Woolrich, M. (2014). Fast transient networks in spontaneous human brain activity. *ELife*, *3*(3), 1867. https://doi.org/10.7554/ELIFE.01867

Barkley, R. A. (1997). Behavioral inhibition, sustained attention, and executive functions: constructing a unifying theory of ADHD. *Psychological Bulletin*, *121*(1), 65–94. https://doi.org/10.1037/0033-2909.121.1.65

Barzegaran, E., Vildavski, V. Y., & Knyazeva, M. G. (2017). Fine Structure of Posterior Alpha Rhythm in Human EEG: Frequency Components, Their Cortical Sources, and Temporal Behavior. *Undefined*, *7*(1). https://doi.org/10.1038/S41598-017-08421-Z

Başar, E. (2013). Brain oscillations in neuropsychiatric disease. *Dialogues in Clinical Neuroscience*, *15*(3), 291. https://doi.org/10.31887/DCNS.2013.15.3/EBASAR

Bauer, A. K. R., Debener, S., & Nobre, A. C. (2020). Synchronisation of Neural Oscillations and Cross-modal Influences. *Trends in Cognitive Sciences*, *24*(6), 481–495. https://doi.org/10.1016/J.TICS.2020.03.003

Becker, R., Reinacher, M., Freyer, F., Villringer, A., & Ritter, P. (2011). How Ongoing Neuronal Oscillations Account for Evoked fMRI Variability. *Journal of Neuroscience*, *31*(30), 11016–11027. https://doi.org/10.1523/JNEUROSCI.0210-11.2011

Beckmann, C. F., DeLuca, M., Devlin, J. T., & Smith, S. M. (2005). Investigations into resting-state connectivity using independent component analysis. *Philosophical Transactions of the Royal Society B: Biological Sciences*, *360*(1457), 1001. https://doi.org/10.1098/RSTB.2005.1634

Benwell, C. S. Y., London, R. E., Tagliabue, C. F., Veniero, D., Gross, J., Keitel, C., & Thut, G. (2019). Frequency and power of human alpha oscillations drift systematically with time-on-task. *NeuroImage*, *192*, 101–114. https://doi.org/10.1016/J.NEUROIMAGE.2019.02.067

Berger, H. (1929). Über das Elektrenkephalogramm des Menschen. *Archiv Für Psychiatrie Und Nervenkrankheiten 1929 87:1*, *87*(1), 527–570. https://doi.org/10.1007/BF01797193

Boillat, Y., Xin, L., van der Zwaag, W., & Gruetter, R. (2020). Metabolite concentration changes associated with positive and negative BOLD responses in the human visual cortex: A functional MRS study at 7 Tesla. *Journal of Cerebral Blood Flow and Metabolism : Official Journal of the International Society of Cerebral Blood Flow and Metabolism*, *40*(3), 488–500. https://doi.org/10.1177/0271678X19831022

Bollimunta, A., Mo, J., Schroeder, C. E., & Ding, M. (2011). Neuronal Mechanisms and Attentional Modulation of Corticothalamic Alpha Oscillations. *The Journal of Neuroscience*, *31*(13), 4935. https://doi.org/10.1523/JNEUROSCI.5580-10.2011

Bonmassar, G., Hadjikhani, N., Ives, J. R., Hinton, D., & Belliveau, J. W. (2001). Influence of EEG electrodes on the BOLD fMRI signal. *Human Brain Mapping*, *14*(2), 108–115. https://doi.org/10.1002/HBM.1045

Bourguignon, M., De Tiège, X., De Beeck, M. O., Ligot, N., Paquier, P., Van Bogaert, P., Goldman, S., Hari, R., & Jousmäki, V. (2013). The pace of prosodic phrasing couples the listener's cortex to the reader's voice. *Human Brain Mapping*, *34*(2), 314–326. https://doi.org/10.1002/HBM.21442

Bowyer, S. M. (2016). Coherence a measure of the brain networks: past and present. *Neuropsychiatric Electrophysiology 2016 2:1*, *2*(1), 1–12. https://doi.org/10.1186/S40810-015-0015-7

Breska, A., & Deouell, L. Y. (2017). Neural mechanisms of rhythm-based temporal prediction: Delta phase-locking reflects temporal predictability but not rhythmic entrainment. *PLOS Biology*, *15*(2), e2001665. https://doi.org/10.1371/JOURNAL.PBIO.2001665

Bright, M. G., Whittaker, J. R., Driver, I. D., & Murphy, K. (2020). Vascular physiology drives functional brain networks. *NeuroImage*, *217*, 116907. https://doi.org/10.1016/J.NEUROIMAGE.2020.116907

Brookes, M. J., Woolrich, M., Luckhoo, H., Price, D., Hale, J. R., Stephenson, M. C., Barnes, G. R., Smith, S. M., & Morris, P. G. (2011). Investigating the electrophysiological basis of resting state networks using magnetoencephalography. *Proceedings of the National Academy of Sciences of the United States of America*, *108*(40), 16783–16788. https://doi.org/10.1073/PNAS.1112685108/-/DCSUPPLEMENTAL

Buffalo, E. A., Fries, P., Landman, R., Buschman, T. J., & Desimone, R. (2011). Laminar differences in gamma and alpha coherence in the ventral stream. *Proceedings of the National Academy of Sciences of the United States of America*, *108*(27), 11262–11267. https://doi.org/10.1073/PNAS.1011284108/-/DCSUPPLEMENTAL

Bullmore, E., & Sporns, O. (2012). The economy of brain network organization. *Nature Reviews Neuroscience 2012 13:5*, *13*(5), 336–349. https://doi.org/10.1038/nrn3214

Busch, N. A., Dubois, J., & VanRullen, R. (2009). The Phase of Ongoing EEG Oscillations Predicts Visual Perception. *Journal of Neuroscience*, *29*(24), 7869–7876. https://doi.org/10.1523/JNEUROSCI.0113-09.2009

Busch, N. A., & Vanrullen, R. (2010). *Spontaneous EEG oscillations reveal periodic sampling of visual attention*. *107*(37). https://doi.org/10.1073/pnas.1004801107

Butler, R., Bernier, P. M., Lefebvre, J., Gilbert, G., & Whittingstall, K. (2017). Decorrelated Input Dissociates Narrow Band γ Power and BOLD in Human Visual Cortex. *Journal of Neuroscience*, *37*(22), 5408–5418. https://doi.org/10.1523/JNEUROSCI.3938-16.2017

Buzsáki, G., Anastassiou, C. A., & Koch, C. (2012). The origin of extracellular fields and currents — EEG, ECoG, LFP and spikes. *Nature Reviews Neuroscience 2012 13:6*, *13*(6), 407–420. https://doi.org/10.1038/nrn3241

Buzsáki, G., & Draguhn, A. (2004). Neuronal oscillations in cortical networks. *Science (New York, N.Y.)*, *304*(5679), 1926–1929. https://doi.org/10.1126/SCIENCE.1099745

Canolty, R. T., & Knight, R. T. (2010). The functional role of cross-frequency coupling. In *Trends in Cognitive Sciences*. https://doi.org/10.1016/j.tics.2010.09.001

Capilla, A., Pazo-Alvarez, P., Darriba, A., Campo, P., & Gross, J. (2011). Steady-State Visual Evoked Potentials Can Be Explained by Temporal Superposition of Transient Event-Related Responses. *PLOS ONE*, *6*(1), e14543. https://doi.org/10.1371/JOURNAL.PONE.0014543

Cecere, R., Rees, G., & Romei, V. (2015). Individual differences in alpha frequency drive crossmodal illusory perception. *Current Biology : CB*, *25*(2), 231–235. https://doi.org/10.1016/J.CUB.2014.11.034

Chang, C., Liu, Z., Chen, M. C., Liu, X., & Duyn, J. H. (2013). EEG correlates of time-varying BOLD functional connectivity. *NeuroImage*, *72*, 227–236. https://doi.org/10.1016/J.NEUROIMAGE.2013.01.049

Clayton, M. S., Yeung, N., & Cohen Kadosh, R. (2018). The many characters of visual alpha oscillations. *European Journal of Neuroscience*, *48*(7), 2498–2508. https://doi.org/10.1111/EJN.13747

Cohen, M. X. (2014). Fluctuations in Oscillation Frequency Control Spike Timing and Coordinate Neural Networks. *Journal of Neuroscience*, *34*(27), 8988–8998. https://doi.org/10.1523/JNEUROSCI.0261-14.2014

Cohen, M. X., Axmacher, N., Lenartz, D., Elger, C. E., Sturm, V., & Schlaepfer, T. E. (2009). Good vibrations: cross-frequency coupling in the human nucleus accumbens during reward processing. *Journal of Cognitive Neuroscience*, *21*(5), 875–889. https://doi.org/10.1162/JOCN.2009.21062

Cohen, M. X., & Gulbinaite, R. (2017). *Rhythmic entrainment source separation: Optimizing analyses of neural responses to rhythmic sensory stimulation*. https://doi.org/10.1101/070862

Colclough, G. L., Brookes, M. J., Smith, S. M., & Woolrich, M. W. (2015). A symmetric multivariate leakage correction for MEG connectomes. *NeuroImage*, *117*, 439–448. https://doi.org/10.1016/J.NEUROIMAGE.2015.03.071

Cox, R., Schapiro, A. C., & Stickgold, R. (2018). Variability and stability of large-scale cortical oscillation patterns. *Network Neuroscience*, *2*(4), 481. https://doi.org/10.1162/NETN_A_00046

Da Silva, F. L. (2009). EEG: Origin and Measurement. *EEG - FMRI: Physiological Basis, Technique, and Applications*, 19–38. https://doi.org/10.1007/978-3-540-87919-0_2

de Graaf, T. A., Gross, J., Paterson, G., Rusch, T., Sack, A. T., & Thut, G. (2013). Alpha-

Band Rhythms in Visual Task Performance: Phase-Locking by Rhythmic Sensory Stimulation. *PLoS ONE*. https://doi.org/10.1371/journal.pone.0060035

De Luca, M., Beckmann, C. F., De Stefano, N., Matthews, P. M., & Smith, S. M. (2005). *fMRI resting state networks define distinct modes of long-distance interactions in the human brain*. https://doi.org/10.1016/j.neuroimage.2005.08.035

Deligianni, F., Centeno, M., Carmichael, D. W., & Clayden, J. D. (2014). Relating resting-state fMRI and EEG whole-brain connectomes across frequency bands. *Frontiers in Neuroscience*, *8*, 258. https://doi.org/10.3389/FNINS.2014.00258/ABSTRACT

Delorme, A., & Makeig, S. (2004). EEGLAB: an open source toolbox for analysis of single-trial EEG dynamics including independent component analysis. *Journal of Neuroscience Methods*, *134*, 9–21. http://www.sccn.ucsd.edu/eeglab/

Demuru, M., & Fraschini, M. (2020). EEG fingerprinting: Subject-specific signature based on the aperiodic component of power spectrum. *Computers in Biology and Medicine*, *120*, 103748. https://doi.org/10.1016/J.COMPBIOMED.2020.103748

Dima, D., Dietrich, D. E., Dillo, W., & Emrich, H. M. (2010). Impaired top-down processes in schizophrenia: a DCM study of ERPs. *NeuroImage*, *52*(3), 824–832. https://doi.org/10.1016/J.NEUROIMAGE.2009.12.086

Dima, D., Roiser, J. P., Dietrich, D. E., Bonnemann, C., Lanfermann, H., Emrich, H. M., & Dillo, W. (2009). Understanding why patients with schizophrenia do not perceive the hollow-mask illusion using dynamic causal modelling. *NeuroImage*, *46*(4), 1180–1186. https://doi.org/10.1016/J.NEUROIMAGE.2009.03.033

Donner, T. H., & Siegel, M. (2011). A framework for local cortical oscillation patterns. *Trends in Cognitive Sciences*, *15*(5), 191–199. https://doi.org/10.1016/J.TICS.2011.03.007

Dosenbach, N. U. F., Fair, D. A., Miezin, F. M., Cohen, A. L., Wenger, K. K., Dosenbach, R. A. T., Fox, M. D., Snyder, A. Z., Vincent, J. L., Raichle, M. E., Schlaggar, B. L., & Petersen, S. E. (2007). Distinct brain networks for adaptive and stable task control in humans. *Proceedings of the National Academy of Sciences*, *104*(26), 11073–11078. https://doi.org/10.1073/PNAS.0704320104

Eickhoff, S. B., Stephan, K. E., Mohlberg, H., Grefkes, C., Fink, G. R., Amunts, K., & Zilles, K. (2005). A new SPM toolbox for combining probabilistic cytoarchitectonic maps and functional imaging data. *NeuroImage*, *25*(4), 1325–1335. https://doi.org/10.1016/j.neuroimage.2004.12.034

Engel, A. K., Fries, P., & Singer, W. (2001). Dynamic predictions: Oscillations and

synchrony in top–down processing. *Nature Reviews Neuroscience 2001 2:10*, *2*(10), 704–716. https://doi.org/10.1038/35094565

Engel, A. K., Gerloff, C., Hilgetag, C. C., & Nolte, G. (2013). Intrinsic coupling modes: multiscale interactions in ongoing brain activity. *Neuron*, *80*(4), 867–886. https://doi.org/10.1016/J.NEURON.2013.09.038

Ergenoglu, T., Demiralp, T., Bayraktaroglu, Z., Ergen, M., Beydagi, H., & Uresin, Y. (2004). Alpha rhythm of the EEG modulates visual detection performance in humans. *Cognitive Brain Research*, *20*(3), 376–383. https://doi.org/https://doi.org/10.1016/j.cogbrainres.2004.03.009

Felleman, D. J., & Van Essen, D. C. (1991). Distributed hierarchical processing in the primate cerebral cortex. *Cerebral Cortex*, *1*(1), 1–47. https://doi.org/10.1093/CERCOR/1.1.1

Fiebelkorn, I. C., & Kastner, S. (2019). A rhythmic theory of attention. *Trends in Cognitive Sciences*, *23*(2), 87. https://doi.org/10.1016/J.TICS.2018.11.009

Fiebelkorn, I. C., Saalmann, Y. B., & Kastner, S. (2013). Rhythmic Sampling within and between Objects despite Sustained Attention at a Cued Location. *Current Biology*, *23*(24), 2553–2558. https://doi.org/10.1016/J.CUB.2013.10.063

Finnema, S. J., Scheinin, M., Shahid, M., Lehto, J., Borroni, E., Bang-Andersen, B., Sallinen, J., Wong, E., Farde, L., Halldin, C., & Grimwood, S. (2015). Application of cross-species PET imaging to assess neurotransmitter release in brain. *Psychopharmacology*, *232*(21–22), 4129. https://doi.org/10.1007/S00213-015-3938-6

Florin, E., & Baillet, S. (2015). The brain's resting-state activity is shaped by synchronized cross-frequency coupling of neural oscillations. *NeuroImage*, *111*, 26–35. https://doi.org/10.1016/J.NEUROIMAGE.2015.01.054

Fontolan, L., Morillon, B., Liegeois-Chauvel, C., & Giraud, A. L. (2014). The contribution of frequency-specific activity to hierarchical information processing in the human auditory cortex. *Nature Communications 2014 5:1*, *5*(1), 1–10. https://doi.org/10.1038/ncomms5694

Fox, M. D., Corbetta, M., Snyder, A. Z., Vincent, J. L., & Raichle, M. E. (2006). Spontaneous neuronal activity distinguishes human dorsal and ventral attention systems. *Proceedings of the National Academy of Sciences*, *103*(26), 10046–10051. https://doi.org/10.1073/PNAS.0604187103

Fox, M. D., Snyder, A. Z., Zacks, J. M., & Raichle, M. E. (2006). Coherent spontaneous activity accounts for trial-to-trial variability in human evoked brain responses. *Nature*

Neuroscience, *9*(1), 23–25. https://doi.org/10.1038/NN1616

Foxe, J. J., & Snyder, A. C. (2011). The role of alpha-band brain oscillations as a sensory suppression mechanism during selective attention. *Frontiers in Psychology*, *2*(JUL), 154. https://doi.org/10.3389/fpsyg.2011.00154

Fries, P. (2005). A mechanism for cognitive dynamics: neuronal communication through neuronal coherence. *Trends in Cognitive Sciences*, *9*(10), 474–480. https://doi.org/10.1016/J.TICS.2005.08.011

Fries, P. (2015). Rhythms For Cognition: Communication Through Coherence. *Neuron*, *88*(1), 220. https://doi.org/10.1016/J.NEURON.2015.09.034

Friston, K. J. (2002). *MODELS OF BRAIN FUNCTION IN NEUROIMAGING*. https://doi.org/10.1146/annurev.psych.56.091103.070311

Friston, K. J., Williams, S., Howard, R., Frackowiak, R. S. J., & Turner, R. (1996). Movement-related effects in fMRI time-series. *Magnetic Resonance in Medicine*, *35*(3), 346–355. https://doi.org/10.1002/MRM.1910350312

Giordano, B. L., Ince, R. A. A., Gross, J., Schyns, P. G., Panzeri, S., & Kayser, C. (2017). *Contributions of local speech encoding and functional connectivity to audio-visual speech perception*. https://doi.org/10.7554/eLife.24763.001

Giraud, A. L., & Poeppel, D. (2012). Cortical oscillations and speech processing: emerging computational principles and operations. *Nature Neuroscience*, *15*(4), 511. https://doi.org/10.1038/NN.3063

Glasser, M. F., Coalson, T. S., Robinson, E. C., Hacker, C. D., Harwell, J., Yacoub, E., Ugurbil, K., Andersson, J., Beckmann, C. F., Jenkinson, M., Smith, S. M., & Van Essen, D. C. (2016). A multi-modal parcellation of human cerebral cortex. *Nature*, *536*(7615), 171. https://doi.org/10.1038/NATURE18933

Goldman, R. I., Stern, J. M., Engel, J., Jr, & Cohen, M. S. (2002). Simultaneous EEG and fMRI of the alpha rhythm. *Neuroreport*, *13*(18), 2487. https://doi.org/10.1097/01.WNR.0000047685.08940.D0

Gross, J., Hoogenboom, N., Thut, G., Schyns, P., Panzeri, S., Belin, P., & Garrod, S. (2013). Speech rhythms and multiplexed oscillatory sensory coding in the human brain. *PLoS Biology*, *11*(12). https://doi.org/10.1371/JOURNAL.PBIO.1001752

Guillery, S. M. S. and R. W. (2005). *Exploring the Thalamus and Its Role in Cortical Function, Second Edition*. http://mitpress.mit.edu/catalog/item/default.asp?tid=10680&ttype=2

Hacker, C. D., Snyder, A. Z., Pahwa, M., Corbetta, M., & Leuthardt, E. C. (2017).

Frequency-specific electrophysiologic correlates of resting state fMRI networks. *NeuroImage*, *149*, 446–457. https://doi.org/10.1016/J.NEUROIMAGE.2017.01.054

Haegens, S., Barczak, A., Musacchia, G., Lipton, M. L., Mehta, A. D., Lakatos, P., & Schroeder, C. E. (2015). Laminar Profile and Physiology of the α Rhythm in Primary Visual, Auditory, and Somatosensory Regions of Neocortex. *Journal of Neuroscience*, *35*(42), 14341–14352. https://doi.org/10.1523/JNEUROSCI.0600-15.2015

Haegens, S., Cousijn, H., Wallis, G., Harrison, P. J., & Nobre, A. C. (2014). Inter- and intra-individual variability in alpha peak frequency. *NeuroImage*, *92*, 46–55. https://doi.org/10.1016/J.NEUROIMAGE.2014.01.049

Haegens, S., Osipova, D., Oostenveld, R., & Jensen, O. (2010). Somatosensory working memory performance in humans depends on both engagement and disengagement of regions in a distributed network. *Human Brain Mapping*, *31*(1), 26–35. https://doi.org/10.1002/HBM.20842

Haegens, S., & Zion Golumbic, E. (2018). Rhythmic facilitation of sensory processing: A critical review. In *Neuroscience and Biobehavioral Reviews* (Vol. 86, pp. 150–165). Elsevier Ltd. https://doi.org/10.1016/j.neubiorev.2017.12.002

Halgren, M., Ulbert, I., Bastuji, H., Fabó, D., Eross, L., Rey, M., Devinsky, O., Doyle, W. K., Mak-McCully, R., Halgren, E., Wittner, L., Chauvel, P., Heit, G., Eskandar, E., Mandell, A., & Cash, S. S. (2019). The generation and propagation of the human alpha rhythm. *Proceedings of the National Academy of Sciences of the United States of America*, *116*(47), 23772–23782. https://doi.org/10.1073/PNAS.1913092116

Händel, B. F., Haarmeier, T., & Jensen, O. (2011). Alpha Oscillations Correlate with the Successful Inhibition of Unattended Stimuli. *Journal of Cognitive Neuroscience*, *23*(9), 2494–2502. https://doi.org/10.1162/JOCN.2010.21557

Händel, B., & Haarmeier, T. (2009). Cross-frequency coupling of brain oscillations indicates the success in visual motion discrimination. *NeuroImage*, *45*(3), 1040–1046. https://doi.org/10.1016/J.NEUROIMAGE.2008.12.013

Hanslmayr, S., Aslan, A., Staudigl, T., Klimesch, W., Herrmann, C. S., & Bäuml, K.-H. (2007). Prestimulus oscillations predict visual perception performance between and within subjects. *NeuroImage*, *37*(4), 1465–1473. https://doi.org/https://doi.org/10.1016/j.neuroimage.2007.07.011

Hari, R., & Salmelin, R. (1997). Human cortical oscillations: a neuromagnetic view through the skull. *Trends Neurosci.*, *44–49*.

Helfrich, R. F., Breska, A., & Knight, R. T. (2019). Neural entrainment and network

resonance in support of top-down guided attention. *Current Opinion in Psychology*, *29*, 82–89. https://doi.org/10.1016/J.COPSYC.2018.12.016

Helfrich, R. F., Herrmann, C. S., Engel, A. K., & Schneider, T. R. (2016). Different coupling modes mediate cortical cross-frequency interactions. *NeuroImage*. https://doi.org/10.1016/j.neuroimage.2015.11.035

Helfrich, R. F., Huang, M., Wilson, G., & Knight, R. T. (2017). Prefrontal cortex modulates posterior alpha oscillations during top-down guided visual perception. *Proceedings of the National Academy of Sciences*. https://doi.org/10.1073/pnas.1705965114

Helfrich, R. F., Schneider, T. R., Rach, S., Trautmann-Lengsfeld, S. A., Engel, A. K., & Herrmann, C. S. (2014). Entrainment of brain oscillations by transcranial alternating current stimulation. *Current Biology : CB*, *24*(3), 333–339. https://doi.org/10.1016/J.CUB.2013.12.041

Hermes, D., Nguyen, M., & Winawer, J. (2017). Neuronal synchrony and the relation between the blood-oxygen-level dependent response and the local field potential. *PLOS Biology*, *15*(7), e2001461. https://doi.org/10.1371/JOURNAL.PBIO.2001461

Herrmann, C. S. (2001). Human EEG responses to 1-100 Hz flicker: Resonance phenomena in visual cortex and their potential correlation to cognitive phenomena. *Experimental Brain Research*. https://doi.org/10.1007/s002210100682

Herrmann, Christoph S., Murray, M. M., Ionta, S., Hutt, A., & Lefebvre, J. (2016). Shaping Intrinsic Neural Oscillations with Periodic Stimulation. *Journal of Neuroscience*, *36*(19), 5328–5337. https://doi.org/10.1523/JNEUROSCI.0236-16.2016

Higgins, C., Liu, Y., Vidaurre, D., Kurth-Nelson, Z., Dolan, R., Behrens, T., & Woolrich, M. (2021). Replay bursts in humans coincide with activation of the default mode and parietal alpha networks. *Neuron*, *109*(5), 882-893.e7. https://doi.org/10.1016/J.NEURON.2020.12.007

Hiltunen, T., Kantola, J., Abou Elseoud, A., Lepola, P., Suominen, K., Starck, T., Nikkinen, J., Remes, J., Tervonen, O., Palva, S., Kiviniemi, V., & Palva, J. M. (2014). Infra-Slow EEG Fluctuations Are Correlated with Resting-State Network Dynamics in fMRI. *Journal of Neuroscience*. https://doi.org/10.1523/JNEUROSCI.0276-13.2014

Hipp, J. F., Hawellek, D. J., Corbetta, M., Siegel, M., & Engel, A. K. (2012). Large-scale cortical correlation structure of spontaneous oscillatory activity. *Nature Neuroscience 2012 15:6*, *15*(6), 884–890. https://doi.org/10.1038/nn.3101

Hipp, J. F., & Siegel, M. (2015). BOLD fMRI Correlation Reflects Frequency-Specific Neuronal Correlation. *Current Biology : CB*, *25*(10), 1368–1374.

https://doi.org/10.1016/J.CUB.2015.03.049

Hunyadi, B., Woolrich, M. W., Quinn, A. J., Vidaurre, D., & De Vos, M. (2019). A dynamic system of brain networks revealed by fast transient EEG fluctuations and their fMRI correlates. *NeuroImage*, *185*, 72–82. https://doi.org/10.1016/J.NEUROIMAGE.2018.09.082

Hutchison, R. M., Womelsdorf, T., Allen, E. A., Bandettini, P. A., Calhoun, V. D., Corbetta, M., Della Penna, S., Duyn, J. H., Glover, G. H., Gonzalez-Castillo, J., Handwerker, D. A., Keilholz, S., Kiviniemi, V., Leopold, D. A., de Pasquale, F., Sporns, O., Walter, M., & Chang, C. (2013). Dynamic functional connectivity: Promise, issues, and interpretations. *NeuroImage*, *80*, 360–378. https://doi.org/10.1016/J.NEUROIMAGE.2013.05.079

Iemi, L., Chaumon, M., Crouzet, S. M., & Busch, N. A. (2017). Spontaneous Neural Oscillations Bias Perception by Modulating Baseline Excitability. *The Journal of Neuroscience*. https://doi.org/10.1523/JNEUROSCI.1432-16.2017

Ito, J., Nikolaev, A. R., & Van Leeuwen, C. (2005). Spatial and temporal structure of phase synchronization of spontaneous alpha EEG activity. *Biological Cybernetics*, *92*(1), 54–60. https://doi.org/10.1007/S00422-004-0533-Z

Iwabuchi, S. J., & Palaniyappan, L. (2017). Abnormalities in the effective connectivity of visuothalamic circuitry in schizophrenia. *Psychological Medicine*, *47*(7), 1300–1310. https://doi.org/10.1017/S0033291716003469

Jann, K., Koenig, T., Dierks, T., Boesch, C., & Federspiel, A. (2010). *Association of individual resting state EEG alpha frequency and cerebral blood ow*. https://doi.org/10.1016/j.neuroimage.2010.02.024

Jann, K., Kottlow, M., Dierks, T., Boesch, C., & Koenig, T. (2010). Topographic Electrophysiological Signatures of fMRI Resting State Networks. *PLOS ONE*, *5*(9), e12945. https://doi.org/10.1371/JOURNAL.PONE.0012945

Jensen, O., & Mazaheri, A. (2010). Shaping functional architecture by oscillatory alpha activity: Gating by inhibition. *Frontiers in Human Neuroscience*, *4*, 186. https://doi.org/10.3389/FNHUM.2010.00186/BIBTEX

Jones, E. G. (2009). Synchrony in the interconnected circuitry of the thalamus and cerebral cortex. *Annals of the New York Academy of Sciences*, *1157*, 10–23. https://doi.org/10.1111/J.1749-6632.2009.04534.X

Keil, J., Pomper, U., & Senkowski, D. (2016). Distinct patterns of local oscillatory activity and functional connectivity underlie intersensory attention and temporal prediction.

Cortex, *74*, 277–288. https://doi.org/10.1016/J.CORTEX.2015.10.023

Keil, J., & Senkowski, D. (2018). Neural Oscillations Orchestrate Multisensory Processing. *Neuroscientist*, *24*(6), 609–626. https://doi.org/10.1177/1073858418755352

Keitel, A., & Gross, J. (2016). Individual Human Brain Areas Can Be Identified from Their Characteristic Spectral Activation Fingerprints. *PLOS Biology*, *14*(6), e1002498. https://doi.org/10.1371/JOURNAL.PBIO.1002498

Keitel, C., Keitel, A., Benwell, C. S. Y., Daube, C., Thut, G., & Gross, J. (2019). Stimulus-Driven Brain Rhythms within the Alpha Band: The Attentional-Modulation Conundrum. *Journal of Neuroscience*, *39*(16), 3119–3129. https://doi.org/10.1523/JNEUROSCI.1633-18.2019

Keitel, C., Quigley, C., & Ruhnau, P. (2014). Stimulus-Driven Brain Oscillations in the Alpha Range: Entrainment of Intrinsic Rhythms or Frequency-Following Response? *The Journal of Neuroscience*, *34*(31), 10137. https://doi.org/10.1523/JNEUROSCI.1904-14.2014

Keller, A. S., Payne, L., & Sekuler, R. (2017). Characterizing the roles of alpha and theta oscillations in multisensory attention. *Neuropsychologia*, *99*, 48. https://doi.org/10.1016/J.NEUROPSYCHOLOGIA.2017.02.021

Klimesch, W. (1997). EEG-alpha rhythms and memory processes. *International Journal of Psychophysiology : Official Journal of the International Organization of Psychophysiology*, *26*(1–3), 319–340. https://doi.org/10.1016/S0167-8760(97)00773-3

Klimesch, W., Doppelmayr, M., Schimke, H., & Pachinger, T. (1996). Alpha frequency, reaction time, and the speed of processing information. *Journal of Clinical Neurophysiology : Official Publication of the American Electroencephalographic Society*, *13*(6), 511–518. https://doi.org/10.1097/00004691-199611000-00006

Klimesch, Wolfgang. (1999). EEG alpha and theta oscillations reflect cognitive and memory performance: a review and analysis. *Brain Research. Brain Research Reviews*, *29*(2–3), 169–195. https://doi.org/10.1016/S0165-0173(98)00056-3

Klimesch, Wolfgang. (2012). Alpha-band oscillations, attention, and controlled access to stored information. In *Trends in Cognitive Sciences*. https://doi.org/10.1016/j.tics.2012.10.007

Klimesch, Wolfgang. (2018). The frequency architecture of brain and brain body oscillations: an analysis. *The European Journal of Neuroscience*, *48*(7), 2431–2453. https://doi.org/10.1111/EJN.14192

Klimesch, Wolfgang, Sauseng, P., & Hanslmayr, S. (2007). EEG alpha oscillations: The

inhibition-timing hypothesis. *Brain Research Reviews*. https://doi.org/10.1016/j.brainresrev.2006.06.003

Kö, A., Bosker, H. R., Takashima, A., Meyer, A., Jensen, O., Correspondence, P. H., & Hagoort, P. (2018). Neural Entrainment Determines the Words We Hear Article Neural Entrainment Determines the Words We Hear. *Current Biology*, *28*, 1–9. https://doi.org/10.1016/j.cub.2018.07.023

Koch, S. P., Koendgen, S., Bourayou, R., Steinbrink, J., & Obrig, H. (2008). Individual alpha-frequency correlates with amplitude of visual evoked potential and hemodynamic response. *NeuroImage*, *41*(2), 233–242. https://doi.org/10.1016/J.NEUROIMAGE.2008.02.018

Kujala, J., Jung, J., Bouvard, S., Lecaignard, F., Lothe, A., Bouet, R., Ciumas, C., Ryvlin, P., & Jerbi, K. (2015). Gamma oscillations in V1 are correlated with GABAA receptor density: A multi-modal MEG and Flumazenil-PET study. *Scientific Reports 2015 5:1*, *5*(1), 1–12. https://doi.org/10.1038/srep16347

Kumral, D., Şansal, F., Cesnaite, E., Mahjoory, K., Al, E., Gaebler, M., Nikulin, V. V., & Villringer, A. (2020). BOLD and EEG signal variability at rest differently relate to aging in the human brain. *NeuroImage*, *207*, 116373. https://doi.org/10.1016/J.NEUROIMAGE.2019.116373

Kwong, K. K., Belliveau, J. W., Chesler, D. A., Goldberg, I. E., Weisskoff, R. M., Poncelet, B. P., Kennedy, D. N., Hoppel, B. E., Cohen, M. S., Turner, R., Cheng -, H. M., Brady, T. J., & Rosen, B. R. (1992). Dynamic magnetic resonance imaging of human brain activity during primary sensory stimulation. *Proceedings of the National Academy of Sciences*, *89*(12), 5675–5679. https://doi.org/10.1073/PNAS.89.12.5675

Lai, M., Demuru, M., Hillebrand, A., & Fraschini, M. (2018). A comparison between scalp- and source-reconstructed EEG networks. *Scientific Reports 2018 8:1*, *8*(1), 1–8. https://doi.org/10.1038/s41598-018-30869-w

Lakatos, P., Gross, J., & Thut, G. (2019). A New Unifying Account of the Roles of Neuronal Entrainment. *Current Biology : CB*, *29*(18), R890–R905. https://doi.org/10.1016/J.CUB.2019.07.075

Lamme, V. A. F., Supèr, H., & Spekreijse, H. (1998). Feedforward, horizontal, and feedback processing in the visual cortex. *Current Opinion in Neurobiology*, *8*(4), 529–535. https://doi.org/10.1016/S0959-4388(98)80042-1

Landau, A. N., & Fries, P. (2012). Attention Samples Stimuli Rhythmically. *Current Biology*, *22*(11), 1000–1004. https://doi.org/10.1016/J.CUB.2012.03.054

Lange, J., Oostenveld, R., & Fries, P. (2013). Reduced Occipital Alpha Power Indexes Enhanced Excitability Rather than Improved Visual Perception. *Journal of Neuroscience*. https://doi.org/10.1523/JNEUROSCI.3755-12.2013

Laufs, H., Kleinschmidt, A., Beyerle, A., Eger, E., Salek-Haddadi, A., Preibisch, C., & Krakow, K. (2003). EEG-correlated fMRI of human alpha activity. *NeuroImage*, *19*(4), 1463–1476. https://doi.org/10.1016/S1053-8119(03)00286-6

Leh, S. E., Chakravarty, M. M., & Ptito, A. (2008). The connectivity of the human pulvinar: a diffusion tensor imaging tractography study. *International Journal of Biomedical Imaging*, *2008*(1). https://doi.org/10.1155/2008/789539

Lemieux, L., Allen, P. J., Franconi, F., Symms, M. R., & Fish, D. R. (1997). Recording of EEG during fMRI experiments: patient safety. *Magnetic Resonance in Medicine*, *38*(6), 943–952. https://doi.org/10.1002/MRM.1910380614

Lenartowicz, A., Delorme, A., Walshaw, P. D., Cho, A. L., Bilder, R. M., McGough, J. J., McCracken, J. T., Makeig, S., & Loo, S. K. (2014). Electroencephalography Correlates of Spatial Working Memory Deficits in Attention-Deficit/Hyperactivity Disorder: Vigilance, Encoding, and Maintenance. *Journal of Neuroscience*, *34*(4), 1171–1182. https://doi.org/10.1523/JNEUROSCI.1765-13.2014

Lenartowicz, A., Lu, S., Rodriguez, C., Lau, E. P., Walshaw, P. D., McCracken, J. T., Cohen, M. S., & Loo, S. K. (2016). Alpha desynchronization and fronto-parietal connectivity during spatial working memory encoding deficits in ADHD: A simultaneous EEG-fMRI study. *NeuroImage. Clinical*, *11*, 210–223. https://doi.org/10.1016/J.NICL.2016.01.023

Lenartowicz, A., Mazaheri, A., Jensen, O., & Loo, S. K. (2018). ABERRANT MODULATION OF BRAIN OSCILLATORY ACTIVITY AND ATTENTIONAL IMPAIRMENT IN ADHD. *Biological Psychiatry. Cognitive Neuroscience and Neuroimaging*, *3*(1), 19. https://doi.org/10.1016/J.BPSC.2017.09.009

Leonardi, N., & Van De Ville, D. (2015). On spurious and real fluctuations of dynamic functional connectivity during rest. *NeuroImage*, *104*, 430–436. https://doi.org/10.1016/J.NEUROIMAGE.2014.09.007

Li, S., Jin, J. N., Wang, X., Qi, H. Z., Liu, Z. P., & Yin, T. (2017). Theta and alpha oscillations during the retention period of working memory by rTMS stimulating the parietal lobe. *Frontiers in Behavioral Neuroscience*, *11*, 170. https://doi.org/10.3389/FNBEH.2017.00170/BIBTEX

Liang, C. L., Ances, B. M., Perthen, J. E., Moradi, F., Liau, J., Buracas, G. T., Hopkins, S. R., & Buxton, R. B. (2013). Luminance contrast of a visual stimulus modulates the BOLD

response more than the cerebral blood flow response in the human brain. *NeuroImage*, *64*(1), 104. https://doi.org/10.1016/J.NEUROIMAGE.2012.08.077

Lindquist, M. A., Meng Loh, J., Atlas, L. Y., & Wager, T. D. (2009). Modeling the Hemodynamic Response Function in fMRI: Efficiency, Bias and Mis-modeling. *Neuroimage*, *45*(1 Suppl), S187. https://doi.org/10.1016/J.NEUROIMAGE.2008.10.065

Liu, T., Zhang, J., Dong, X., Li, Z., Shi, X., Tong, Y., Yang, R., Wu, J., Wang, C., & Yan, T. (2019). Occipital alpha connectivity during resting-state electroencephalography in patients with ultra-high risk for psychosis and schizophrenia. *Frontiers in Psychiatry*, *10*, 553. https://doi.org/10.3389/FPSYT.2019.00553/BIBTEX

Liu, Yong, Liang, M., Zhou, Y., He, Y., Hao, Y., Song, M., Yu, C., Liu, H., Liu, Z., & Jiang, T. (2008). Disrupted small-world networks in schizophrenia. *Brain : A Journal of Neurology*, *131*(Pt 4), 945–961. https://doi.org/10.1093/BRAIN/AWN018

Liu, Yuelu, Bengson, J., Huang, H., Mangun, G. R., & Ding, M. (2016). Top-down Modulation of Neural Activity in Anticipatory Visual Attention: Control Mechanisms Revealed by Simultaneous EEG-fMRI. *Cerebral Cortex (New York, NY)*, *26*(2), 517. https://doi.org/10.1093/CERCOR/BHU204

Logothetis, N. K. (2008). What we can do and what we cannot do with fMRI. *Nature 2008 453:7197*, *453*(7197), 869–878. https://doi.org/10.1038/nature06976

Lopes da Silva, F. (2013). EEG and MEG: relevance to neuroscience. *Neuron*, *80*(5), 1112–1128. https://doi.org/10.1016/J.NEURON.2013.10.017

Lowe, M. J., Mock, B. J., & Sorenson, J. A. (1998). Functional Connectivity in Single and Multislice Echoplanar Imaging Using Resting-State Fluctuations. *NeuroImage*, *7*(2), 119–132. https://doi.org/10.1006/NIMG.1997.0315

Lowet, E., Roberts, M. J., Bonizzi, P., Karel, J., & De Weerd, P. (2016). Quantifying Neural Oscillatory Synchronization: A Comparison between Spectral Coherence and Phase-Locking Value Approaches. *PLOS ONE*, *11*(1), e0146443. https://doi.org/10.1371/JOURNAL.PONE.0146443

Lynall, M. E., Bassett, D. S., Kerwin, R., McKenna, P. J., Kitzbichler, M., Muller, U., & Bullmore, E. (2010). Functional Connectivity and Brain Networks in Schizophrenia. *The Journal of Neuroscience*, *30*(28), 9477. https://doi.org/10.1523/JNEUROSCI.0333-10.2010

Manning, J. R., Jacobs, J., Fried, I., & Kahana, M. J. (2009). Broadband Shifts in Local Field Potential Power Spectra Are Correlated with Single-Neuron Spiking in Humans. *Journal of Neuroscience*, *29*(43), 13613–13620. https://doi.org/10.1523/JNEUROSCI.2041-

09.2009

Mantini, D., Perrucci, M. G., Del Gratta, C., Romani, G. L., Corbetta, M., & Raichle, M. E. (2007). *Electrophysiological signatures of resting state networks in the human brain* (Vol. 104, Issue 32).

Marshall, T. R., Bergmann, T. O., & Jensen, O. (2015). Frontoparietal Structural Connectivity Mediates the Top-Down Control of Neuronal Synchronization Associated with Selective Attention. *PLoS Biology*, *13*(10), 1–17. https://doi.org/10.1371/JOURNAL.PBIO.1002272

Marzetti, L., Della Penna, S., Snyder, A. Z., Pizzella, V., Nolte, G., de Pasquale, F., Romani, G. L., & Corbetta, M. (2013). Frequency specific interactions of MEG resting state activity within and across brain networks as revealed by the multivariate interaction measure. *NeuroImage*, *79*, 172–183. https://doi.org/10.1016/J.NEUROIMAGE.2013.04.062

Mathewson, K. E., Gratton, G., Fabiani, M., Beck, D. M., & Ro, T. (2009). To See or Not to See: Prestimulus α Phase Predicts Visual Awareness. *Journal of Neuroscience*, *29*(9), 2725–2732. https://doi.org/10.1523/JNEUROSCI.3963-08.2009

Mathewson, K. E., Lleras, A., Beck, D. M., Fabiani, M., Ro, T., & Gratton, G. (2011). Pulsed out of awareness: EEG alpha oscillations represent a pulsed-inhibition of ongoing cortical processing. In *Frontiers in Psychology*. https://doi.org/10.3389/fpsyg.2011.00099

Mathewson, K. E., Prudhomme, C., Fabiani, M., Beck, D. M., Lleras, A., & Gratton, G. (2012). *Making Waves in the Stream of Consciousness: Entraining Oscillations in EEG Alpha and Fluctuations in Visual Awareness with Rhythmic Visual Stimulation*.

Maurer, U., Brem, S., Liechti, M., Maurizio, S., Michels, L., & Brandeis, D. (2015). Frontal Midline Theta Reflects Individual Task Performance in a Working Memory Task. *Brain Topography*, *28*(1), 127–134. https://doi.org/10.1007/S10548-014-0361-Y/FIGURES/3

Mayhew, S. D., & Bagshaw, A. P. (2017). Dynamic spatiotemporal variability of alpha-BOLD relationships during the resting-state and task-evoked responses. *NeuroImage*, *155*, 120–137. https://doi.org/10.1016/J.NEUROIMAGE.2017.04.051

Mazaheri, A., Coffey-Corina, S., Mangun, G. R., Bekker, E. M., Berry, A. S., & Corbett, B. A. (2010). Functional disconnection of frontal cortex and visual cortex in attention-deficit/hyperactivity disorder. *Biological Psychiatry*, *67*(7), 617–623. https://doi.org/10.1016/J.BIOPSYCH.2009.11.022

Mazaheri, A., Fassbender, C., Coffey-Corina, S., Hartanto, T. A., Schweitzer, J. B., &

Mangun, G. R. (2014). Differential oscillatory electroencephalogram between attention-deficit/hyperactivity disorder subtypes and typically developing adolescents. *Biological Psychiatry*, *76*(5), 422–429. https://doi.org/10.1016/J.BIOPSYCH.2013.08.023

Michalareas, G., Vezoli, J., van Pelt, S., Schoffelen, J. M., Kennedy, H., & Fries, P. (2016). Alpha-Beta and Gamma Rhythms Subserve Feedback and Feedforward Influences among Human Visual Cortical Areas. *Neuron*, *89*(2), 384–397. https://doi.org/10.1016/J.NEURON.2015.12.018

Michel, C. M., Murray, M. M., Lantz, G., Gonzalez, S., Spinelli, L., & Grave De Peralta, R. (2004). EEG source imaging. *Clinical Neurophysiology : Official Journal of the International Federation of Clinical Neurophysiology*, *115*(10), 2195–2222. https://doi.org/10.1016/J.CLINPH.2004.06.001

Mierau, A., Klimesch, W., & Lefebvre, J. (2017). State-dependent alpha peak frequency shifts: Experimental evidence, potential mechanisms and functional implications. *Neuroscience*, *360*, 146–154. https://doi.org/10.1016/J.NEUROSCIENCE.2017.07.037

Miller, K. J., Zanos, S., Fetz, E. E., Den Nijs, M., & Ojemann, J. G. (2009). Decoupling the Cortical Power Spectrum Reveals Real-Time Representation of Individual Finger Movements in Humans. *Journal of Neuroscience*, *29*(10), 3132–3137. https://doi.org/10.1523/JNEUROSCI.5506-08.2009

Monto, S., Palva, S., Voipio, J., & Palva, J. M. (2008). Very Slow EEG Fluctuations Predict the Dynamics of Stimulus Detection and Oscillation Amplitudes in Humans. *Journal of Neuroscience*, *28*(33), 8268–8272. https://doi.org/10.1523/JNEUROSCI.1910-08.2008

Mostame, P., & Sadaghiani, S. (2021). Oscillation-Based Connectivity Architecture Is Dominated by an Intrinsic Spatial Organization, Not Cognitive State or Frequency. *Journal of Neuroscience*, *41*(1), 179–192. https://doi.org/10.1523/JNEUROSCI.2155-20.2020

Murakami, S., & Okada, Y. (2006). Contributions of principal neocortical neurons to magnetoencephalography and electroencephalography signals. *The Journal of Physiology*, *575*(Pt 3), 925–936. https://doi.org/10.1113/JPHYSIOL.2006.105379

Murta, T., Chaudhary, U. J., Tierney, T. M., Dias, A., Leite, M., Carmichael, D. W., Figueiredo, P., & Lemieux, L. (2017). Phase-amplitude coupling and the BOLD signal: A simultaneous intracranial EEG (icEEG) - fMRI study in humans performing a finger-tapping task. *NeuroImage*, *146*, 438–451. https://doi.org/10.1016/J.NEUROIMAGE.2016.08.036

Musall, S., Von Pföstl, V., Rauch, A., Logothetis, N. K., & Whittingstall, K. (2014). Effects

of neural synchrony on surface EEG. *Cerebral Cortex (New York, N.Y. : 1991)*, *24*(4), 1045–1053. https://doi.org/10.1093/CERCOR/BHS389

Muthukumaraswamy, S. D., Edden, R. A. E., Jones, D. K., Swettenham, J. B., & Singh, K. D. (2009). Resting GABA concentration predicts peak gamma frequency and fMRI amplitude in response to visual stimulation in humans. *Proceedings of the National Academy of Sciences of the United States of America*, *106*(20), 8356–8361. https://doi.org/10.1073/PNAS.0900728106

Muthukumaraswamy, S. D., & Singh, K. D. (2011). A cautionary note on the interpretation of phase-locking estimates with concurrent changes in power. *Clinical Neurophysiology : Official Journal of the International Federation of Clinical Neurophysiology*, *122*(11), 2324–2325. https://doi.org/10.1016/J.CLINPH.2011.04.003

Nentwich, M., Ai, L., Madsen, J., Telesford, Q. K., Haufe, S., Milham, M. P., & Parra, L. C. (2020). Functional connectivity of EEG is subject-specific, associated with phenotype, and different from fMRI. *NeuroImage*, *218*, 117001. https://doi.org/10.1016/J.NEUROIMAGE.2020.117001

Newson, J. J., & Thiagarajan, T. C. (2019). EEG Frequency Bands in Psychiatric Disorders: A Review of Resting State Studies. *Frontiers in Human Neuroscience*, *12*, 521. https://doi.org/10.3389/FNHUM.2018.00521/BIBTEX

Niedermeyer, E., & Lopes da Silva, F. H. (1999). *Electroencephalography : basic principles, clinical applications, and related fields*. 1258. https://books.google.com/books/about/Electroencephalography.html?id=zoGPQgAACAAJ

Nolte, G., Bai, O., Wheaton, L., Mari, Z., Vorbach, S., & Hallett, M. (2004). Identifying true brain interaction from EEG data using the imaginary part of coherency. *Clinical Neurophysiology : Official Journal of the International Federation of Clinical Neurophysiology*, *115*(10), 2292–2307. https://doi.org/10.1016/J.CLINPH.2004.04.029

Notbohm, A., & Herrmann, C. S. (2016). Flicker Regularity Is Crucial for Entrainment of Alpha Oscillations. *Frontiers in Human Neuroscience*. https://doi.org/10.3389/fnhum.2016.00503

Notbohm, A., Kurths, J., & Herrmann, C. S. (2016). Modification of Brain Oscillations via Rhythmic Light Stimulation Provides Evidence for Entrainment but Not for Superposition of Event-Related Responses. *Frontiers in Human Neuroscience*. https://doi.org/10.3389/fnhum.2016.00010

Nunez, P. L., Silberstein, R. B., Cadusch, P. J., Wijesinghe, R. S., Westdorp, A. F., &

Srinivasan, R. (1994). A theoretical and experimental study of high resolution EEG based on surface Laplacians and cortical imaging. *Electroencephalography and Clinical Neurophysiology*, *90*(1), 40–57. https://doi.org/10.1016/0013-4694(94)90112-0

Nunez, P., & Srinivasan, R. (2006). Electric Fields of the Brain : the neurophysics of EEG. In *JAMA: The Journal of the American Medical Association* (Vol. 247, Issue 13). Oxford University Press,.

Ogawa, S., Tank, D. W., Menon, R., Ellermann, J. M., Kim, S. G., Merkle, H., & Ugurbil, K. (1992). Intrinsic signal changes accompanying sensory stimulation: functional brain mapping with magnetic resonance imaging. *Proceedings of the National Academy of Sciences of the United States of America*, *89*(13), 5951–5955. https://doi.org/10.1073/PNAS.89.13.5951

Ohki, T., Gunji, A., Takei, Y., Takahashi, H., Kaneko, Y., Kita, Y., Hironaga, N., Tobimatsu, S., Kamio, Y., Hanakawa, T., Inagaki, M., & Hiraki, K. (2016). Neural oscillations in the temporal pole for a temporally congruent audio-visual speech detection task. *Scientific Reports*, *6*. https://doi.org/10.1038/SREP37973

Ojemann, G. A., Ramsey, N. F., & Ojemann, J. (2013). Relation between functional magnetic resonance imaging (fMRI) and single neuron, local field potential (LFP) and electrocorticography (ECoG) activity in human cortex. *Frontiers in Human Neuroscience*, *7*(JAN). https://doi.org/10.3389/FNHUM.2013.00034

Oostenveld, R., Fries, P., Maris, E., & Schoffelen, J. M. (2011). FieldTrip: Open source software for advanced analysis of MEG, EEG, and invasive electrophysiological data. *Computational Intelligence and Neuroscience*, *2011*. https://doi.org/10.1155/2011/156869

Osipova, D., Hermes, D., & Jensen, O. (2008). Gamma power is phase-locked to posterior alpha activity. *PloS One*, *3*(12). https://doi.org/10.1371/JOURNAL.PONE.0003990

Otero, M., Prado-Gutiérrez, P., Weinstein, A., Escobar, M. J., & El-Deredy, W. (2020). Persistence of EEG Alpha Entrainment Depends on Stimulus Phase at Offset. *Frontiers in Human Neuroscience*, *14*, 139. https://doi.org/10.3389/FNHUM.2020.00139/BIBTEX

Ozus, B., Liu, H. L., Chen, L., Iyer, M. B., Fox, P. T., & Gao, J. H. (2001). Rate dependence of human visual cortical response due to brief stimulation: an event-related fMRI study. *Magnetic Resonance Imaging*, *19*(1), 21–25. https://doi.org/10.1016/S0730-725X(01)00219-3

Palva, S., & Palva, J. M. (2011). Functional roles of alpha-band phase synchronization in

local and large-scale cortical networks. In *Frontiers in Psychology*. https://doi.org/10.3389/fpsyg.2011.00204

Parkes, L. M., Fries, P., Kerskens, C. M., & Norris, D. G. (2004). Reduced BOLD response to periodic visual stimulation. *NeuroImage*, *21*(1), 236–243. https://doi.org/10.1016/j.neuroimage.2003.08.025

Patel, A. X., Kundu, P., Rubinov, M., Jones, P. S., Vértes, P. E., Ersche, K. D., Suckling, J., & Bullmore, E. T. (2014). A wavelet method for modeling and despiking motion artifacts from resting-state fMRI time series. *NeuroImage*, *95*(100), 287–304. https://doi.org/10.1016/J.NEUROIMAGE.2014.03.012

Pfurtscheller, G., Stancák, A., & Neuper, C. (1996). Event-related synchronization (ERS) in the alpha band--an electrophysiological correlate of cortical idling: a review. *International Journal of Psychophysiology : Official Journal of the International Organization of Psychophysiology*, *24*(1–2), 39–46. https://doi.org/10.1016/S0167-8760(96)00066-9

Pikovsky, A., Rosenblum, M., & Kurths, J. (2001). Synchronization - A Universal Concept in Nonlinear Sciences. *Undefined*.

Pikovsky, Arkady, Rosenblum, M., Kurths, J., & Hilborn, R. C. (2002). Synchronization: A Universal Concept in Nonlinear Science. *American Journal of Physics*, *70*(6), 655. https://doi.org/10.1119/1.1475332

Pomper, U., Keil, J., Foxe, J. J., & Senkowski, D. (2015). Intersensory selective attention and temporal orienting operate in parallel and are instantiated in spatially distinct sensory and motor cortices. *Human Brain Mapping*, *36*(8), 3246–3259. https://doi.org/10.1002/HBM.22845

Portnova, G. V., Tetereva, A., Balaev, V., Atanov, M., Skiteva, L., Ushakov, V., Ivanitsky, A., & Martynova, O. (2018). Correlation of BOLD signal with linear and nonlinear patterns of EEG in resting state EEG-informed fMRI. *Frontiers in Human Neuroscience*, *11*, 654. https://doi.org/10.3389/FNHUM.2017.00654/BIBTEX

Qin, P., Duncan, N. W., Wiebking, C., Gravel, P., Lyttelton, O., Hayes, D. J., Verhaeghe, J., Kostikov, A., Schirrmacher, R., Reader, A. J., & Northoff, G. (2012). GABAA receptors in visual and auditory cortex and neural activity changes during basic visual stimulation. *Frontiers in Human Neuroscience*, *0*(DEC), 337. https://doi.org/10.3389/FNHUM.2012.00337/BIBTEX

Rajkumar, R., Régio Brambilla, C., Veselinović, T., Bierbrier, J., Wyss, C., Ramkiran, S., Orth, L., Lang, M., Rota Kops, E., Mauler, J., Scheins, J., Neumaier, B., Ermert, J.,

Herzog, H., Langen, K. J., Binkofski, F. C., Lerche, C., Shah, N. J., & Neuner, I. (2021). Excitatory–inhibitory balance within EEG microstates and resting-state fMRI networks: assessed via simultaneous trimodal PET–MR–EEG imaging. *Translational Psychiatry 2021 11:1*, *11*(1), 1–15. https://doi.org/10.1038/s41398-020-01160-2

Regan, D. (1982). COMPARISON OF TRANSIENT AND STEADY-STATE METHODS*. *Annals of the New York Academy of Sciences*, *388*(1), 45–71. https://doi.org/10.1111/J.1749-6632.1982.TB50784.X

Rohenkohl, G., & Nobre, A. C. (2011). Alpha Oscillations Related to Anticipatory Attention Follow Temporal Expectations. *Journal of Neuroscience*, *31*(40), 14076–14084. https://doi.org/10.1523/JNEUROSCI.3387-11.2011

Rolls, E. T., Huang, C. C., Lin, C. P., Feng, J., & Joliot, M. (2020). Automated anatomical labelling atlas 3. *NeuroImage*, *206*(August 2019), 116189. https://doi.org/10.1016/j.neuroimage.2019.116189

Romei, V., Brodbeck, V., Michel, C., Amedi, A., Pascual-Leone, A., & Thut, G. (2008). Spontaneous Fluctuations in Posterior α-Band EEG Activity Reflect Variability in Excitability of Human Visual Areas. *Cerebral Cortex (New York, NY)*, *18*(9), 2010–2018. https://doi.org/10.1093/cercor/bhm229

Ronconi, L., Busch, N. A., & Melcher, D. (2018). Alpha-band sensory entrainment alters the duration of temporal windows in visual perception. *Scientific Reports*, *8*(1), 1–10. https://doi.org/10.1038/s41598-018-29671-5

Ross, C. A., Margolis, R. L., Reading, S. A. J., Pletnikov, M., & Coyle, J. T. (2006). Neurobiology of Schizophrenia. *Neuron*, *52*(1), 139–153. https://doi.org/10.1016/J.NEURON.2006.09.015

Roux, F., & Uhlhaas, P. J. (2014). Working memory and neural oscillations: alpha–gamma versus theta–gamma codes for distinct WM information? *Trends in Cognitive Sciences*, *18*(1), 16–25. https://doi.org/10.1016/J.TICS.2013.10.010

Rudie, J. D., Shehzad, Z., Hernandez, L. M., Colich, N. L., Bookheimer, S. Y., Iacoboni, M., & Dapretto, M. (2012). Reduced Functional Integration and Segregation of Distributed Neural Systems Underlying Social and Emotional Information Processing in Autism Spectrum Disorders. *Cerebral Cortex*, *22*(5), 1025–1037. https://doi.org/10.1093/CERCOR/BHR171

Saalmann, Y. B., & Kastner, S. (2011). Cognitive and Perceptual Functions of the Visual Thalamus. *Neuron*, *71*(2), 209. https://doi.org/10.1016/J.NEURON.2011.06.027

Saalmann, Y. B., Pinsk, M. A., Wang, L., Li, X., & Kastner, S. (2012). The pulvinar

regulates information transmission between cortical areas based on attention demands. *Science*. https://doi.org/10.1126/science.1223082

Sadaghiani, S., Scheeringa, R., Lehongre, K., Morillon, B., Giraud, A.-L., D'Esposito, M., & Kleinschmidt, A. (2012). Alpha-Band Phase Synchrony Is Related to Activity in the Fronto-Parietal Adaptive Control Network. *Journal of Neuroscience*. https://doi.org/10.1523/JNEUROSCI.1358-12.2012

Sadaghiani, Sepideh, Brookes, M. J., & Baillet, S. (2022). Connectomics of human electrophysiology. *NeuroImage*, *247*, 118788. https://doi.org/10.1016/J.NEUROIMAGE.2021.118788

Sadaghiani, Sepideh, Scheeringa, R., Lehongre, K., Morillon, B., Giraud, A. L., D'Esposito, M., & Kleinschmidt, A. (2012). Alpha-band phase synchrony is related to activity in the fronto-parietal adaptive control network. *Journal of Neuroscience*, *32*(41), 14305–14310. https://doi.org/10.1523/JNEUROSCI.1358-12.2012

Sadaghiani, Sepideh, & Wirsich, J. (2020). Intrinsic connectome organization across temporal scales: New insights from cross-modal approaches. *Network Neuroscience*, *4*(1), 1. https://doi.org/10.1162/NETN_A_00114

Samaha, J., Bauer, P., Cimaroli, S., & Postle, B. R. (2015). Top-down control of the phase of alpha-band oscillations as a mechanism for temporal prediction. *Proceedings of the National Academy of Sciences*. https://doi.org/10.1073/pnas.1503686112

Samaha, J., Iemi, L., & Postle, B. R. (2017). Prestimulus alpha-band power biases visual discrimination confidence, but not accuracy. *Consciousness and Cognition*. https://doi.org/10.1016/j.concog.2017.02.005

Samaha, J., & Postle, B. R. (2015). The Speed of Alpha-Band Oscillations Predicts the Temporal Resolution of Visual Perception. *Current Biology*. https://doi.org/10.1016/j.cub.2015.10.007

Sargent, K., Chavez-Baldini, U. Y., Master, S. L., Verweij, K. J. H., Lok, A., Sutterland, A. L., Vulink, N. C., Denys, D., Smit, D. J. A., & Nieman, D. H. (2021). Resting-state brain oscillations predict cognitive function in psychiatric disorders: A transdiagnostic machine learning approach. *NeuroImage: Clinical*, *30*, 102617. https://doi.org/10.1016/J.NICL.2021.102617

Sauseng, P., Klimesch, W., Gruber, W., Doppelmayr, M., Stadler, W., & Schabus, M. (2002). The interplay between theta and alpha oscillations in the human electroencephalogram reflects the transfer of information between memory systems. *Neuroscience Letters*, *324*(2), 121–124. https://doi.org/10.1016/S0304-3940(02)00225-2

Sauseng, Paul, Conci, M., Wild, B., & Geyer, T. (2015). Predictive coding in visual search as revealed by cross-frequency EEG phase synchronization. In *Frontiers in Psychology*. https://doi.org/10.3389/fpsyg.2015.01655

Sauseng, Paul, Klimesch, W., Heise, K. F., Gruber, W. R., Holz, E., Karim, A. A., Glennon, M., Gerloff, C., Birbaumer, N., & Hummel, F. C. (2009). Brain Oscillatory Substrates of Visual Short-Term Memory Capacity. *Current Biology*, *19*(21), 1846–1852. https://doi.org/10.1016/J.CUB.2009.08.062

Scheeringa, R., Mazaheri, A., Bojak, I., Norris, D. G., & Kleinschmidt, A. (2011). Modulation of Visually Evoked Cortical fMRI Responses by Phase of Ongoing Occipital Alpha Oscillations. *Journal of Neuroscience*. https://doi.org/10.1523/JNEUROSCI.4697-10.2011

Scheeringa, René, & Fries, P. (2019). Cortical layers, rhythms and BOLD signals. *NeuroImage*, *197*, 689–698. https://doi.org/10.1016/J.NEUROIMAGE.2017.11.002

Scheeringa, René, Koopmans, P. J., van Mourik, T., Jensen, O., & Norris, D. G. (2016). The relationship between oscillatory EEG activity and the laminar-specific BOLD signal. *Proceedings of the National Academy of Sciences*. https://doi.org/10.1073/pnas.1522577113

Scheeringa, René, Petersson, K. M., Kleinschmidt, A., Jensen, O., & Bastiaansen, M. C. m. (2012). EEG Alpha Power Modulation of fMRI Resting-State Connectivity. *Brain Connectivity*, *2*(5), 254–264. https://doi.org/10.1089/brain.2012.0088

Scheeringa, René, Petersson, K. M., Oostenveld, R., Norris, D. G., Hagoort, P., & Bastiaansen, M. C. M. (2009). Trial-by-trial coupling between EEG and BOLD identifies networks related to alpha and theta EEG power increases during working memory maintenance. *NeuroImage*, *44*(3), 1224–1238. https://doi.org/10.1016/j.neuroimage.2008.08.041

Schoffelen, J. M., & Gross, J. (2009a). Source connectivity analysis with MEG and EEG. *Human Brain Mapping*, *30*(6), 1857–1865. https://doi.org/10.1002/HBM.20745

Schoffelen, J. M., & Gross, J. (2009b). Source connectivity analysis with MEG and EEG. *Human Brain Mapping*, *30*(6), 1857–1865. https://doi.org/10.1002/HBM.20745

Schroeder, C. E., & Lakatos, P. (2009). Low-frequency neuronal oscillations as instruments of sensory selection. *Trends in Neurosciences*. https://doi.org/10.1016/j.tins.2008.09.012

Sedley, W., Gander, P. E., Kumar, S., Kovach, C. K., Oya, H., Kawasaki, H., Howard, M. A., & Griffiths, T. D. (2016). Neural signatures of perceptual inference. *ELife*, *5*(MARCH2016). https://doi.org/10.7554/ELIFE.11476

Shah, N. J., Arrubla, J., Rajkumar, R., Farrher, E., Mauler, J., Kops, E. R., Tellmann, L., Scheins, J., Boers, F., Dammers, J., Sripad, P., Lerche, C., Langen, K. J., Herzog, H., & Neuner, I. (2017). Multimodal Fingerprints of Resting State Networks as assessed by Simultaneous Trimodal MR-PET-EEG Imaging. *Scientific Reports 2017 7:1*, *7*(1), 1–13. https://doi.org/10.1038/s41598-017-05484-w

Sherman, S. M., & Guillery, R. W. (2013). Chapter 4: Classification of afferents in thalamus en cortex. *Functional Connections of Cortical Areas; a New View from the Thalamus*.

Shine, J. M., Bissett, P. G., Bell, P. T., Koyejo, O., Balsters, J. H., Gorgolewski, K. J., Moodie, C. A., & Poldrack, R. A. (2016). The Dynamics of Functional Brain Networks: Integrated Network States during Cognitive Task Performance. *Neuron*, *92*(2), 544–554. https://doi.org/10.1016/J.NEURON.2016.09.018/ATTACHMENT/0AF718CF-9952-4E6C-9838-A5BA94DC5042/MMC1.PDF

Siegel, M., Donner, T. H., & Engel, A. K. (2012). *Spectral fingerprints of large-scale neuronal interactions*.

Simon, D. M., Noel, J. P., & Wallace, M. T. (2017). Event Related Potentials Index Rapid Recalibration to Audiovisual Temporal Asynchrony. *Frontiers in Integrative Neuroscience*, *11*. https://doi.org/10.3389/FNINT.2017.00008

Singh, M., Kim, S., & Kim, T.-S. (2003). Correlation between BOLD-fMRI and EEG signal changes in response to visual stimulus frequency in humans. *Magnetic Resonance in Medicine*, *49*(1), 108–114. https://doi.org/10.1002/mrm.10335

Smout, C. A., Tang, M. F., Garrido, M. I., & Mattingley, J. B. (2019). Attention promotes the neural encoding of prediction errors. *PLOS Biology*, *17*(2), e2006812. https://doi.org/10.1371/JOURNAL.PBIO.2006812

Snyder, A. C., & Foxe, J. J. (2010). Anticipatory attentional suppression of visual features indexed by oscillatory alpha-band power increases: a high-density electrical mapping study. *The Journal of Neuroscience : The Official Journal of the Society for Neuroscience*, *30*(11), 4024–4032. https://doi.org/10.1523/JNEUROSCI.5684-09.2010

Spaak, E., de Lange, F. P., & Jensen, O. (2014). Local Entrainment of Alpha Oscillations by Visual Stimuli Causes Cyclic Modulation of Perception. *Journal of Neuroscience*. https://doi.org/10.1523/JNEUROSCI.4385-13.2014

Spaak, Eelke, Bonnefond, M., Maier, A., Leopold, D. A., & Jensen, O. (2012). Layer-specific entrainment of gamma-band neural activity by the alpha rhythm in monkey visual cortex. *Current Biology : CB*, *22*(24), 2313. https://doi.org/10.1016/J.CUB.2012.10.020

Spillmann, L., & Werner, J. S. (1996). *Article in Trends in Neurosciences*.

https://doi.org/10.1016/0166-2236(96)10038-2

Stein, B. E., Meredith, M. A., & Wallace, M. T. (1993). The visually responsive neuron and beyond: multisensory integration in cat and monkey. *Progress in Brain Research*, *95*(C), 79–90. https://doi.org/10.1016/S0079-6123(08)60359-3

Stephan, K. E., & Friston, K. J. (2009). Functional Connectivity. *Encyclopedia of Neuroscience*, 391–397. https://doi.org/10.1016/B978-008045046-9.00308-9

Steriade, M., & Deschenes, M. (1984). The thalamus as a neuronal oscillator. *Brain Research*, *320*(1), 1–63. https://doi.org/10.1016/0165-0173(84)90017-1

Thilakavathi, B., Shenbaga Devi, S., Malaiappan, M., & Bhanu, K. (2019). EEG power spectrum analysis for schizophrenia during mental activity. *Australasian Physical & Engineering Sciences in Medicine*, *42*(3), 887–897. https://doi.org/10.1007/S13246-019-00779-W

Thut, G., Nietzel, A., Brandt, S. A., & Pascual-Leone, A. (2006). α-Band Electroencephalographic Activity over Occipital Cortex Indexes Visuospatial Attention Bias and Predicts Visual Target Detection. *The Journal of Neuroscience*, *26*(37), 9494. http://www.jneurosci.org/content/26/37/9494.abstract

Thut, G., Schyns, P. G., & Gross, J. (2011). Entrainment of Perceptually Relevant Brain Oscillations by Non-Invasive Rhythmic Stimulation of the Human Brain. *Frontiers in Psychology*, *2*(JUL). https://doi.org/10.3389/FPSYG.2011.00170

Thut, G., Veniero, D., Romei, V., Miniussi, C., Schyns, P., & Gross, J. (2011). Rhythmic TMS causes local entrainment of natural oscillatory signatures. *Current Biology*. https://doi.org/10.1016/j.cub.2011.05.049

Tomasi, D., Wang, G. J., & Volkow, N. D. (2013). Energetic cost of brain functional connectivity. *Proceedings of the National Academy of Sciences of the United States of America*, *110*(33), 13642–13647. https://doi.org/10.1073/PNAS.1303346110/-/DCSUPPLEMENTAL

Trajkovic, J., Di Gregorio, F., Ferri, F., Marzi, C., Diciotti, S., & Romei, V. (2021). Resting state alpha oscillatory activity is a valid and reliable marker of schizotypy. *Scientific Reports 2021 11:1*, *11*(1), 1–13. https://doi.org/10.1038/s41598-021-89690-7

Uhlhaas, P. J., & Singer, W. (2006). Neural synchrony in brain disorders: relevance for cognitive dysfunctions and pathophysiology. *Neuron*, *52*(1), 155–168. https://doi.org/10.1016/J.NEURON.2006.09.020

Van Diepen, Rosanne M., Foxe, J. J., & Mazaheri, A. (2019). The functional role of alpha-band activity in attentional processing: the current zeitgeist and future outlook.

Undefined, *29*, 229–238. https://doi.org/10.1016/J.COPSYC.2019.03.015

Van Diepen, Rosanne M, Foxe, J. J., & Mazaheri, A. (2019). The functional role of alpha-band activity in attentional processing: the current zeitgeist and future outlook. *Current Opinion in Psychology*, *29*, 229–238. https://doi.org/10.1016/j.copsyc.2019.03.015

Van Diepen, Rosanne Maria, & Mazaheri, A. (2018). The Caveats of observing Inter-Trial Phase-Coherence in Cognitive Neuroscience. *Scientific Reports 2018 8:1*, *8*(1), 1–9. https://doi.org/10.1038/s41598-018-20423-z

Van Dijk, H., Schoffelen, J. M., Oostenveld, R., & Jensen, O. (2008). Prestimulus Oscillatory Activity in the Alpha Band Predicts Visual Discrimination Ability. *Journal of Neuroscience*, *28*(8), 1816–1823. https://doi.org/10.1523/JNEUROSCI.1853-07.2008

Van Kerkoerle, T., Self, M. W., Dagnino, B., Gariel-Mathis, M. A., Poort, J., Van Der Togt, C., & Roelfsema, P. R. (2014). Alpha and gamma oscillations characterize feedback and feedforward processing in monkey visual cortex. *Proceedings of the National Academy of Sciences of the United States of America*, *111*(40), 14332–14341. https://doi.org/10.1073/PNAS.1402773111/-/DCSUPPLEMENTAL

VanRullen, R., Busch, N. A., Drewes, J., & Dubois, J. (2011). Ongoing EEG Phase as a Trial-by-Trial Predictor of Perceptual and Attentional Variability. *Frontiers in Psychology*, *2*(APR). https://doi.org/10.3389/FPSYG.2011.00060

VanRullen, Rufin. (2016). Perceptual Cycles. In *Trends in Cognitive Sciences*. https://doi.org/10.1016/j.tics.2016.07.006

Varela, F., Lachaux, J. P., Rodriguez, E., & Martinerie, J. (2001). The brainweb: Phase synchronization and large-scale integration. *Nature Reviews Neuroscience 2001 2:4*, *2*(4), 229–239. https://doi.org/10.1038/35067550

Vidaurre, D., Hunt, L. T., Quinn, A. J., Hunt, B. A. E., Brookes, M. J., Nobre, A. C., & Woolrich, M. W. (2018). Spontaneous cortical activity transiently organises into frequency specific phase-coupling networks. *Nature Communications 2018 9:1*, *9*(1), 1–13. https://doi.org/10.1038/s41467-018-05316-z

Vijayan, S., & Kopell, N. J. (2012). Thalamic model of awake alpha oscillations and implications for stimulus processing. *Proceedings of the National Academy of Sciences of the United States of America*, *109*(45), 18553–18558. https://doi.org/10.1073/PNAS.1215385109/-/DCSUPPLEMENTAL

Villien, M., Wey, H. Y., Mandeville, J. B., Catana, C., Polimeni, J. R., Sander, C. Y., Zürcher, N. R., Chonde, D. B., Fowler, J. S., Rosen, B. R., & Hooker, J. M. (2014). Dynamic functional imaging of brain glucose utilization using fPET-FDG. *NeuroImage*,

100, 192–199. https://doi.org/10.1016/J.NEUROIMAGE.2014.06.025

Vincent, J. L., Kahn, I., Snyder, A. Z., Raichle, M. E., & Buckner, R. L. (2008). Evidence for a Frontoparietal Control System Revealed by Intrinsic Functional Connectivity. *Journal of Neurophysiology*, *100*(6), 3328. https://doi.org/10.1152/JN.90355.2008

Vinke, L., & Ling, S. (2018). Luminance response functions in the human visual cortex. *Journal of Vision*, *18*(10), 363–363. https://doi.org/10.1167/18.10.363

Vollebregt, M. A., Zumer, J. M., ter Huurne, N., Buitelaar, J. K., & Jensen, O. (2016). Posterior alpha oscillations reflect attentional problems in boys with Attention Deficit Hyperactivity Disorder. *Clinical Neurophysiology : Official Journal of the International Federation of Clinical Neurophysiology*, *127*(5), 2182–2191. https://doi.org/10.1016/J.CLINPH.2016.01.021

Voytek, B., & Knight, R. T. (2010). Prefrontal cortex and basal ganglia contributions to visual working memory. *Proceedings of the National Academy of Sciences*. https://doi.org/10.1073/pnas.1007277107

Wei, Y., Chang, M., Womer, F. Y., Zhou, Q., Yin, Z., Wei, S., Zhou, Y., Jiang, X., Yao, X., Duan, J., Xu, K., Zuo, X. N., Tang, Y., & Wang, F. (2018). Local functional connectivity alterations in schizophrenia, bipolar disorder, and major depressive disorder. *Journal of Affective Disorders*, *236*, 266–273. https://doi.org/10.1016/J.JAD.2018.04.069

Whitfield-Gabrieli, S., & Nieto-Castanon, A. (2012). Conn: a functional connectivity toolbox for correlated and anticorrelated brain networks. *Brain Connectivity*, *2*(3), 125–141. https://doi.org/10.1089/BRAIN.2012.0073

Wills, A. J., Lavric, A., Croft, G. S., & Hodgson, T. L. (2007). Predictive learning, prediction errors, and attention: evidence from event-related potentials and eye tracking. *Journal of Cognitive Neuroscience*, *19*(5), 843–854. https://doi.org/10.1162/JOCN.2007.19.5.843

Winawer, J., Kay, K. N., Foster, B. L., Rauschecker, A. M., Parvizi, J., & Wandell, B. A. (2013). Asynchronous broadband signals are the principal source of the BOLD response in human visual cortex. *Current Biology : CB*, *23*(13), 1145–1153. https://doi.org/10.1016/J.CUB.2013.05.001

Wirsich, J., Giraud, A. L., & Sadaghiani, S. (2020). Concurrent EEG- and fMRI-derived functional connectomes exhibit linked dynamics. *NeuroImage*, *219*. https://doi.org/10.1016/J.NEUROIMAGE.2020.116998

Wirsich, J., Ridley, B., Besson, P., Jirsa, V., Bénar, C., Ranjeva, J. P., & Guye, M. (2017). Complementary contributions of concurrent EEG and fMRI connectivity for predicting

structural connectivity. *NeuroImage*, *161*, 251–260. https://doi.org/10.1016/J.NEUROIMAGE.2017.08.055

Womelsdorf, T., Valiante, T. A., Sahin, N. T., Miller, K. J., & Tiesinga, P. (2014). Dynamic circuit motifs underlying rhythmic gain control, gating and integration. *Nature Neuroscience*, *17*(8), 1031–1039. https://doi.org/10.1038/NN.3764

Worden, M. S., Foxe, J. J., Wang, N., & Simpson, G. V. (2000). *Anticipatory Biasing of Visuospatial Attention Indexed by Retinotopically Specific-Band Electroencephalography Increases over Occipital Cortex*. http://www.jneurosci.org/cgi/content/full/4016

Wöstmann, M., Waschke, L., & Obleser, J. (2019). Prestimulus neural alpha power predicts confidence in discriminating identical auditory stimuli. *The European Journal of Neuroscience*, *49*(1), 94–105. https://doi.org/10.1111/EJN.14226

Xia, M., Wang, J., & He, Y. (2013). BrainNet Viewer: A Network Visualization Tool for Human Brain Connectomics. *PLoS ONE*, *8*(7). https://doi.org/10.1371/journal.pone.0068910

Xia, M., Womer, F. Y., Chang, M., Zhu, Y., Zhou, Q., Edmiston, E. K., Jiang, X., Wei, S., Duan, J., Xu, K., Tang, Y., He, Y., & Wang, F. (2019). Shared and Distinct Functional Architectures of Brain Networks Across Psychiatric Disorders. *Schizophrenia Bulletin*, *45*(2), 450–463. https://doi.org/10.1093/SCHBUL/SBY046

Yan, W. X., Mullinger, K. J., Brookes, M. J., & Bowtell, R. (2009). Understanding gradient artefacts in simultaneous EEG/fMRI. *NeuroImage*, *46*(2), 459–471. https://doi.org/10.1016/J.NEUROIMAGE.2009.01.029

Yan, W. X., Mullinger, K. J., Geirsdottir, G. B., & Bowtell, R. (2010). Physical modeling of pulse artefact sources in simultaneous EEG/fMRI. *Human Brain Mapping*, *31*(4), 604–620. https://doi.org/10.1002/HBM.20891

Yordanova, J., Kolev, V., & Rothenberger, A. (2013). Event-related oscillations reflect functional asymmetry in children with attention deficit/hyperactivity disorder. *Supplements to Clinical Neurophysiology*, *62*, 289–301. https://doi.org/10.1016/B978-0-7020-5307-8.00018-1

Yuan, P., Hu, R., Zhang, X., Wang, Y., & Jiang, Y. (2021). Cortical entrainment to hierarchical contextual rhythms recomposes dynamic attending in visual perception. *ELife*, *10*. https://doi.org/10.7554/ELIFE.65118

Zalesky, A., Fornito, A., & Bullmore, E. T. (2010). Network-based statistic: identifying differences in brain networks. *NeuroImage*, *53*(4), 1197–1207.

https://doi.org/10.1016/J.NEUROIMAGE.2010.06.041

Zhuang, X., Yang, Z., & Cordes, D. (2020). A technical review of canonical correlation analysis for neuroscience applications. *Human Brain Mapping*, *41*(13), 3807–3833. https://doi.org/10.1002/HBM.25090

Zoefel, B., ten Oever, S., & Sack, A. T. (2018). The involvement of endogenous neural oscillations in the processing of rhythmic input: More than a regular repetition of evoked neural responses. In *Frontiers in Neuroscience* (Vol. 12, Issue MAR, p. 95). Frontiers Media S.A. https://doi.org/10.3389/fnins.2018.00095

Zumer, J. M., Scheeringa, R., Schoffelen, J. M., Norris, D. G., & Jensen, O. (2014). Occipital Alpha Activity during Stimulus Processing Gates the Information Flow to Object-Selective Cortex. *PLOS Biology*, *12*(10), e1001965. https://doi.org/10.1371/JOURNAL.PBIO.1001965

ACKNOWLEDGEMENTS

First and foremost, I would like to thank my supervisor Dr. Afra Wohlschläger for believing in me from the beginning, giving me the opportunity to test my many ideas, and providing guidance and support. I would also particularly like to thank the members of my PhD committee, Dr. Christian Sorg and Prof Dr. Paul Sauseng, who gave fruitful advice and helped me conceptualize many of my ideas.

I want to thank my colleagues at TUMNIC and the NKZ for their support. I am especially thankful for Rachel, Juliana and Sebastian for their sincere help prepping endless electrodes, great scientific advice, and many shared laughs. A special thank you also goes out to Martin for the great discussions over a cup of coffee and his continuous technical and programming support. I also want to especially thank Dr. Franziska Knolle, who provided wonderful insight. I would like to also thank Dr. Christine Preibisch for sharing valuable MR knowledge and helping me solve any scanner-related issues.

I would also like to express my gratitude to Professor Claus Zimmer and the Anesthesiology department for funding my research and providing the neuroimaging equipment and infrastructure.

I would also like to thank the GSN for providing an excellent academic program and organizing many social and scientific events that helped meet many great scientists.

I am incredibly grateful for the wonderful friends I have met during my PhD. Thank you, Fabian and Meg, for whisking me away to the mountains and pushing me to my physical limits. Thank you, Lili for always being there for a good talk, hosting our thesis writing parties, and keeping me motivated till the very end. Judi, your cheerful attitude and advice helped me tremendously, and I will cherish our many art and cultural adventures. Sachith, I am especially grateful to you for exchanging scientific insight and our many long discussions. To the brains on tour, thank you Issy and Samira for the great outdoor adventures, the many laughs, and wonderful moments.

I would also like to thank the Soapbox Science Organization Team. It has been great to work alongside so many talented and inspiring women and I am very happy to have seen the organization become so successful over the years.

I am also very grateful for the Tricamp family who have nurtured my passion for endurance sports and have kept me on my feet these past few years.

I cannot express enough gratitude to some of my oldest and dearest friends, Liza and Nay, who remain my biggest role models and supporters even from across the globe.

Without the amazing support of my friends, my PhD would not have been possible.

My final and biggest thank you goes to those closest and dearest to me. Becky, thank you for always being there for me, especially in these last few very stressful months. I could not have done this without your encouragement and support. To my two sisters, Luisa and Felina, who are always there to make me laugh, best adventure companions, and always push me to do better. To my grandparents, Moma and Mopa, whose constant love and support always encouraged me to follow my aspirations. Lastly, and most importantly, I would like to thank my parents. Thank you for always encouraging me to follow my dreams, believing in me, even when I didn't, and being my biggest supporters. I cannot express in words; how proud and grateful I am to have you as my parents. As a small token of appreciation, I wrote this thesis for you.

LIST OF PUBLICATIONS

Published:

Jaeger C, Glim S, Dimulescu C, Ries A, Sorg C, Wohlschläger AM. Segregated Co-activation Patterns in the Emergence of Decision Confidence During Visual Perception. *Front. Syst. Neurosci.* 14, 2020.

Unpublished:

Jaeger C, Nuttall R, Zimmermann J, Dowsett J, Preibisch C, Sorg C, Wohlschlaeger AM. Targeted rhythmic visual stimulation at individual subjects' intrinsic alpha frequency causes selective increase of occipitoparietal BOLD-fMRI and EEG functional connectivity.

Jaeger C, Nuttall R, Scheider S, Zimmermann J, Dowsett J, Sorg C, Wohlschlaeger AM. Alpha-mediated long-range connectivity during visual stimulation in concurrent EEG-fMRI study

AFFIDAVIT

Hiermit versichere ich an Eides statt, dass ich die vorliegende Dissertation selbstständig angefertigt habe, mich außer der angegebenen keiner weiteren Hilfsmittel bedient und alle Erkenntnisse, die aus dem Schrifttum ganz oder annähernd übernommen sind, als solche kenntlich gemacht und nach ihrer Herkunft unter Bezeichnung der Fundstelle einzeln nachgewiesen habe.

I hereby confirm that the dissertation is the result of my own work and that I have only used sources or materials listed and specified in the dissertation.

München, den 16.03.2022

_____

Cilia Jaeger

DECLARATION OF AUTHORSHIP:

Project I:	Targeted rhythmic visual stimulation at individual subjects' intrinsic alpha frequency causes selective increase of occipitoparietal BOLD-fMRI and EEG functional connectivity
Authors:	Cilia Jaeger, Rachel Nuttall, Juliana Zimmermann, James Dowsett, Christine Preibisch, Christian Sorg, Afra Wohlschlaeger
Author Contribution:	CS and AW conceived the experiment. JD, RN, **CJ**, CP, CS, and AW designed the experiment. RN, JZ, **CJ** collected the data. **CJ** analyzed and interpreted the data, wrote the manuscript, and created the figures. AW interpreted the data and reviewed the manuscript and figures.

Project II:	Alpha-mediated long-range connectivity during visual stimulation in concurrent EEG-fMRI study
Authors:	Cilia Jaeger, Rachel Nuttall, Sebastian Schneider, Juliana Zimmermann, James Dowsett, Christian Sorg, Afra Wohlschlaeger
Author Contribution:	CS, and AW conceived the experiment. **CJ**, RN, and JD designed the experiment. **CJ,** RN, JZ, and SS collected data. **CJ** analyzed and interpreted the data, wrote the manuscript and created the figures. AW reviewed the manuscript.

_____ _____

Cilia Jaeger — Place, date

(First Author)

_____ _____

Dr. Afra M. Wohlschlaeger — Place, date

(Supervisor)